The Structure of Atmospheric Parameters in Wavenumber-Space

By
David Wackter

Department of Atmospheric Science
Colorado State University
Fort Collins, Colorado

This research was supported by the National Science Foundation under
Grants GA-41542 and DES 74-001917 A01.
Principal investigator: Bernhard Haurwitz
March 1976

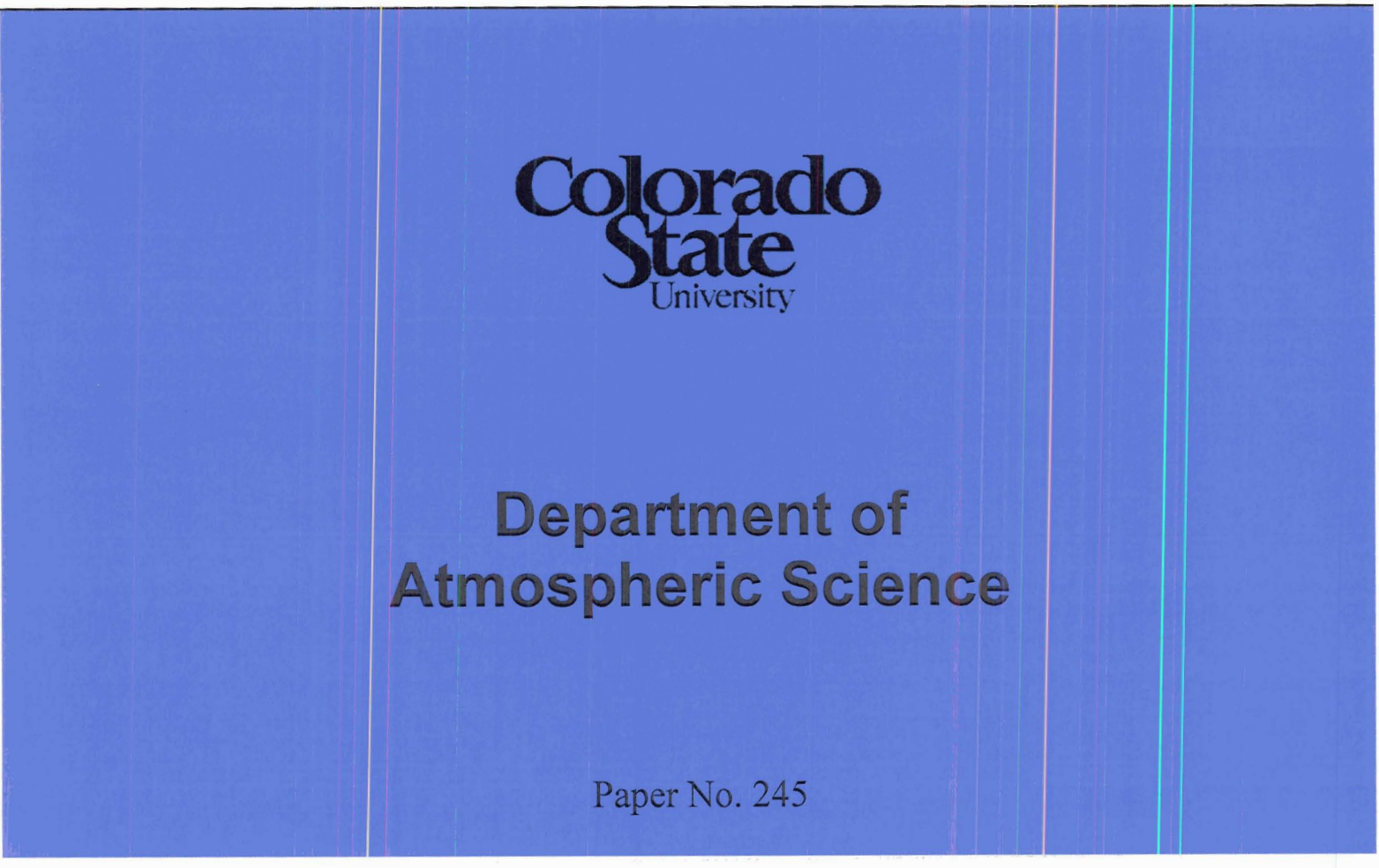

THE STRUCTURE OF ATMOSPHERIC PARAMETERS IN WAVENUMBER-SPACE

by

David Wackter

This research was supported by the National Science Foundation under Grants GA-41542 and DES 74-001917 A01. Principal Investigator Bernhard Haurwitz.

Department of Atmospheric Science

Colorado State University

Fort Collins, Colorado

80523

March, 1976

Atmospheric Science Paper Number 245

ABSTRACT OF THESIS

THE STRUCTURE OF ATMOSPHERIC PARAMETERS IN WAVENUMBER-SPACE

Zonal harmonic analysis of geopotential heights was performed at each fifth degree of latitude from 20°N to 85°N and at fourteen standard pressure levels from 1000 mb to 10 mb for each day of 1971. Computed parameters include the first twelve harmonic amplitudes, phase angles of contour heights, geostrophic wind components, kinetic energies of the zonal and meridional geostrophic flow, and the meridional fluxes of relative westerly momentum. Two types of calculations were used to compute monthly means, thereby allowing the introduction of "standing" and "transient" wave contributions.

The most dominant feature of the seasonal amplitude distributions was the disappearance of the strong wavenumbers one and two in the stratosphere following the spring breakdown of the polar night vortex.

Wavenumbers one through three dominated the zonal kinetic energy spectrum in January and July, and also the meridional kinetic energy spectrum at high latitudes and levels. An appreciable part of the meridional kinetic energy was contained in the wavenumber band from five through twelve at lower and mid-latitudes of the troposphere.

The standing and transient components of the wave energy showed preferred modes with, in general, the transient waves predominantly responsible for the meridional kinetic energy and the standing waves responsible for a major part of the zonal kinetic energy.

The development of a stratospheric sudden warming was analyzed in the same manner, but on a daily basis. When amplitudes of wavenumbers one and two were high there occurred a noticeable westerly tilt with

height. Waves two and three appear to gain energy at the expense of wave one and the mean zonal current as the polar night vortex begins to break down.

David Wackter
Atmospheric Science Department
Colorado State University
Fort Collins, Colorado 80523
Spring, 1976

ACKNOWLEDGEMENTS

The author would like to express his gratitude to Dr. Bernhard Haurwitz for his constructive criticisms and inspiring suggestions in the preparation of this thesis and throughout the author's graduate career. Many thanks also are due to Ms. Juanita Veen, Ms. Grace Holt, and Ms. Ann Spahr who collectively typed the manuscript, and especially to my wife Ronnie for her cooperation, patience, and encouragement.

Most of the numerical computing and contour plotting was performed at the National Center for Atmospheric Research Computing Facility (NCAR is sponsored by the National Science Foundation). The research contained in this report was sponsored by National Science Foundation under grants GA-41542 and DES 74-00197 A01.

TABLE OF CONTENTS

ABSTRACT iii

ACKNOWLEDGEMENTS. v

TABLE OF CONTENTS vi

LIST OF TABLES vii

LIST OF FIGURES viii

LIST OF SYMBOLS xi

1. INTRODUCTION. 1

2. COMPUTATIONAL PROCEDURES. 6

2.1 Fourier Analysis of Geopotential Height 6

2.2 Computation of Geostrophic Winds in the Spectral Domain. . 7

2.3 Spectral Kinetic Energy and Flux of Relative Westerly Momentum 9

2.4 Averaging Notation 11

2.5 Data 14

3. MONTHLY MEAN QUANTITIES 16

3.1 Amplitude and Phase. 16

3.2 Zonal and Meridional Kinetic Energy Spectra. 32

3.3 Transport of Relative Westerly Momentum 50

4. STRATOSPHERIC SUDDEN WARMING OF JANUARY, 1971. 61

4.1 Synoptic Discussion. 62

4.2 Amplitude and Phase of Long Waves 65

4.3 Kinetic Energy and Relative Momentum Flux 74

5. SUMMARY AND CONCLUSIONS 88

REFERENCES. 92

LIST OF TABLES

Table		Page
1.1	Variation of wavelength (km) with latitude for k = 1,2,3,6 and 12 at 20, 40, 60 and 80 degrees latitude ($L_k = \frac{2\pi E \cos\phi}{k}$ where E is the earth's radius). . .	4
3.1	Percent of January monthly mean height variance accounted for by (a) the first two harmonics, and (b) the first six harmonics.	17
3.2	Percent of July monthly mean height variance accounted for by (a) the first two harmonics, and (b) the first six harmonics	18
3.3	Spectral percentage of zonal, meridional, and total (zonal plus meridional) kinetic energies to the assumed total of the respective quantities (meaning the sum of waves one through twelve) at 500 mb for (a) January and (b) July single-barred monthly means	36-38

LIST OF FIGURES

Figure		Page
3.1	Pressure/latitude distribution of monthly mean January amplitudes (gpm) and corresponding phase angles of the first ridge line east of Greenwich (from 0 to 2π) for wavenumbers: one, (a) and (b), respectively; two, (c) and (d); three, (e) and (f); and the wave four amplitude, (g).	21-22
3.2	Same as Figure 3.1 except for April	27-28
3.3	Same as Figure 3.1 except for July	30-31
3.4	Same as Figure 3.1 except for October	33-34
3.5	Pressure/latitude distribution of the January wave one: double-barred zonal kinetic energy; (b) single-barred zonal kinetic energy; (c) double-barred meridional kinetic energy; and (d) single-barred meridional kinetic energy. Isopleths are at increments of 10 m^2/s^2	41
3.6	Same as Figure 3.5 except for wavenumber two . . .	42
3.7	Sum of January (a) double-barred zonal kinetic energy by waves one through four, (b) single-barred zonal kinetic energy by waves one through four, (c) double-barred zonal kinetic energy by waves one through twelve, and (d) single-barred zonal kinetic energy by waves one through twelve. Isopleths are at increments of 10 m^2/s^2	44
3.8	Same as Figure 3.7 except for meridional kinetic energy.	45
3.9	Same as Figure 3.7 except for July	47
3.10	Same as Figure 3.7 except for the July meridional kinetic energy	48
3.11	January meridional flux of relative westerly momentum by wave (a) one (double-barred), (b) one (single-barred), (c) two (double-barred), (d) two (single-barred, (e) three (double-barred), and (f) three (single-barred). Solid lines indicate northward (or zero) flux; dashed lines indicate southward flux. Isopleth interval is 10 m^2/s^2	53-54

LIST OF FIGURES (Cont'd.)

Figure		Page
3.12	January meridional flux of relative westerly momentum by waves (a) one through four (double-barred), (b) one through four (single-barred), (c) one through twelve (double-barred), and (d) one through twelve (single-barred).	56
3.13	Same as Figure 3.12 except for July	60
4.1	50 mb Northern Hemisphere synoptic charts for (a) 1 January 1971 and (b) 19 January 1971. Solid lines are contour heights (decameters) and dashed lines are isotherms (°C)	63
4.2	January day-to-day variation of the zonally averaged geostrophic zonal wind at 62.5°N (solid line) and 72.5°N (dashed line) at the 10 mb level. Units are m/s	64
4.3	January day-to-day variation of the wave one (a) amplitude and (b) longitude of the first ridge line east of Greenwich at 10 mb (solid line), 70 mb (dashed line), 200 mb (dashed-dotted line), and 500 mb (dotted line) at 70°N.	66
4.4	Same as Figure 4.3 except for wave two.	68
4.5	Wave one amplitude distribution for every 6th day of January. Contour interval of 20 m except 50 m at amplitudes above 300 m.	70-71
4.6	Same as Figure 4.5 except for wave two	72-73
4.7	Same as Figure 4.5 except for wave three	75
4.8	Kinetic energy of the zonal current (k=0) for every 6th day of January. Contour interval of 50 m^2/s^2. .	77
4.9	Kinetic energy of the zonal flow by wave one for every 6th day of January. Contour interval of 10 m^2/s^2	79
4.10	Same as Figure 4.9 except for the meridional flow .	80
4.11	Meridional flux of relative westerly momentum by wave one for every 6th day of January. Solid lines indicate northward (or zero) flux; dashed lines indicate southward flux. Contour interval of 10 m^2/s^2 . . .	81

LIST OF FIGURES (Cont'd.)

Figure		Page
4.12	Same as Figure 4.9 except by wave two	83
4.13	Same as Figure 4.9 except for wave two meridional flow	84
4.14	Same as Figure 4.11 except by wave two	85

LIST OF SYMBOLS

A_k	Amplitude of k'th harmonic wave of geopotential heights
a_k, b_k	Fourier coefficients of geopotential heights
a_k^u, b_k^u	Fourier coefficients of geostrophic zonal wind
a_k^v, b_k^v	Fourier coefficients of geostrophic meridional wind
E	earth's radius; mean kinetic energy around a latitude circle
E_m	meridional kinetic energy averaged around a latitude circle
E_z	zonal kinetic energy averaged around a latitude circle
e_k^v	k'th harmonic component of meridional kinetic energy
e_k^u	k'th harmonic component of zonal kinetic energy
f	Coriolis parameter
g	acceleration of gravity
k	zonal wavenumber
L_k	wavelength of k'th harmonic for a given latitude
2N	number of data points equally spaced around a latitude circle
u	geostrophic zonal wind
v	geostrophic meridional wind
$\overline{x}$	monthly mean of the daily values of x, if x is determined from a_k and b_k
$\overline{\overline{x}}$	value of x computed from $\overline{a}_k$ and $\overline{b}_k$ for a given month
Z	height of an isobaric surface
λ	longitude
λ_r	longitude of r'th data point east of Greenwich
λ_k	longitude of first ridge line of k'th harmonic
λ_R	set of ridge lines around a latitude circle
λ_T	set of trough lines around a latitude circle
π	3.14159

τ	northward flux of relative westerly momentum
τ_k	k'th harmonic component of τ
ϕ	latitude
Ω	earth's angular velocity

1. INTRODUCTION

Upon examination of Northern Hemisphere weather maps one characteristically observes planetary scale waves superimposed on a basic zonal current. Through the use of zonal harmonic analysis these perturbations of varying time and space scales can be studied selectively.

Harmonic analysis of the geopotential height field of an isobaric surface (or the field of any other meteorological parameter) is a mathematical technique used for determining the importance of various scales of atmospheric disturbances as a function of latitude and pressure level. The significance of individual wavenumbers (where the wavenumber k is defined as the number of wave cycles around a given latitude circle) with respect to daily, seasonal, or interannual variations of the general circulation can also be determined. This is accomplished here by the analysis of computed spectral modes of appropriate meteorological parameters, namely the amplitudes and phases of standard pressure level heights, and derived quantities, that is the geostrophic wind contribution to the zonal and meridional kinetic energies and the meridional transport of relative westerly momentum.

An extensive bibliography and summary of previous works in the wavenumber-space domain has been compiled by Van Mieghem (1961). Most of the earlier works were hindered by the laborious and time consuming calculations necessary for harmonic analyses. Also, harmonic analyses generate large quantities of statistics which require further analysis, and for these reasons the vertical and meridional structure of differing scales of atmospheric disturbances have been studied theoretically and empirically in only very limited space and time domains.

Thus, Eliasen (1958) analyzed the mid-latitude contour height fields at 1000 mb and 500 mb on a daily basis for a period of six weeks. Van Mieghem, et al. (1960) studied the monthly normal geostrophic flow patterns at the 500-mb level for every fifth degree of latitude from 20°N to 70°N for each of the twelve months. More recently, the vertical structure of planetary scale waves in January has been investigated by van Loon, et al. (1973) for seven Januaries, ten standard levels from near the earth's surface to 10 mb, and for each fifth degree of latitude north of 10°N. Iwashima (1973) studied four stratospheric levels at each fifth degree of latitude north of 30°N for 121 consecutive days, and Sato (1974) analyzed six pressure levels for eight winters (each consisting of three-month means) and two latitudes. For comparative purposes some of the results of these and other papers will be mentioned briefly in context with the results of this investigation.

On the basis of previous studies of the general circulation using harmonic analysis, the spectra of atmospheric disturbances in the troposphere have been roughly divided (Van Mieghem, 1973) into three subdivisions as follows:

i) the quasi-stationary planetary waves, with zonal wavenumbers from one through four which are forced primarily by the distribution of continents and oceans (k = 2), mountain barriers and topographic features (k = 3), and the distribution of heat sources and sinks;

ii) the long transient waves, with zonal wavenumbers five through ten, which are produced primarily by the baroclinic instability of the circumpolar flow, and hence, are linked to the various

generations of and conversions between available potential energy and kinetic energy; and

iii) the traveling synoptic scale systems of mid-latitude (wavenumbers greater than ten) which are generated and dissipated in the lower layers of the troposphere, losing intensity fairly rapidly with height.

It might also be mentioned here that Kertz (1956) performed harmonic analyses of the continent-ocean distribution at every tenth degree of latitude and found a predominance of wavenumbers one and two in the Northern Hemisphere.

A difficulty with studies of the general circulation using harmonic analysis arises from the lack of reliable meteorological data over large areas of sparse observations. The lack of data results in errors inherent in subjective analyses through the smoothing of synoptic scale features. The smaller scales of motion corresponsing to higher frequency disturbances also are systematically filtered out when using period means with time scales on the order of a month, season, or year.

Since high wavenumber variations are pretty much smoothed out by an inadequate data network, zonal harmonic analyses currently seem best suited to the study of large scale phenomena. However, the computations here have been carried through wavenumber twelve in order to account for what will be assumed as the total variance of the flow pattern.

Of course, the length of an individual harmonic wave varies with the cosine of the latitude. This is tabulated for a few wavebumbers and latitudes in Table 1.1.

	ϕ=	20°	40°	60°	80°
K =	1	37,616	30,665	20,015	6,951
	2	18,808	15,332	10,007	3,475
	3	12,539	10,222	6,672	2,317
	6	6,269	5,111	3,336	1,158
	12	3,135	2,555	1,668	579

Table 1.1. Variation of wavelength (km) with latitude for k = 1,2,3,6 and 12 at 20, 40, 60 and 80 degrees latitude ($L_k = \frac{2\pi E\cos\phi}{k}$, where E is the earth's radius).

The primary purpose of this study was to investigate the important modes of atmospheric disturbances by studying daily and seasonal differences in latitudinal distribution and vertical structure of various parameters in wavenumber-space. The monthly means of zonal and meridional kinetic energies and of momentum flux were calculated in two ways in order to determine the importance of day-to-day variations of the wave motions. The data for January are presented in more detail to enable a more complete spectral representation of the flow patterns during a rather strong stratospheric sudden warming (Barnett, et al., 1971). Data for January, April, July, and October are presented as typical for the respective seasons. This assumption, although somewhat crude, at least eliminates the redundant verbosity that would have been required to present the data in its entirety.

Zonal harmonic analyses are performed for each day at each fifth degree of latitude from 20°N to 85°N and at fourteen pressure levels ranging from 1000 mb to 10 mb for the entire year 1971. To simplify matters the data from only ten pressure levels were studied in the final

analysis. Monthly means of the first twelve amplitudes and phase angles were then computed for each of the twelve months.

It appears desirable at this point to describe in some detail the numerical procedures which were used to derive various quantities from the basic data (that is, the heights of the pressure surfaces at each tenth degree of longitude around a given latitude circle).

2. COMPUTATIONAL PROCEDURES

2.1 Fourier Analysis of Geopotential Height.

Since the height of a pressure level $Z(\lambda)$ along a latitude circle ϕ is a cyclic function of longitude (λ) with a period of 2π, a Fourier approximation can be assumed in the form

$$Z(\lambda) \approx a_o + \sum_{k=1}^{n} (a_k \cos k\lambda + b_k \sin k\lambda) \qquad 1.1$$

(Hildebrand, 1950). The zonal wavenumber k defines the number of waves around the earth at a given latitude (it should be remembered that each wave consists of a ridge and a trough). The value of n is determined by one half the number of data points.

The coefficients of the Fourier expansion, a_k and b_k, can be calculated from empirical data if $Z(\lambda)$ is known at a discrete set of equally spaced points over the fundamental period interval $[0,2\pi]$ going eastward around the hemisphere from the prime meridian. If 2N points are designated at longitudes $0, \pi/N, 2\pi/N, \ldots, (2N-1)\pi N$, then we have 2N independent values of Z which can be expected to determine the coefficients of the terms in Equation 1.1. The abscissa ranges from 0 to $2\pi - \frac{\pi}{N}$ and can be denoted by the subscript r, as

$$\lambda_r = (r-1)\ \pi/N \quad (r = 1,2,\ldots,2N)$$

If the least squares criterion is utilized along with the orthogonality of sines and cosines, the following relations can be derived:

$$a_o = \frac{1}{2N} \sum_{r=1}^{2N} Z(\lambda_r), \qquad 1.2$$

$$a_k = \frac{1}{N} \sum_{r=1}^{2N} Z(\lambda_r) \cos k\lambda_r, \qquad 1.3$$

$$b_k = \frac{1}{N} \sum_{r=1}^{2N} Z(\lambda_r) \sin k\lambda_r . \qquad 1.4$$

The Fourier series of Equation 1.1 can also be written in another form which is convenient for our purposes:

$$Z(\lambda) = a_o + \sum_{k=1}^{n} A_k \cos k(\lambda - \lambda_k) \qquad 1.5$$

where the amplitude, A_k, and the phase angle, λ_k, are related to the Fourier coefficients as follows:

$$A_k = (a_k^2 + b_k^2)^{\frac{1}{2}} \qquad 1.6$$

$$\lambda_k = \frac{1}{k} \tan^{-1} \frac{b_k}{a_k} . \qquad 1.7$$

The amplitude A_k is the spectral contribution to the height field with a wavelength of $L_k = \frac{2\pi E \cos \phi}{k}$ (where E is the earth's radius) with a distribution corresponding to the phase angle.

The ridges of the k'th harmonic are determined from the harmonic coefficients, and will be found at longitudes

$$\lambda_R = \lambda_k + \frac{2\pi n}{k} \quad (n=0,1,2,\ldots,k-1) \qquad 1.8$$

Conversely, the troughs of the k'th harmonic will be found at longitudes $\lambda_T = \lambda_R + \pi/k$. The first ridge (trough) to the east of the Greenwich Meridian will then be the first positive value of λ_R (λ_T).

2.2 Computation of Geostrophic Winds in the Spectral Domain.

The wind components for the zonal (westward) and meridional (northward) directions, using the geostrophic assumption, and spherical

coordinates become

$$u = -\frac{g}{fE}\frac{\partial Z}{\partial \phi}, \qquad v = \frac{g}{fE\cos\phi}\frac{\partial Z}{\partial \lambda} \tag{2.1}$$

where g is the acceleration of gravity, f is the Coriolis parameter ($2\Omega \sin\phi$), Ω is the earth's angular velocity, λ is the longitude, ϕ is latitude, and E is the earth's radius.

The decomposition of u and v into Fourier series is similar to that for $Z(\lambda)$ around a given latitude circle (see Equation 1.1):

$$u(\lambda) = a_o^u + \sum_{k=1}^{n} (a_k^u \cos k\lambda + b_k^u \sin k\lambda) \tag{2.2}$$

$$v(\lambda) = \sum_{k=1}^{n} (a_k^v \cos k\lambda + b_k^v \sin k\lambda) \tag{2.3}$$

where the mean meridional wind component around a latitude circle (a_o^v) is zero because of the geostrophic assumption. The coefficients a_k^u, b_k^u, a_k^v, and b_k^v are found from the determinations of a_k and b_k by substituting Equation 1.1 in Equations 2.1 along with the Fourier series for u and v (Equations 2.2 and 2.3). The resulting formulae are:

$$a_k^u = -\frac{g}{fE}\frac{\partial a_k}{\partial \phi} \tag{2.4}$$

$$b_k^u = -\frac{g}{fE}\frac{\partial b_k}{\partial \phi} \tag{2.5}$$

$$a_k^v = \frac{gk}{fE\cos\phi}\, b_k \tag{2.6}$$

$$b_k^v = \frac{-gk}{fE\cos\phi}\, a_k. \tag{2.7}$$

In the actual computations, the coefficients defined in Equations 2.4 and 2.5 were found from the differences of a_k and b_k at two consecutive latitudes. The computed values of a_k^u and b_k^u, then, refer to the intermediate latitudes 22.5°N, 27.5°N, etc. To determine the

coefficients defined in Equations 2.6 and 2.7 at the same latitudes, the means of b_k and a_k at two consecutive latitudes were used in the computations of a_k^v and b_k^v, respectively. The values for f and cos ϕ in Equations 2.4 - 2.7 are also determined for the intermediate latitudes.

2.3 Spectral Kinetic Energy and Flux of Relative Westerly Momentum.

Because the actual wind is nearly geostrophic in middle and high latitudes and above the planetary boundary layer, we can compute derived quantities like the kinetic energy of the wind components and the northward flux of relative westerly momentum to a reasonable degree of accuracy using the geostrophic assumption.

The mean kinetic energy per unit mass (in units of $m^2 s^{-2}$) around a given latitude circle and at a given pressure level can be expressed as

$$E = \frac{1}{2\pi} \int_0^{2\pi} 1/2(u^2 + v^2)\, d\lambda \qquad 3.1$$

where the first term is the kinetic energy of the zonal flow, and the second term is the kinetic energy of the meridional flow. Also, the kinetic energy per unit volume (or kinetic energy density) can be formed by multiplying the kinetic energy times the density.

Taking each term of Equation 3.1 separately and substituting the appropriate Fourier series from Equations 2.2 and 2.3, we obtain for the zonal kinetic energy (assumed as per unit mass)

$$E_z = \frac{1}{4\pi} \int_0^{2\pi} [a_o^u + \sum_{k=1}^{n} (a_k^u \cos k\lambda + b_k^u \sin k\lambda)]^2\, d\lambda$$

which can be simplified using Parseval's theorem to obtain

$$E_z = 1/2(a_o^u)^2 + 1/4 \sum_{k=1}^{n} [(a_k^u)^2 + (b_k^u)^2] \qquad 3.2$$

$$= e_o^u + \sum_{k=1}^{n} e_k^u.$$

In this equation e_o^u is the kinetic energy of the zonal flow averaged around a given latitude circle. The e_k^u's are the zonal kinetic energies produced by each harmonic wave. Similarly for the meridional kinetic energy component, we get

$$E_m = 1/4 \sum_{k=1}^{n} [(a_k^v)^2 + (b_k^v)^2] \qquad 3.3$$

$$= \sum_{k=1}^{n} e_k^v$$

where e_o^v is zero since the mean geostrophic meridional wind is zero.

It is now easily shown by substituting the meridional wind coefficients (Equations 2.6 and 2.7) into Equation 3.3 that the spectral kinetic energy of the meridional flow is proportional to the square of the product of the zonal wavenumber k times its amplitude, and inversely proportional to the square of the cosine of the latitude and f^2:

$$e_k^v = \frac{g^2}{4E^2} \cdot \frac{k^2 A_k^2}{f^2 \cos^2\phi}. \qquad 3.4$$

The northward flux of relative westerly momentum (again, per unit mass) is determined from the following equation:

$$\tau = \sum_{k=1}^{n} \tau_k = \frac{1}{2\pi} \int_o^{2\pi} uv d\lambda. \qquad 3.5$$

By substituting the Fourier series for u and v, and then simplifying we find

$$\tau = 1/2 \sum_{k=1}^{n} (a_k^u a_k^v + b_k^u b_k^v). \qquad 3.6$$

For a physical interpretation this equation is changed into a different form. If Equations 2.4-2.7 are substituted for the coefficients and the differentiated form of Equation 1.7,

$$a_k \partial b_k/\partial\phi - b_k \partial a_k/\partial\phi = k(a_k^2 + b_k^2)\partial\lambda_k/\partial\phi,$$

is introduced, Equation 3.6 takes on the following form:

$$\tau_k = \frac{1}{2 \cos \phi} \left(\frac{gkA_k}{fE}\right)^2 \partial\lambda_k/\partial\phi. \qquad 3.7$$

This equation expresses the well-known fact that the sign of the flux of relative westerly momentum is determined by the tilt of the trough and ridge lines with latitude (Palmén and Newton, 1969). Because of this geometric consequence, we can have a flux of relative westerly momentum poleward without a net mass flux of air at a given level. This latter situation occurs in the Northern Hemisphere when planetary scale waves are oriented from southwest to northeast and consequently, northward-moving air particles are associated with a greater west wind component than are southward-moving particles. A corresponding southerly flux occurs with waves tilted from southeast to northwest. Wavenumber two frequently has this orientation and, consequently, produces a southward flux while at the same time the net flux ($\Sigma\tau_k$, k = 1 - 12) is northward (see Section 3.3).

2.4 Averaging Notation.

Synoptic experience has taught us that the long planetary waves tend to be quasi-stationary persisting in preferred geographic locations on

monthly normal weather charts. Monthly means of atmospheric parameters can be determined in a number of different ways, sometimes producing contrasting results depending on the form of the terms being averaged. The monthly mean Fourier coefficients of the geopotential height field can be determined in two different ways, and because of the linearity of the formulae, with identical results:

i) By computing $\overline{a}_k$ and $\overline{b}_k$ (where the bar denotes a monthly mean) directly from the monthly mean values of the height fields; and

ii) By computing $\overline{a}_k$ and $\overline{b}_k$ directly from the daily values of a_k and b_k.

The monthly mean amplitudes and phase angles are determined from the monthly means of the coefficients, a_k and b_k, rather than from the mean of the daily amplitudes. As would be expected, the amplitude of the monthly mean wave (computed from $\overline{a}_k$ and $\overline{b}_k$) is generally smaller than the monthly mean of the daily amplitudes (Eliasen, 1958), or $\overline{(a_k^2 + b_k^2)^{1/2}}$. The difference between the two types of mean amplitudes gives a measure of the day-to-day variability of the waves.

Similarly, the Fourier coefficients (a_k^u, a_k^v, b_k^u, and b_k^v) of the monthly mean geostrophic winds can be determined in two different ways with identical results because the geostrophic wind relations are linear:

i) From the daily values of a_k and b_k; or

ii) Directly from $\overline{a}_k$ and $\overline{b}_k$.

Two different methods can also be used in determining the monthly means of the spectral modes of the kinetic energies and relative westerly momentum flux:

i) By computing daily values of these quantities from the daily values of the Fourier wind coefficients and then computing the monthly means of the quantities, which will now be denoted with a single bar: $\bar{e}_k^u$, $\bar{e}_k^v$, and $\bar{\tau}_k$; or

ii) Directly from the monthly means of the wind coefficients, which will now be denoted with a double bar: $\bar{\bar{e}}_k^u$, $\bar{\bar{e}}_k^v$, and $\bar{\bar{\tau}}_k$.

The single-barred and double-barred monthly mean energies and relative momentum fluxes have different values because of the non-linearity of the formulae defining them. The difference between the two types of means for a given parameter gives a measure of the intensity of the day-to-day variations (or variance in time) of the spectral modes of the flow and pressure patterns for a given month. This is probably best seen by an example:

Consider the spectral term of the meridional kinetic energy, e_k^v. As mentioned earlier, for a given latitude this term is proportional to $A_k^2 = a_k^2 + b_k^2$. The squared amplitude of the monthly mean wave is $(\bar{A}_k)^2 = (\bar{a}_k)^2 + (\bar{b}_k)^2$, and the monthly mean squared amplitude from the daily amplitudes is $\overline{A_k^2} = \overline{a_k^2} + \overline{b_k^2}$. If we now take the difference between the proportionalities (for the two types of mean meridional kinetic energy), we see that for a given latitude $(\bar{e}_k^v - \bar{\bar{e}}_k^v) \propto \overline{A_k^2} - (\bar{A}_k)^2$. It can easily be shown that this difference represents the variance of the spectral amplitude over a period of averaging (Panofsky and Brier, 1958, p. 209). An analysis of this type, then, will allow us to determine which harmonics contribute significantly to the daily variations of the pressure and flow patterns, and which harmonics are more persistent.

It might be noted here that another measure of the variance is also easily computed from either the amplitudes or the meridional kinetic energies: that is, the variance of height, $Z(\lambda)$, around a latitude circle (which is equivalent to the sum of the square of each of the harmonic amplitudes). This is possible since the harmonics are all uncorrelated (Haney, 1961) so no two harmonics can explain the same part of the variance of Z. The total variance was here assumed to be produced by the first twelve harmonics. The fraction of the total variance attributable to the first m harmonics can now be determined from the following formula:

$$\frac{\sum_{k=1}^{m} A_k^2}{\sum_{k=1}^{12} A_k^2} = \frac{\sum_{k=1}^{m} \frac{e_k^2}{k^2}}{\sum_{k=1}^{12} \frac{e_k^2}{k^2}} \qquad 4.1$$

In this paper, the single-barred quantities will be referred to as the "total" quantity, while the double-barred quantities are called the "standing" or "stationary" contributions. Then the difference between the types of means will be referred to as the "transient" component. The daily harmonic coefficients can also be Fourier analyzed with respect to time as was done by Deland (1973) and then analyzed for the movement of the traveling wave components.

2.5 Data.

The data used in this study was obtained on tape from the National Center for Atmospheric Research (NCAR) and consisted of "cleaned" National Meteorological Center (NMC) data interpolated from the 1977 point NMC octagonal grid to each 5th degree of latitude from 20°N to

85°N, and to each 10° of longitude. Daily data (at 00GMT) for the year 1971 were then Fourier analyzed at each of these latitudes and for the following pressure surfaces: 1000 mb, 850 mb, 700 mb, 500 mb, 400 mb, 300 mb, 250 mb, 200 mb, 150 mb, 100 mb, 70 mb, 50 mb, 30 mb, and 10 mb. The Fourier coefficients for the first twelve harmonics were then retained on magnetic tape. From this basic data set, the parameters described previously were derived.

Further information about NCAR data sets, and the objective analysis methods used in determining meteorological fields on a regularly spaced grid by applying corrections to a first guess can be found in Jenne (1975) and Cressman (1959), respectively.

3. MONTHLY MEAN QUANTITIES

Some of the primary objectives of this study were to obtain a better understanding of daily and seasonal variations, vertical structure, and latitudinal distribution, of long wave atmospheric disturbances, particularly at middle and high latitudes. Therefore the data and parameters discussed previously will be presented here for the monthly mean quantities, with particular emphasis on the months of January and July. When appropriate, comparisons will be made between data presented here and that of other authors for similar quantities and period means.

3.1 Amplitude and Phase of Contour Heights.

Obviously, not all of the zonal harmonic wave spectrum can be interpreted in physical terms. However, there are characteristic features of the atmosphere which can be explained by discrete wavelengths. But, as mentioned in the Introduction, it is generally accepted that the quasi-stationary planetary scale waves are forced by the distribution of continents, oceans, mountains, heat sources, and heat sinks. The smaller scale traveling waves produced by baroclinic instability are to a large degree smoothed when monthly means of the Fourier coefficients are computed. Thus a large percentage of the height variance around a latitude circle is determined by the longest waves. This is reflected in Tables 3.1 and 3.2 which show the cumulative spectral percentage of the total height variance for waves 1-2 and 1-6 in January (Table 3.1) and July (Table 3.2). The variances were computed using Equation 4.1 (Chapter 2) for the double-barred meridional kinetic energies. An examination of the tables reveals some interesting features. As noted by Haney (1961), the larger part of the monthly mean height variance along a latitude circle can be accounted for by the first few harmonics.

Table 3.1. Percent of January monthly mean height variance accounted for by (a) the first two harmonics, and (b) the first six harmonics.

(a)

Pressure (mb)							
10	99.96	99.47	98.38	97.45	90.16	56.07	60.64
30	99.97	99.75	98.86	97.15	91.07	56.34	50.95
50	99.99	99.87	99.03	96.02	87.67	61.02	58.71
100	99.94	99.66	98.99	95.28	80.99	56.21	73.59
200	99.88	98.75	96.31	93.71	75.37	58.08	78.54
300	99.86	97.00	91.33	90.68	74.68	63.41	67.99
500	99.77	96.78	87.88	88.95	76.74	66.76	72.25
700	99.74	99.05	85.51	87.71	79.37	56.05	76.45
1000	99.23	95.00	91.61	86.47	89.55	48.72	43.52
Latitude	82.5	72.5	62.5	52.5	42.5	32.5	22.5

(b)

Pressure (mb)							
10	100.00	100.00	100.00	99.99	99.83	98.41	96.39
30	100.00	100.00	100.00	99.96	99.90	97.92	97.52
50	100.00	100.00	100.00	99.91	99.66	97.75	98.37
100	100.00	100.00	99.99	99.91	99.21	95.03	95.88
200	100.00	99.98	99.92	99.92	99.68	95.73	95.43
300	100.00	99.98	99.92	99.88	99.68	97.15	92.16
500	100.00	99.87	99.81	99.89	99.54	97.91	95.02
700	100.00	99.83	99.17	99.72	99.30	97.17	95.45
1000	100.00	99.65	98.85	99.52	98.98	91.57	88.08
Latitude	82.5	72.5	62.5	52.5	42.5	32.5	22.5

Table 3.2. Percent of July monthly mean height variance accounted for by (a) the first two harmonics, and (b) the first six harmonics.

(a)

Pressure (mb)							
10	98.83	95.96	97.90	93.75	81.90	49.86	66.62
30	99.15	86.54	81.26	86.33	71.32	71.24	64.05
50	99.21	90.31	79.57	84.18	88.93	92.95	73.46
100	90.22	84.63	60.41	73.68	84.57	88.72	80.73
200	93.46	86.92	58.47	46.98	57.19	75.73	67.62
300	94.77	84.87	53.70	40.13	19.07	50.20	28.93
500	86.94	80.69	49.54	53.37	55.61	57.49	69.89
700	88.12	71.88	44.50	62.75	83.13	92.70	94.34
1000	78.92	68.88	84.27	77.55	89.03	83.69	91.09
Latitude	82.5	72.5	62.5	52.5	42.5	32.5	22.5

(b)

Pressure (mb)							
10	100.00	99.96	99.93	99.60	98.37	92.01	91.94
30	100.00	100.00	99.42	98.38	96.41	96.26	94.07
50	100.00	100.00	99.68	98.85	97.59	97.31	95.59
100	100.00	99.95	99.59	98.52	97.26	98.37	98.09
200	100.00	99.81	98.29	93.60	84.20	97.10	97.10
300	100.00	99.78	98.16	93.69	62.25	89.25	90.67
500	100.00	99.62	98.18	96.15	82.14	84.59	95.15
700	100.00	99.57	97.91	97.42	95.89	96.93	99.13
1000	100.00	97.35	96.52	97.34	98.10	96.64	98.15
Latitude	82.5	72.5	62.5	52.5	42.5	32.5	22.5

This becomes even more pronounced poleward and at higher levels. For example, in January the first two harmonics averaged for all levels in Table 3.1, account for 64.75% of the total variance at 22.5°N and 99.81% at 82.5°N. The increase with height is not quite as pronounced with 83.41%, averaged for all latitudes in Table 3.1a at 700 mb, and ranging up to 86.02% at 10 mb. The first six harmonics in January nearly always account for more than 95% of the total height variance. The corresponding values in July show that the first two waves account for less of the total variance than they did in January, and while the first six waves still account for less of the total variance than they did in January, they do account for more than 90% of the July total height variance in most cases.

The importance of higher wave numbers at lower latitudes is in part attributable to the increasing wavelength of a given wave number with decreasing latitude. The summer shift emphasizing shorter wavelengths is a consequence of the disproportionate summer decrease in amplitudes of the long waves with respect to the shorter waves. Some of this amplitude data will be shown, subsequently, in this section.

An interesting feature of the first harmonic (k=1) is that it describes the asymmetry of the zonal flow with respect to the pole, or analogously, the eccentricity with respect to the latitude circles (LaSeur, 1954). Hence, this harmonic is the only one which allows flow across the pole.

The meaning of the second harmonic can be described as the ellipticity of the circumpolar flow, which can be readily seen by superimposing the second harmonic on the mean zonal current (or zero order harmonic). The amount of ellipticity is determined by the amplitude, and the

longitude of the peak amplitude is determined by the phase angle. The remaining harmonics define the true wave-like character of atmospheric perturbations as can be observed on synoptic weather charts.

Figures 3.1 - 3.4 depict the vertical and latitudinal structure of the first four harmonic waves from monthly means characteristic of the four seasons for 1971 (January, April, July, and October). Shown are the amplitude distributions of the first four harmonics and the phase angle distributions of the first three waves. The phase angles plotted refer to the longitude (in degrees) of the first ridge line east of Greenwich.

In Figure 3.1a the highest amplitudes for wave number one in January are found in the polar stratosphere, reaching 800 meters at 70°N and at the 10 mb level. The latitude of this maximum amplitude remains constant through the troposphere, with a secondary tropospheric maximum occurring at 35°N and near the 250 mb level. The longitude of the ridge (Fig. 3.1b) corresponding to the high amplitude part of wave one during January has a slight westerly tilt with height and is located over the northwestern corner of North America where the amplitude (Fig. 3.1a) is large, i.e. at high latitudes. The corresponding trough, then is located in the vicinity of Scandinavia. The spatial distribution of waves one and two correspond quite well with the asymmetry and ellipticity of mean January circumpolar flow patterns at high latitudes in the troposphere (Palmén and Newton, 1969; p. 68) and in the stratosphere (Craig, 1965; p. 45). The abnormally high amplitude located in the stratosphere (as compared to seven year means by van Loon, et al., 1973) is probably coincident with the asymmetry of the polar night vortex, which happened to experience a rather strong sudden breakdown and reversal in mid-month

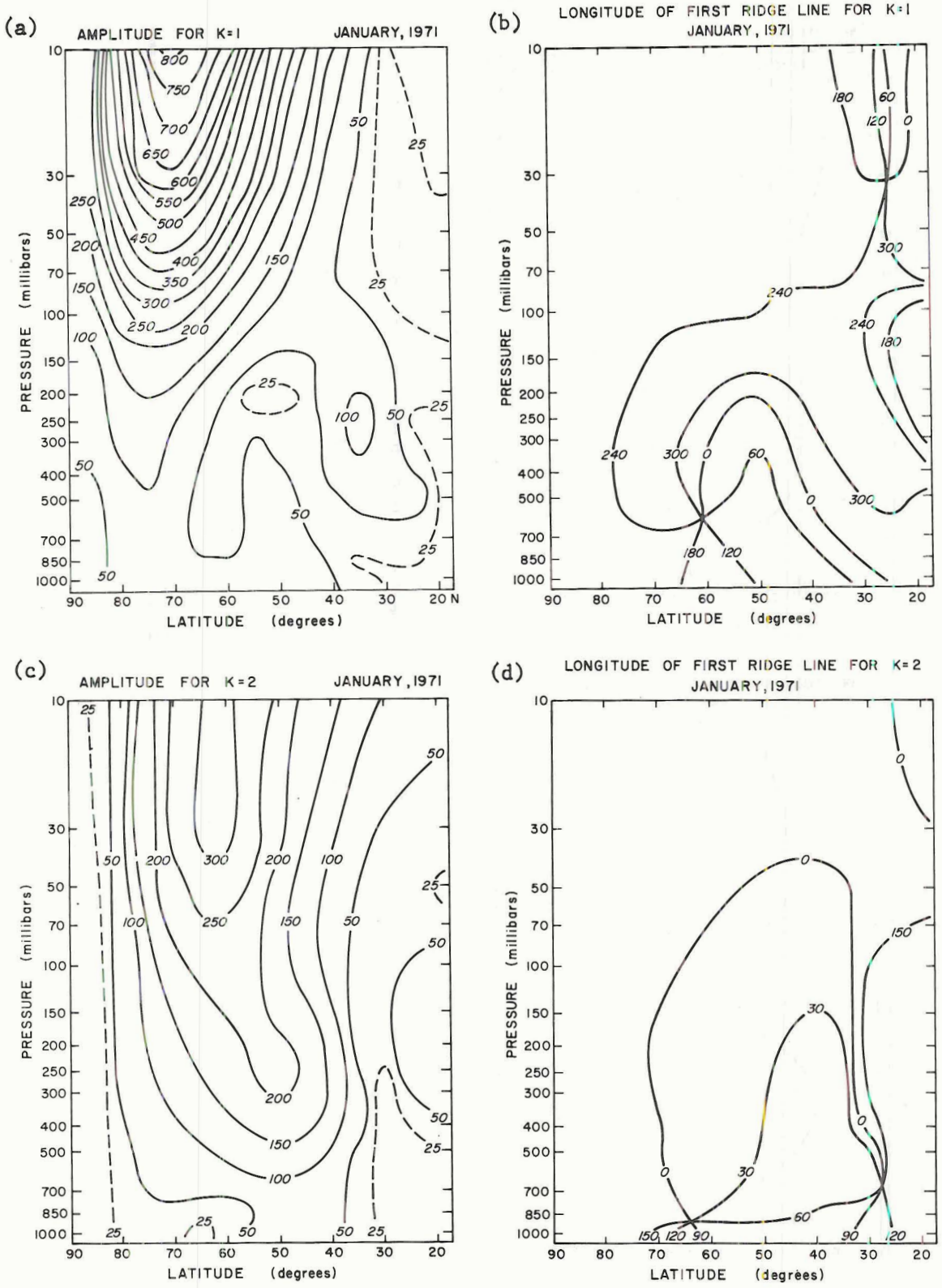

Figure 3.1 Pressure/latitude distribution of monthly mean January amplitudes (gpm) and corresponding phase angles of the first ridge line east of Greenwich (from 0 to 2π) for wavenumbers: one, (a) and (b), respectively; two, (c) and (d); three, (e) and (f); and the wave four amplitude, (g).

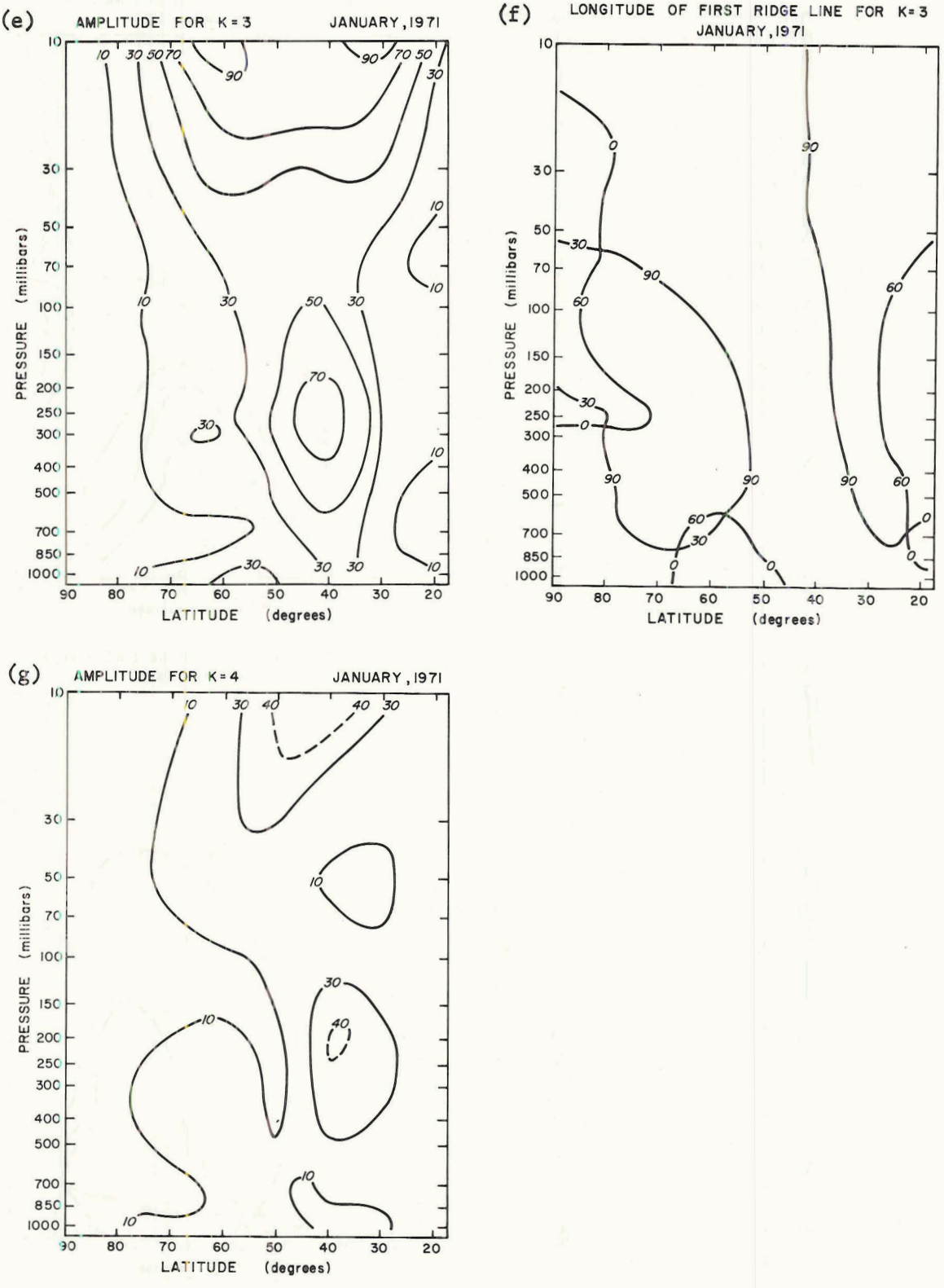

Figure 3.1 Continued.

which was preceded by an extremely strong asymmetric pattern of the circumpolar flow. Rocket measurements have shown that the jet core of the polar night westerlies exists in the lower mesosphere near 40°N (Murgatroyd, 1969), suggesting that this wave probably extends high into the stratosphere having a southerly tilt with height. The vertical tilt of the phase angles is determined in these diagrams by observing the change of the phase angle in the vertical at a given latitude. Another feature of these diagrams is the convergence of the phase angles at certain latitudes and levels which obviously must correspond to points where the amplitude of the wave is zero.

The secondary wave one amplitude maximum (Fig. 3.1a) near 35°N and 250 mb appears slightly to the north of the mean latitude of the subtropical westerly jet stream. At this latitude the phase angle of wave one (Fig. 3.1b) shifts quite markedly to the west with height. The ridge line at 35°N varies from 60°E longitude at 100 mb to 90°W (270°E) longitude at the 150 mb level. Since a westerly tilt of the long waves with height can produce an upward propagation of wave energy from the troposphere to the stratosphere (Hirota and Sato, 1969), it appears that wave one in the monthly mean may do likewise.

Returning to Figure 3.1b, we see that within the troposphere the tilt of the ridge lines with latitude reverses from a southwest to northeast tilt south of about 50°N latitude to a southeast to northwest tilt at higher tropospheric levels north of 50°N. The meridional tilt of the ridge lines is determined from these diagrams by observing the change of the phase angle with increasing latitude at a given pressure level. As mentioned previously (Eq. 3.7: Chap. 2) the consequences of these geometric orientations produce a meridional flux of relative westerly

momentum. The magnitude, sign and distribution of these fluxes are presented in Section 3.3.

The amplitude distribution for wavenumber two (Fig. 3.1c) in January resembles that of wavenumber one primarily because the region of maximum amplitude increases upward into the stratosphere. However, the latitude of this peak for wave two is about ten degrees south of the wave one peak, and the magnitude is only about half as large. There also appears to be a latitudinal shift of the wave two peak between the troposphere and the stratosphere, with respective peaks at 50°N and 60°N. Another interesting point relating distributions of the peak amplitudes of waves one and two is the apparent negative correlation with respect to latitude in the troposphere: i.e. the wave two maximum at 50°N and 250 mb is located at the corresponding minimum position for wave one. Wave one appears to dominate the polar stratosphere, polar troposphere, and subtropical troposphere, while wave two appears to predominate in the mid-latitude troposphere. Compared to the phase angle distribution of wave one, the phase angle of wave two in January (Fig. 3.2d) is fairly constant with height, in agreement with the findings of van Loon, et al. (1973) from long term monthly (January) means. However, there is a noticeable tilt of the ridge lines from southeast to northwest in the middle troposphere suggesting a southward flux of relative westerly momentum at most levels in the troposphere between about 40°N and 70°N. The positions of the troughs of this wave are just to the east of the Himalayas in Asia and just east of the North American continent at high latitudes. (It should remembered that the trough positions are shifted by one-half of the wavelength from the ridge positions depicted in these diagrams.)

The peak amplitude of wave three in January (Fig. 3.1e) is considerably smaller than that of waves one and two, especially in the stratosphere where, at high latitudes, more than 95% of the height variance can be accounted for by the first two harmonics (Table 3.1). Wave three in the middle stratosphere (around 10 mb) has a double-peaked distribution with maximums at about 60°N and 35°N. The tropospheric peak appearing at 40°N and 250 mb is just to the south of the peak for wave two, and to the north of the secondary peak for wave one. There is very little vertical variation of the phase angles (Fig.3.1f) with height except in the polar regions (north of 60°N) where there is an eastward vertical tilt in the lower stratosphere. However, the amplitude of wave three in this region is quite small. There also appears to be a southwest to northeast tilt of the ridges at most levels south of 45°N, and southeast to northwest tilt at higher latitudes.

The amplitude of wave four (Fig. 3.1g) in January is smaller still than wave three, with its peak shifted slightly further south of the peak amplitude for wave three. In fact, the percent of the total height variance due to wave four at its level and latitude of peak amplitude is less than four percent.

An account of the annual variation for 1971 can be obtained through a perusal of the amplitude and phase diagrams for January, April, July and October (Figs. 3.1 - 3.4). Some of the interesting features will be described here.

There is a drastic change in the mean amplitudes of the first two harmonics with the onset of spring (Fig. 3.2). By April, the polar night vortex has broken down, with the first two waves retaining only about 10% of their mid-winter intensities at 10 mb. However, while wave

two has decreased its amplitude in the troposphere, the first wave has increased in magnitude in the troposphere, where again, a double-peaked distribution exists. One peak, again located in the vicinity of the subtropical jet at 30-35°N and 200 mb, has approximately the same magnitude as it did for wave one in January. However, its center is located at a pressure level 50 mb higher, possibly in response to an expansion of the troposphere (or lifting of the tropopause) since the tropopause level possesses an annual variability (Palmén and Newton, 1969). The other peak for wave one, at 55°N and 300 mb, is at the latitude where wave one was a minimum and wave two a maximum in January. Again the peak amplitudes for wave one and wave two appear at different latitudes.

The phase angle distribution of the first harmonic in April (Fig. 3.2b) has considerably different characteristics than it did in January. The most obvious difference is the absence of any tilt in the vertical where the amplitude of wave one has any significant magnitude. Also, the two amplitude peaks in the troposphere mentioned previously possess ridges which are 180° out of phase with each other (i.e. a ridge appears in the western Pacific at low latitudes and a trough at mid-high latitudes). There is a substantial southeast to northwest (horizontal) tilt of the phase angles at mid-latitudes throughout the troposphere and lower stratosphere as can be verified by observing the change of the phase angle in Figure 3.2b between 40°N and 70°N at any pressure level.

Where the amplitude of wave two in April (Fig. 3.2c) is highest the phase angle (Fig. 3.2d) is not significantly different from the January values. The amplitudes of the third and fourth harmonics (Figs. 3.2e and g) in April have virtually the same intensities as they did in January. Furthermore, the latitudinal distribution of the peak amplitudes of the

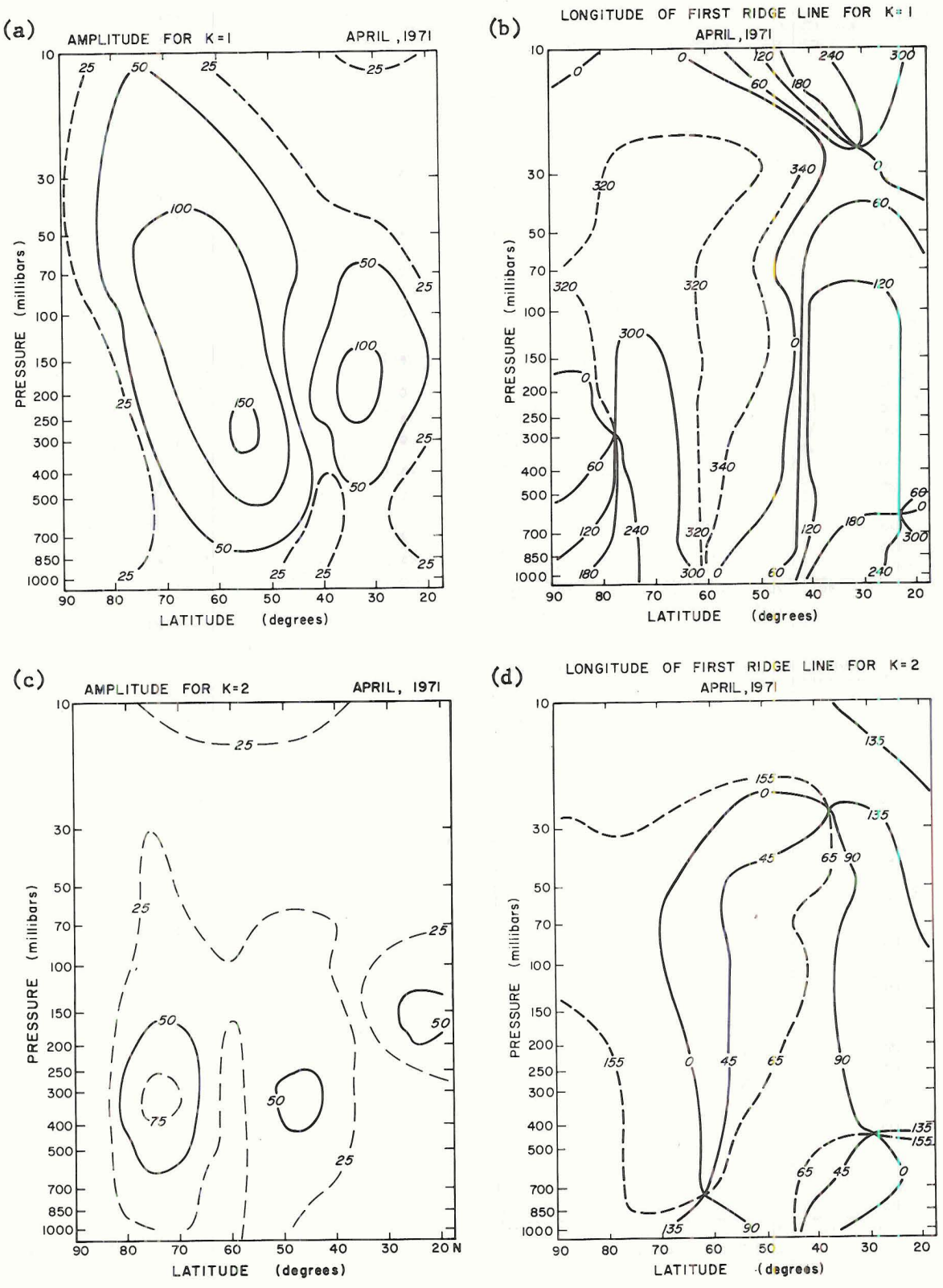

Figure 3.2 Same as Figure 3.1 except for April.

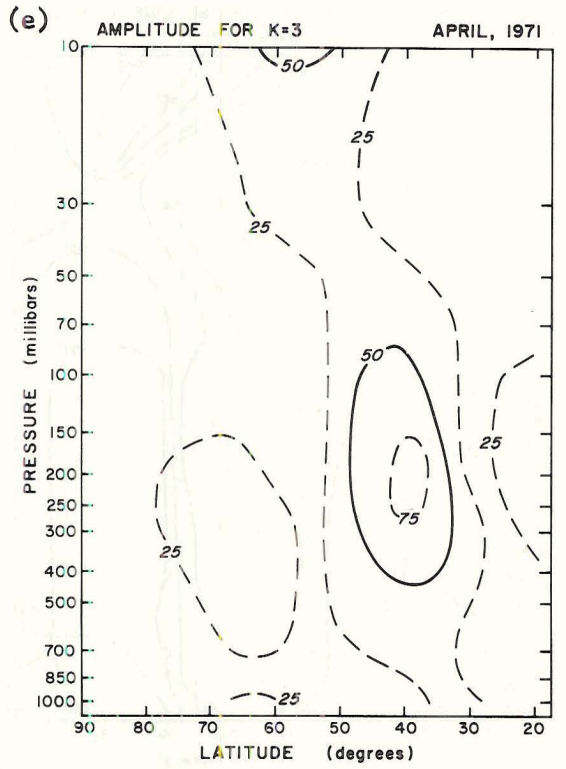

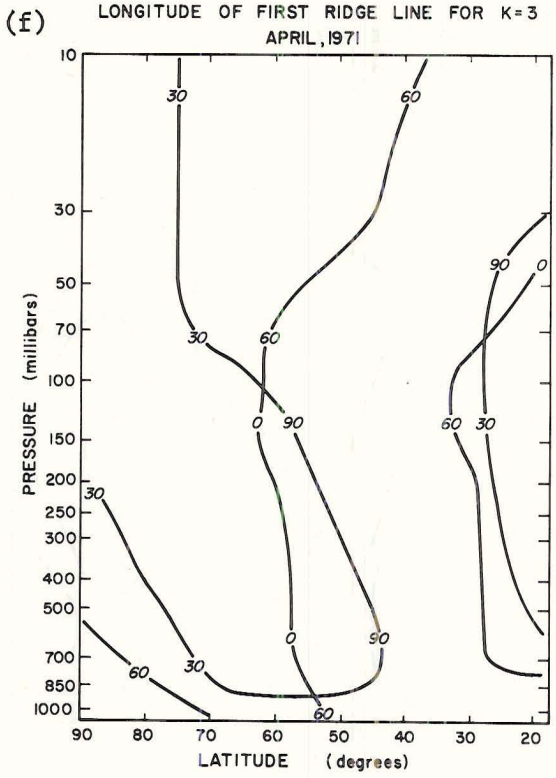

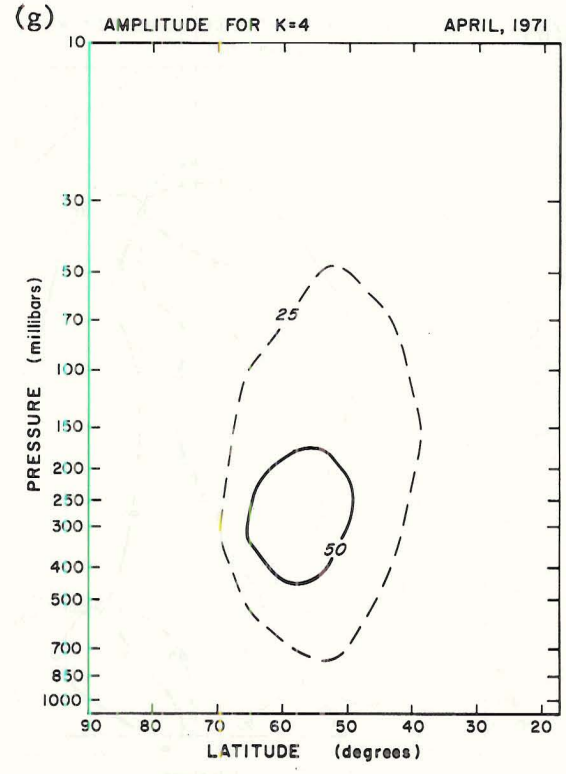

Figure 3.2 Continued.

first three waves in April is such that the domain of each harmonic amplitude peak is in a differnt latitude belt. Thus, relative maxima for wave one occur at 55°N and 30-35°N, wave two at 70-75°N, and wave three at 40°N.

An interesting feature of the long waves in July (Fig. 3.3) is that for wave one the ridge lines are in many cases displaced 180° from the January values. This is particularly true in regions where the amplitude is high. This variation from winter to summer would be expected in view of the seasonal reversal of the roles of the continents and oceans as large scale heat sources and sinks. van Loon, et al. (1973) and Eliassen (1958) also found a difference of phase between extreme seasons for wave one at the surface, but diminishing upward into the middle troposphere. They concluded that wave one was forced primarily by large scale heat sources and sinks near the surface, and by orographic features at higher levels in the troposphere. A similar conclusion was deduced by Van Mieghem et al. (1959 and 1961).

In July, the peak amplitudes of wave two (Fig. 3.3c), at 70°N and 35°N, occur at the same latitudes and levels as those of wave one. Waves three and four (Figs. 3.3e and 3.3g) have their peak July amplitudes further south, at 55-60°N and 30°N and are more nearly of the same magnitude as waves one and two at all levels than they were in January. It is interesting to note that the first four waves in July possess double-peaked distributions, with the southerly maxima in the vicinity of 35°N.

After the fall equinox, the polar stratosphere gradually loses its source of heat and begins to cool. At the same time, the low latitude stratosphere is still being heated by solar radiation producing a strong

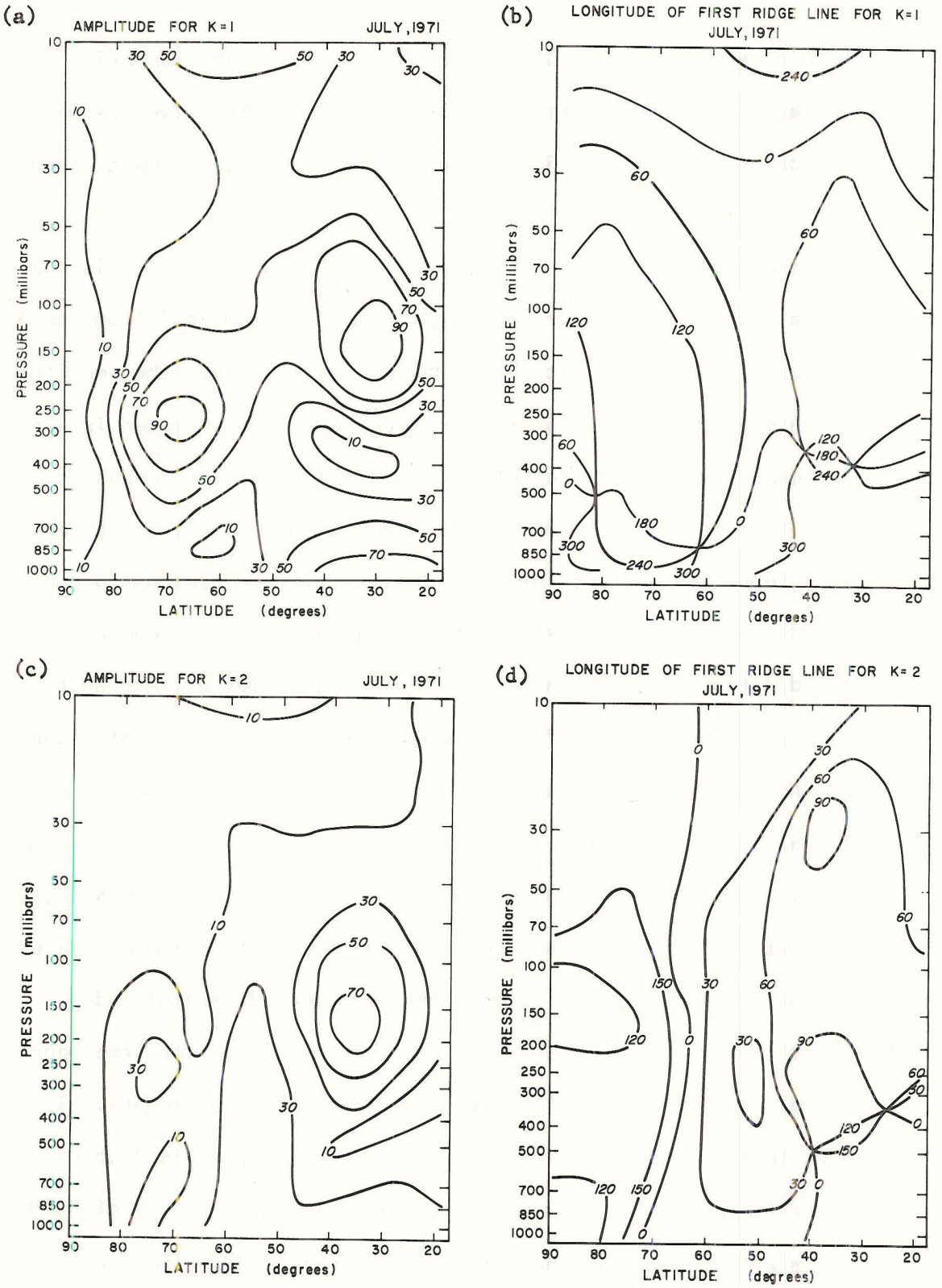

Figure 3.3 Same as Figure 3.1 except for July.

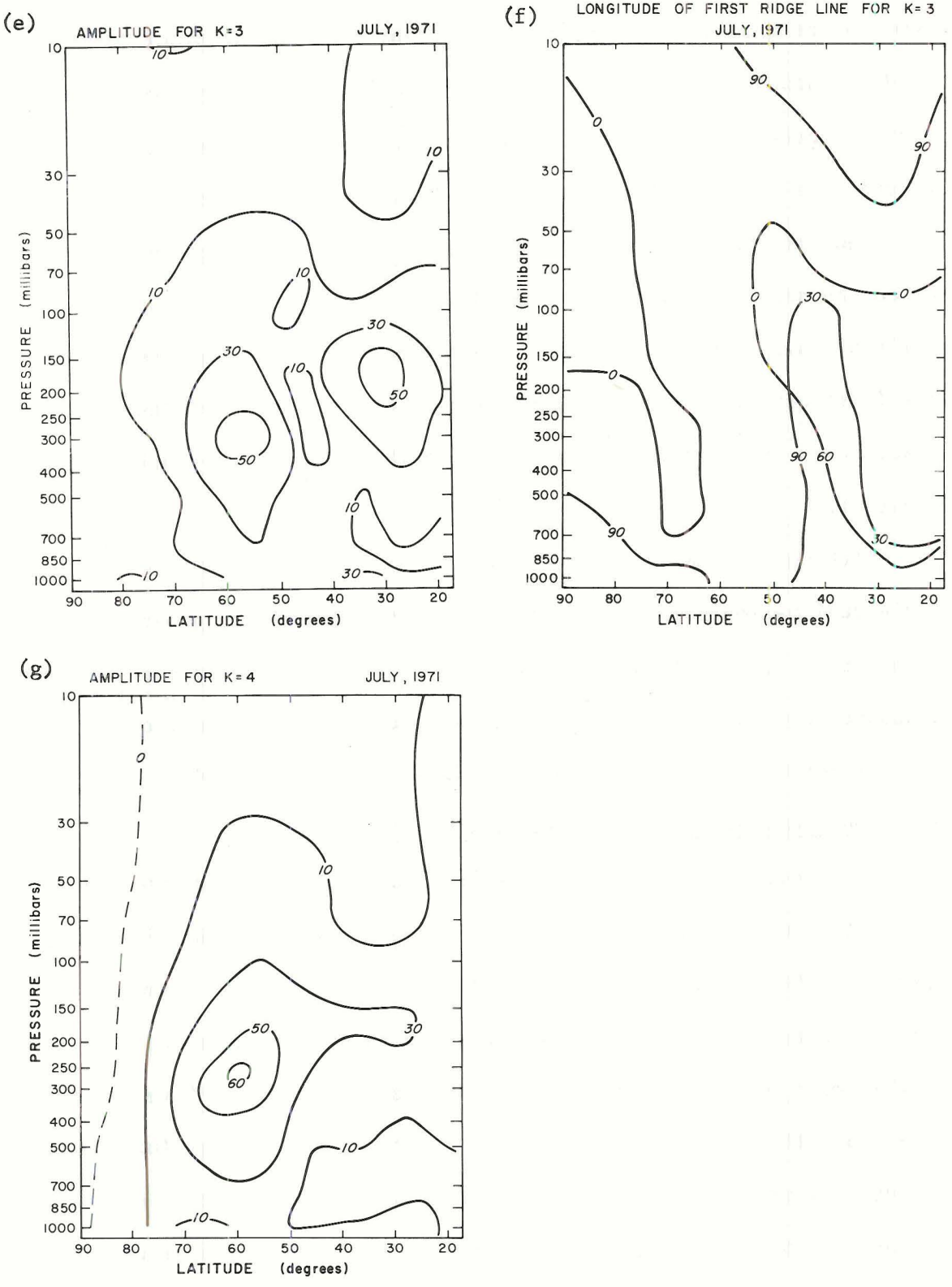

Figure 3.3 Continued.

temperature gradient near 65°N. Consequently the polar night westerlies suddenly appear and begin to amplify in October. This phenomenon consistently appears on monthly mean charts and is often asymmetric with respect to the pole and elliptical in shape. This corresponds to an increase in amplitude of the first two harmonic waves in the stratosphere in October, as can be seen in Figures 3.4a and 3.4c. Simultaneously, a southerly shift of waves one through four is detected in the troposphere. Again, the first wave shifts to the west with height in mid-latitudes (Fig. 3.4b), with the vertical distribution of the other waves remaining fairly constant.

Although the amplitudes give valuable information regarding the individual harmonic waves, a better understanding of the general circulation necessitates a look at the parameters with more dynamic significance discussed previously, namely, the zonal and meridional kinetic energies and the meridional transport of relative westerly momentum.

3.2 Zonal and Meridional Kinetic Energy Spectra.

As discussed in Chapter 2, the zonal and meridional components of the monthly mean kinetic energy spectra are computed in two different ways: the "single-barred" mean quantities from the daily harmonic coefficients; and the "double-barred" mean quantities computed from the monthly mean harmonic coefficients. The derived energies have the units m^2/s^2, and therefore are proportional to the kinetic energy for a given air density or kinetic energy per unit mass. In this section we shall discuss the percentages of individual wave number energies as part of the total spectrum (assumed as the sum of the spectral energies for wave number one through twelve) for given latitudes and levels in January, and subsequently make comparisons to analogous calculations in July.

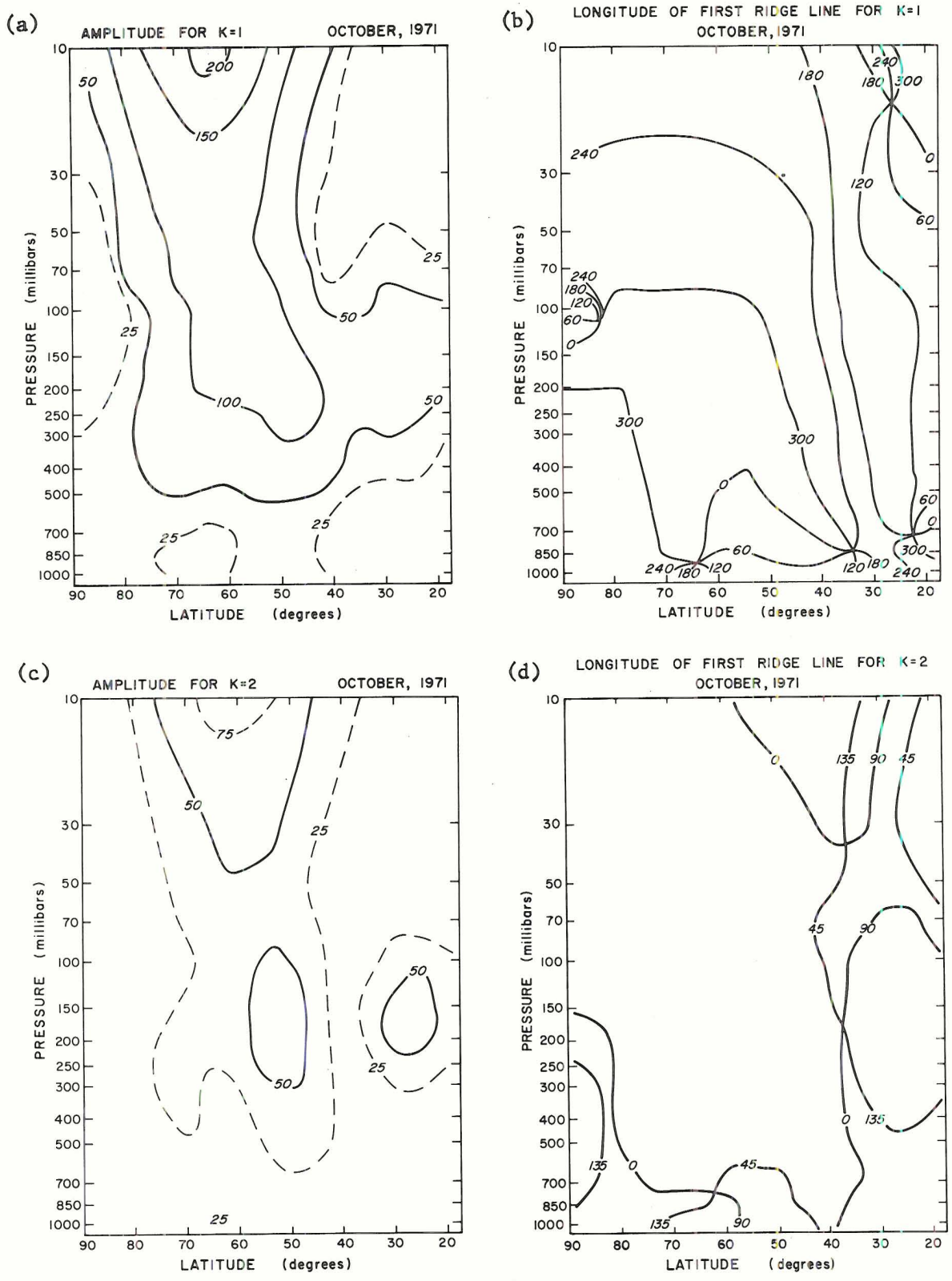

Figure 3.4 Same as Figure 3.1 except for October.

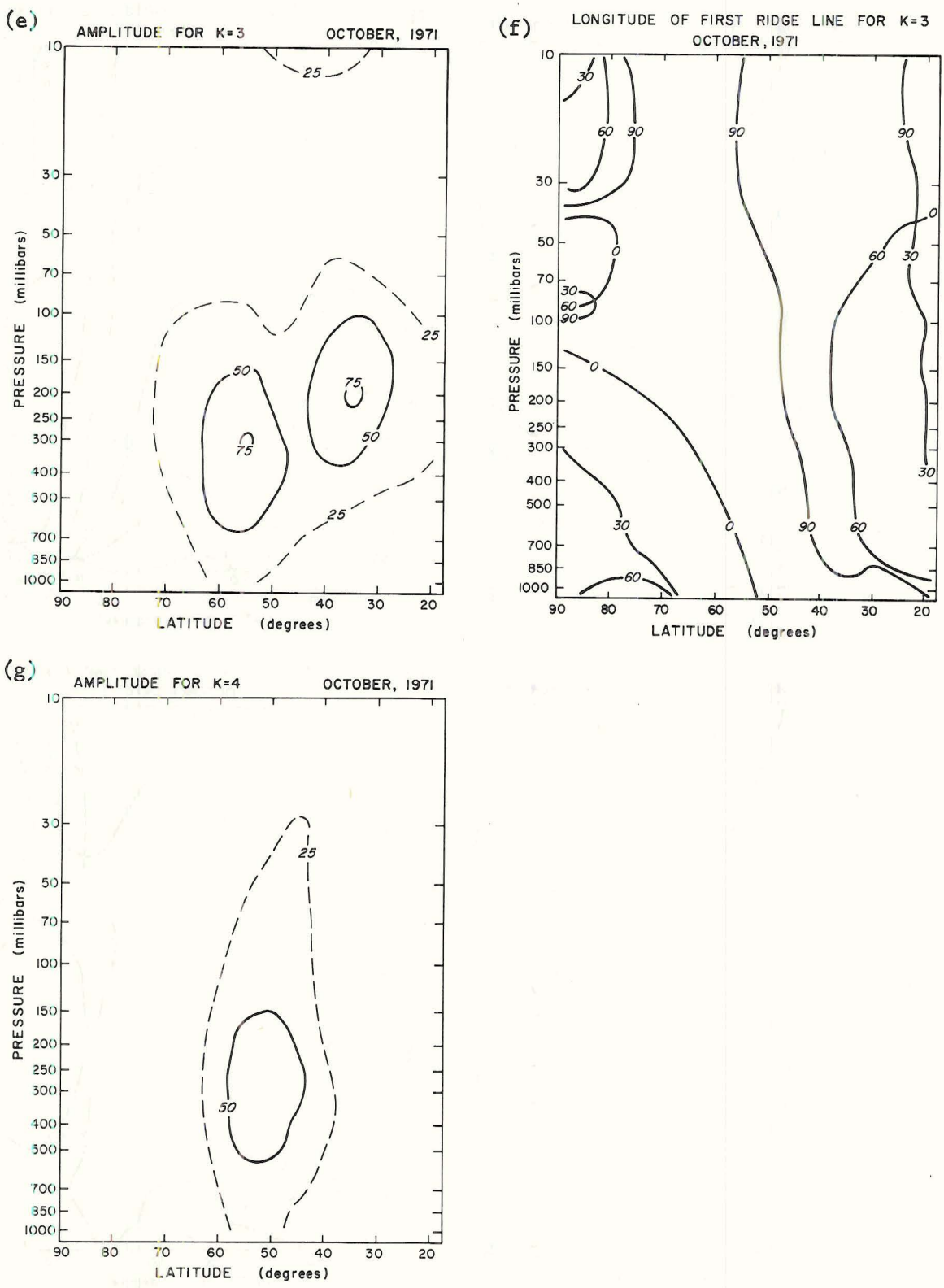

Figure 3.4 Continued.

Then, the annual distribution of individual wave number energies and their vertical structures will be analyzed.

The percentages are a measure of the relative importance of each of the first twelve waves. Only some of the statistics from the single-barred energies will be presented here however, since the single-barred means best represent the total (standing plus transient) contribution of each harmonic. Since the total energy spectrum is calculated from the first twelve wave numbers, it excludes the kinetic energy of the mean zonal current (k=0) which, in general, is considerably greater than the other spectral terms, particularly in the vicinity of the major jet streams.

In Table 3.3 the spectral percentages of zonal, meridional, and total (zonal plus meridional) kinetic energy are presented for each of the first twelve wave numbers at 500 mb and 50 mb at selected latitudes for January and July. This table shows again the predominance of the long waves at high levels and latitudes, particularly for the zonal kinetic energy. In the troposphere at sub-polar latitudes the meridional kinetic energy spectrum generally has peak values in the wave number range from four to seven in both January and July, while the zonal kinetic energy spectrum is still dominated by the first three waves. In July there is a noticeable shift towards higher wave numbers for both the zonal and meridional kinetic energies. Also at 22.5°N the shorter waves (k=8 through 12) contain an appreciable part of the total meridional kinetic energy spectrum. In January these five waves account for 36.8 and 29.4 percent of the meridional kinetic energy at 500 mb and 50 mb, respectively. The corresponding values for the double-barred meridional kinetic energies, (not shown) are 22.9 and 7.4 percent,

Table 3.3. Spectral percentage of zonal, meridional, and total (zonal) plus meridional) kinetic energies to the assumed total of the respective quantities (meaning the sum of waves one through twelve) at 500 mb for (a) January and (b) July single-barred monthly means.

(a) January: 500 mb

	Wave	Zonal	Meridional	Total
22.5N				
	1	44.72	2.48	32.59
	2	8.20	3.52	6.85
	3	12.83	4.28	10.37
	4	5.63	10.78	7.11
	5	8.25	12.40	9.44
	6	7.76	16.10	10.15
	7	3.22	13.66	6.22
	8	3.89	13.39	6.62
	9	1.74	6.67	3.16
	10	1.51	7.66	3.28
	11	1.25	4.28	2.12
	12	1.00	4.78	2.09
42.5N				
	1	30.56	.65	17.56
	2	25.63	9.59	18.66
	3	15.03	7.41	11.72
	4	8.73	9.31	8.98
	5	5.80	16.11	10.28
	6	5.60	20.23	11.96
	7	2.82	8.89	5.46
	8	2.21	8.73	5.04
	9	1.22	5.88	3.25
	10	.83	4.00	2.21
	11	.94	6.31	3.27
	12	.64	2.88	1.61
62.5N				
	1	33.93	3.70	17.06
	2	18.28	24.80	21.92
	3	15.98	10.43	12.88
	4	11.19	17.21	14.55
	5	9.83	14.36	12.36
	6	5.30	11.09	8.53
	7	2.40	6.84	4.88
	8	1.32	3.70	2.65
	9	.77	3.44	2.26
	10	.46	1.90	1.27
	11	.34	1.66	1.08
	12	.19	.87	.57

50 mb

Wave	Zonal	Meridional	Total
1	22.41	1.16	15.51
2	23.06	9.06	18.52
3	26.36	10.61	21.24
4	9.93	16.20	11.97
5	4.27	10.61	6.33
6	3.20	13.98	6.70
7	2.23	8.97	4.42
8	2.27	6.75	3.73
9	1.44	6.75	3.16
10	2.18	5.11	3.13
11	1.76	5.50	2.98
12	.88	5.30	2.32
1	41.79	6.81	32.07
2	44.01	30.43	40.23
3	7.63	22.15	11.67
4	2.74	9.38	4.58
5	1.39	15.27	5.25
6	.98	7.49	2.79
7	.48	3.21	1.24
8	.41	1.68	.76
9	.23	1.57	.61
10	.15	.93	.37
11	.12	.50	.23
12	.07	.57	.21
1	81.72	20.79	41.60
2	7.94	62.45	43.83
3	5.39	7.50	6.78
4	2.14	5.32	4.23
5	1.58	1.80	1.72
6	.66	1.26	1.06
7	.23	.38	.33
8	.15	.18	.17
9	.08	.14	.12
10	.05	.07	.06
11	.04	.06	.05
12	.03	.05	.04

Table 3.3 (continued)

(a) January:

	500 mb			50 mb			
	Wave	Zonal	Meridional	Total	Wave	Zonal	Meridional	Total
82.5N								
	1	42.32	31.66	35.65	1	77.08	77.43	77.28
	2	46.54	51.95	49.93	2	22.29	21.58	21.87
	3	7.88	10.66	9.62	3	.48	.63	.57
	4	2.74	4.44	3.80	4	.13	.27	.21
	5	.37	.79	.64	5	.02	.05	.04
	6	.11	.31	.24	6	.01	.03	.02
	7	.04	.07	.06	7	.00	.01	.01
	8	.00	.02	.01	8	.00	.00	.00
	9	.00	.02	.01	9	.00	.00	.00
	10	.00	.02	.01	10	.00	.00	.00
	11	.00	.02	.01	11	.00	.00	.00
	12	.00	.02	.01	12	.00	.00	.00

(b) July:

	500 mb			50 mb			
	Wave	Zonal	Meridional	Total	Wave	Zonal	Meridional	Total
22.5N								
	1	11.94	2.74	8.50	1	51.97	2.65	39.38
	2	10.06	6.45	8.71	2	10.41	2.95	8.51
	3	23.71	9.88	18.75	3	5.81	3.98	5.35
	4	9.40	6.86	8.45	4	9.56	11.21	9.98
	5	6.46	5.62	6.15	5	4.65	7.67	5.42
	6	8.91	5.76	7.74	6	4.40	7.52	5.20
	7	5.64	16.32	9.63	7	2.33	10.03	4.29
	8	4.25	7.27	5.38	8	5.11	12.68	7.04
	9	6.38	12.35	8.61	9	1.67	15.63	5.23
	10	4.91	7.00	5.69	10	1.82	8.26	3.46
	11	4.99	7.82	6.05	11	1.16	7.37	2.75
	12	3.35	11.93	6.56	12	1.11	10.03	3.39
42.5N								
	1	14.06	.80	8.85	1	34.20	8.60	24.16
	2	27.30	.84	16.89	2	30.38	8.60	21.84
	3	11.55	2.14	7.85	3	9.38	7.80	8.76
	4	19.16	5.90	13.94	4	8.85	12.10	10.13
	5	7.03	19.88	12.09	5	4.51	11.29	7.17
	6	6.66	14.13	9.60	6	3.82	15.05	8.23
	7	4.89	14.75	8.77	7	2.08	13.98	6.75
	8	3.43	11.41	6.57	8	2.08	6.45	3.80
	9	2.01	15.09	7.16	9	1.39	4.03	2.43
	10	1.52	6.40	3.44	10	1.56	4.30	2.64
	11	1.47	5.25	2.95	11	.87	4.30	2.22
	12	.92	3.41	1.90	12	.87	3.49	1.90

Table 3.3 (continued)

(b) July:

	500 mb			50 mb			
	Wave	Zonal	Meridional	Total	Wave	Zonal	Meridional	Total
62.5N								
	1	27.85	1.31	13.44	1	54.24	9.59	26.53
	2	26.14	9.10	16.89	2	25.85	34.97	31.51
	3	10.04	12.69	11.48	3	5.93	19.43	14.31
	4	15.05	26.65	21.35	4	6.78	22.80	16.72
	5	7.46	11.17	9.47	5	2.97	4.40	3.86
	6	5.75	12.53	9.43	6	1.69	3.89	3.05
	7	2.74	7.51	5.33	7	.85	1.81	1.45
	8	1.80	9.16	5.80	8	.85	1.55	1.29
	9	1.74	3.30	2.59	9	.42	.52	.48
	10	.78	3.48	2.24	10	.42	.52	.48
	11	.37	1.31	.88	11	.00	.26	.16
	12	.28	1.80	1.11	12	.00	.26	.16
82.5N								
	1	49.59	37.02	41.61	1	62.90	61.03	61.76
	2	33.85	36.85	35.75	2	30.65	28.21	29.15
	3	10.86	15.17	13.60	3	4.84	6.67	5.96
	4	4.66	8.29	6.96	4	.81	2.05	1.57
	5	.81	1.87	1.48	5	.81	1.54	1.25
	6	.22	.55	.43	6	.00	.51	.31
	7	.00	.08	.05	7	.00	.00	.00
	8	.00	.04	.03	8	.00	.00	.00
	9	.00	.00	.00	9	.00	.00	.00
	10	.00	.04	.03	10	.00	.00	.00
	11	.00	.04	.03	11	.00	.00	.00
	12	.00	.04	.03	12	.00	.00	.00

respectively. From these data it can be concluded that the transient part of the shorter waves produces more of the meridional kinetic energy than the standing part at 22.5°. This result will be expounded upon later in this section.

Figures 3.5 - 3.8 depict the meridional cross sections of the January double- and single-barred zonal and meridional kinetic energies for wavenumbers one and two, the sum of waves one through four, and the sum of waves one through twelve. These figures, along with some others that will be presented later, are plotted using the smoothed version of an NCAR subroutine called CONREC (see Adams, et al., 1975), which was modified slightly to transform the vertical (pressure) coordinate. This contour package sometimes produces spurious results, like crossing isopleths, and discontinuities. Naturally, the reader should overlook these obvious discrepancies. The coordinates used in these figures are latitude (abscissa) decreasing to the right from 82.5°N to 22.5°N and pressure (ordinate) decreasing upward from 1000 mb to 10 mb. The contour interval is 10 m^2/s^2. Points of relative maxima and minima are denoted by H and L, respectively.

By examining Figure 3.5 it becomes immediately apparent that diagrams b and d (single-barred energies) have considerably higher magnitudes than diagrams a and c (double-barred energies). The top two diagrams (a and b) depict the wave one zonal kinetic energy, and the bottom two diagrams (c and d) depict the wave one meridional kinetic energy. The difference between the diagrams on the right and the left gives the magnitude of the kinetic energy of the transient waves, while the diagrams on the left give the stationary wave contribution to the kinetic energy. The distributions of the two types of means are very

similar with maximums and minimums corresponding quite well. The largest relative differences for the wave one zonal kinetic energy (b minus a in Fig. 3.5) occur in the troposphere north of the mean subtropical jet stream near 40-45°N. In this region the transient and stationary components of the wave one zonal kinetic energy appear to be nearly equal in magnitude. In most other regions, the transient contribution of wave one to the total zonal kinetic energy of wave one is roughly half as large as the stationary contribution.

Other interesting features of the wave one zonal kinetic energy distribution in January are the maximum values in the stratosphere near 50°N and the minimum values throughout the atmosphere near 70°N in Figures 3.5a and 3.5b.

The wave one meridional kinetic energy (Fig. 3.5c: double-barred; and Fig. 3.5d: single-barred) shows a pronounced increase with height and latitude. From Equation 3.4 (Chapter 2), the spectral meridional kinetic energy is proportional to the amplitude squared over sin 2ϕ squared. The factor $1/\sin^2 2\phi$ varies from 3 at 22.5°N down to 1 at 45°N and then up to 14.9 at 82.5°N. This increase from 45° to the pole along with the high amplitude of wave one in the polar stratosphere is responsible for the meridional kinetic energy distribution of Figures 3.5c and 3.5d. The difference between theses two diagrams shows that the relative importance of the transient part of wave one in determining the meridional kinetic energy is less than what is observed for the zonal component and decreases with elevation.

In Figure 3.6 the January wave two kinetic energies are shown, revealing a considerably different picture from the wave one distributions. The peak zonal energy of wave two (Fig.3.6b) appears centered

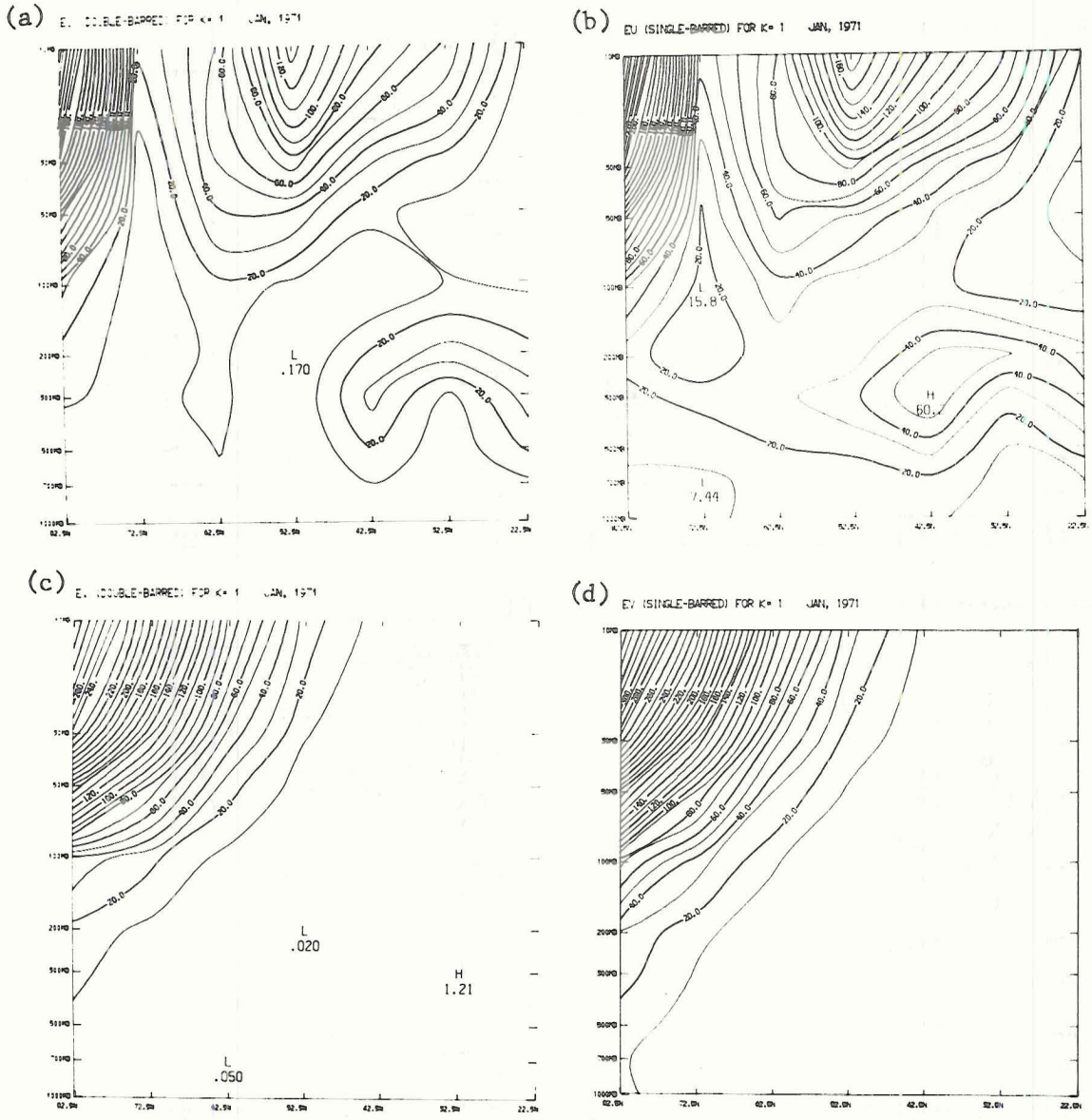

Figure 3.5 Pressure/latitude distribution of the January wave one: (a) double-barred zonal kinetic energy; (b) single-barred zonal kinetic energy; (c) double-barred meridional kinetic energy; and (d) single-barred meridional kinetic energy. Isopleths are at increments of 10 m^2/s^2.

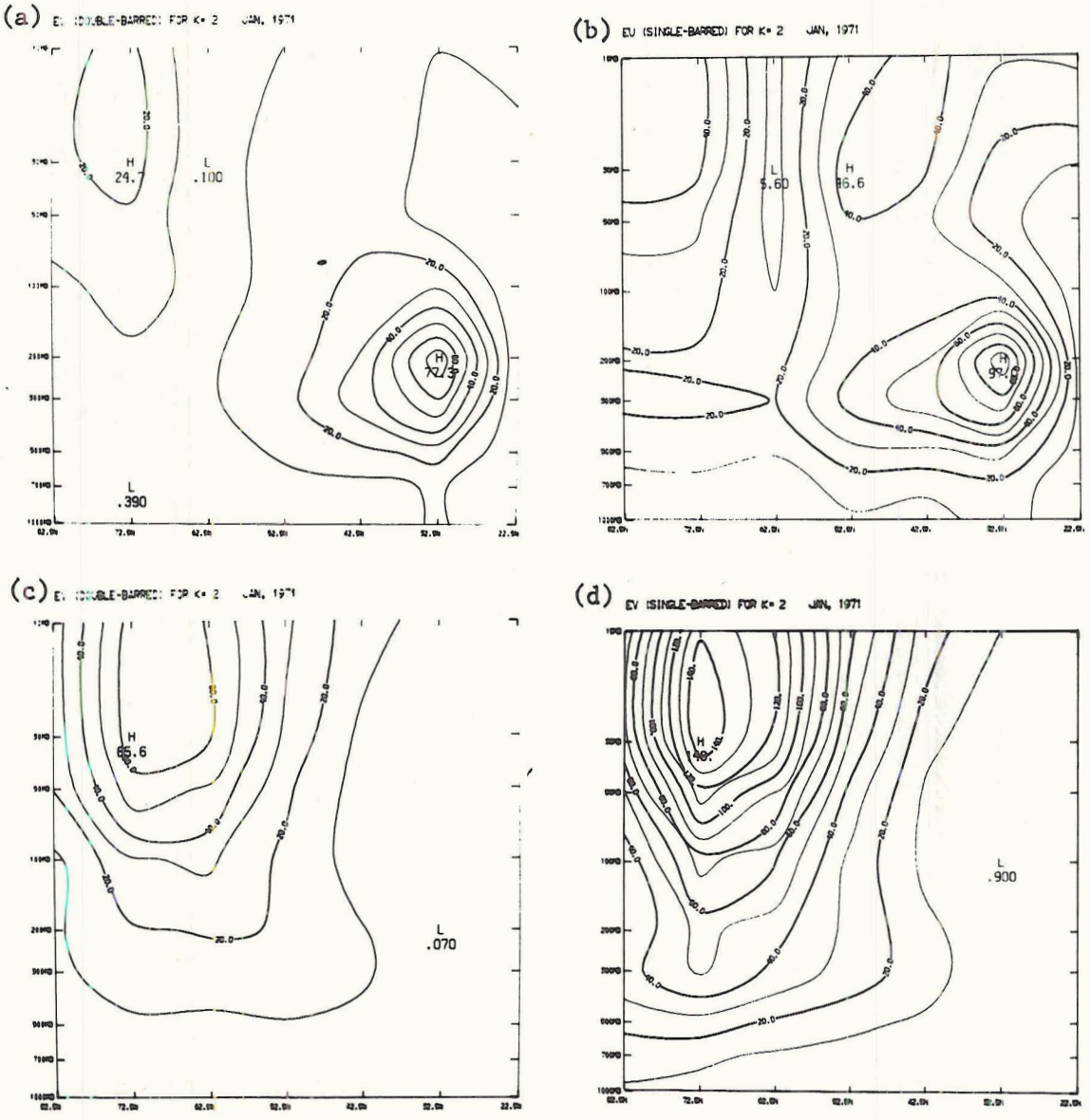

Figure 3.6 Same as Figure 3.5 except for wavenumber two.

on the subtropical jet stream, while the peak meridional energy (Fig. 3.6d) is located in the vicinity of the polar night jet stream. The transient part of the total wave two zonal kinetic energy is fairly constant throughout the atmosphere with a magnitude of roughly 20 m^2/s^2 except at 60°N where a minimum occurs, near 45°N in the stratosphere where a maximum occurs, and very close to the surface. On the other hand, the transient part of the total wave two meridional kinetic energy is at least twice as large as the stationary part at all latitudes and levels.

Figures 3.7 and 3.8 show the zonal and meridional kinetic energy distributions, respectively, for both types of means summed over wavenumbers one through four and one through twelve. The predominance of waves one and two (Figs. 3.5 and 3.6) shows up remarkably well, particularly in the stratosphere. The largest differences between the first four waves and first twelve waves appear (by an analysis of Fig. 3.6) to be due to the meridional kinetic energy of the shorter transient waves throughout most of the troposphere. This is best seen from Figure 3.8 by a graphical subtraction of b from d resulting in the meridional kinetic energy of the short waves (wave numbers five through twelve). The meridional kinetic energy of the short transient waves can be obtained by graphical subtraction of the meridional kinetic energy of the short stationary waves (c minus d) from the former quantity (d minus b). The result is

$$\sum_{k=5}^{12} \overline{e_k}^{v} - \sum_{k=5}^{12} \overline{e_k}^{v} .$$

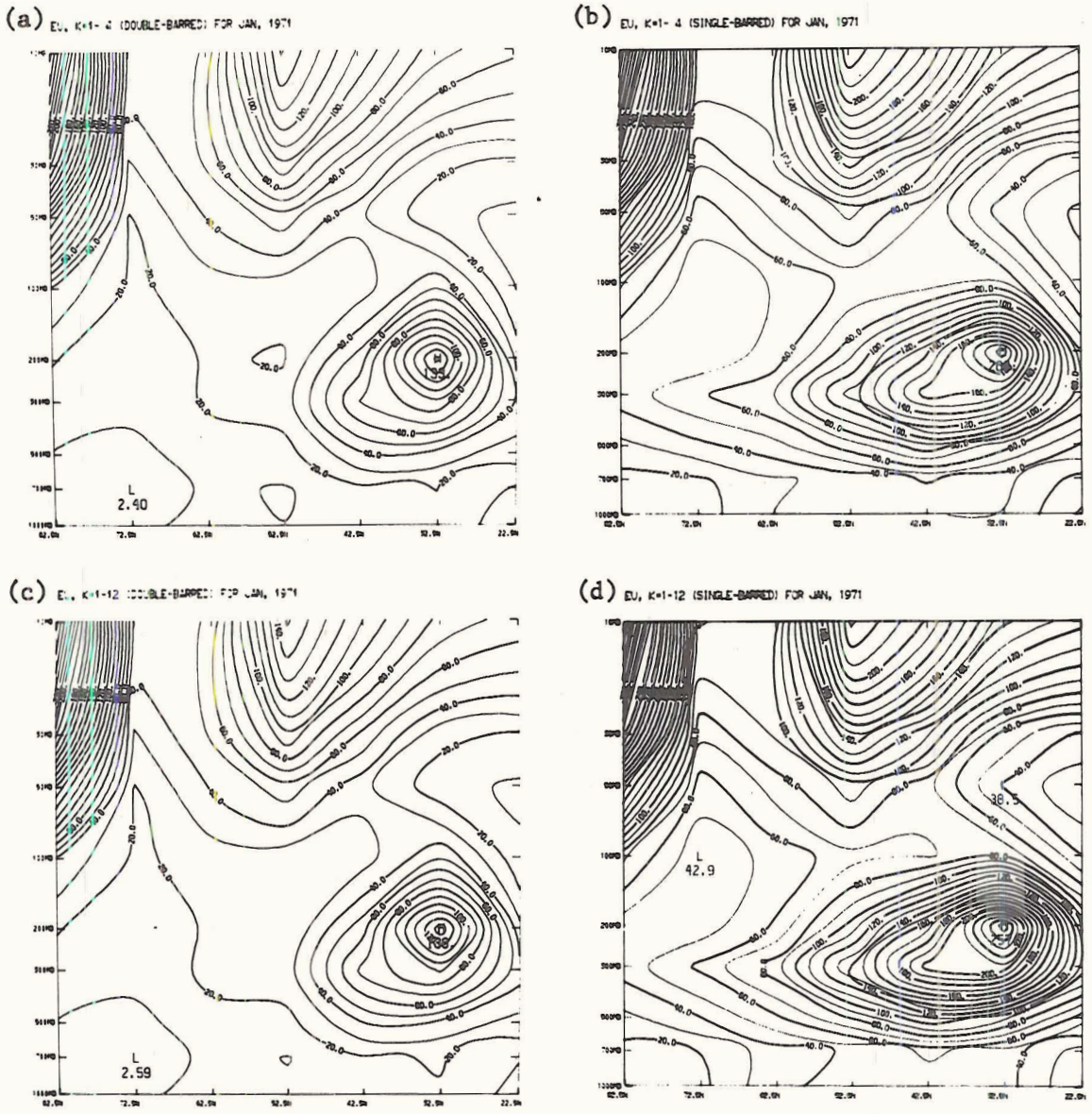

Figure 3.7 Sum of January (a) double-barred zonal kinetic energy by waves one through four, (b) single-barred zonal kinetic energy by waves one through four, (c) double-barred zonal kinetic energy by waves one through twelve, and (d) single-barred zonal kinetic energy by waves one through twelve. Isopleths are at increments of 10 m^2/s^2.

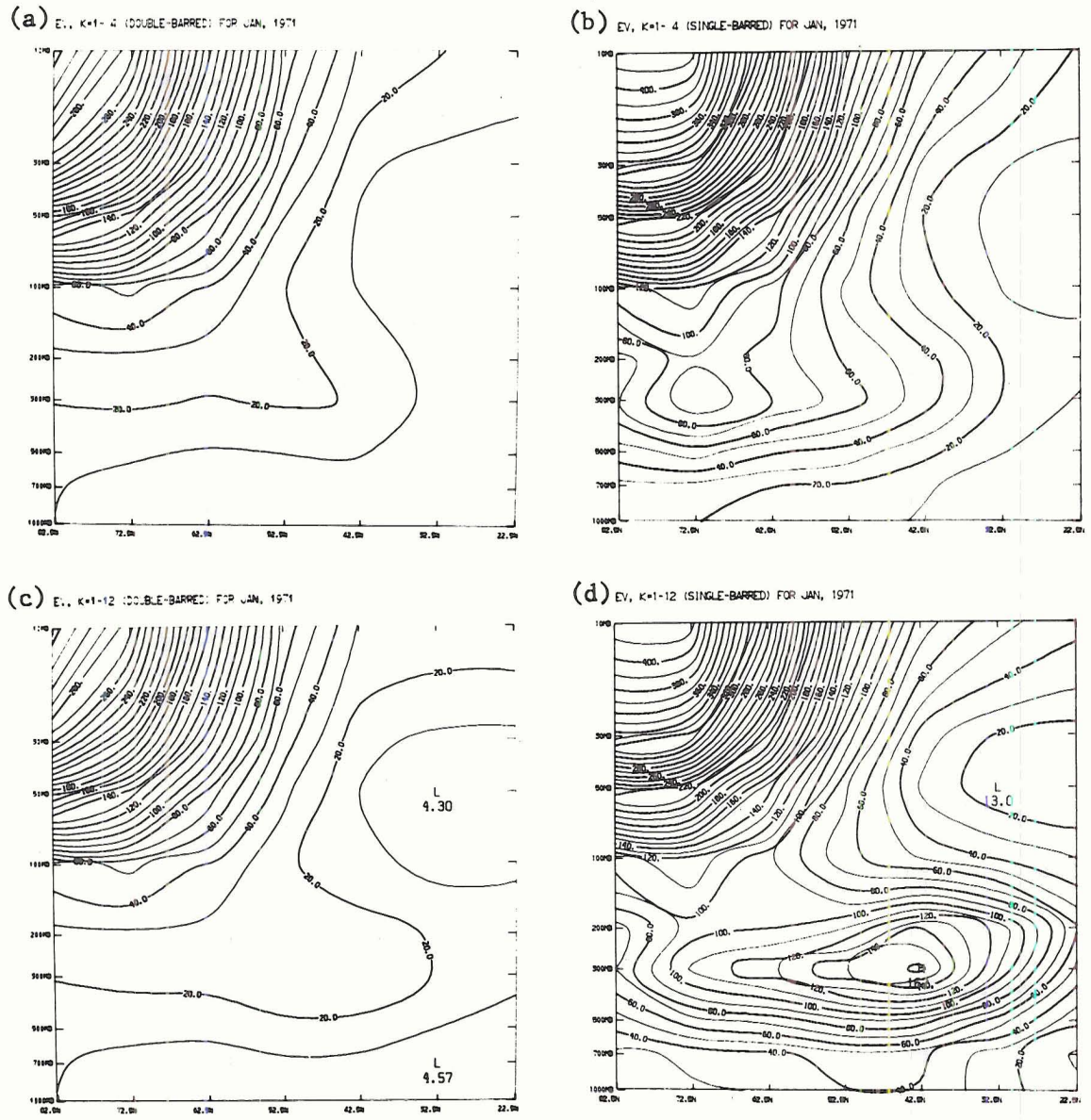

Figure 3.8 Same as Figure 3.7 except for meridional kinetic energy.

The transient waves of all lengths (Fig. 3.8: d minus c) appear responsible for the major part of the tropospheric meridional kinetic energy with the long waves (1-4) predominating in polar latitudes (north of about 65°N) and the shorter waves (5-12) elsewhere. The meridional and zonal kinetic energy contributions by the short standing waves are negligible throughout the atmosphere; and while the zonal energy contribution by the short transient waves (from analysis of Fig. 3.7) is small, what there is appears most concentrated in the vicinity of the subtropical jet stream.

In the summer, the large scale perturbations of the atmospheric circulation have subsided considerably, and the atmosphere's kinetic energy is correspondingly smaller. For this reason, only the sum of waves one through four and one through twelve of the July kinetic energy components will be presented here.

From Figure 3.9 the transient waves (d minus c) are responsible for most of the zonal kinetic energy in July with the long transient waves (b minus a) accounting for roughly half of the total zonal kinetic energy excluding that of the mean zonal current (k=0). Also, the stratosphere contains very little eddy kinetic energy. However, during July a strong easterly zonal flow existed in high levels of the stratosphere, particularly at lower latitudes. During July the mean kinetic erergy per unit mass for this zonal flow at 10 mb and 22.5°N amounted to 277 m^2/s^2.

Again in July, the meridional kinetic energy in the troposphere (Fig. 3.10) is produced mainly by the transient shorter waves at lower latitudes and by the transient long waves at polar latitudes.

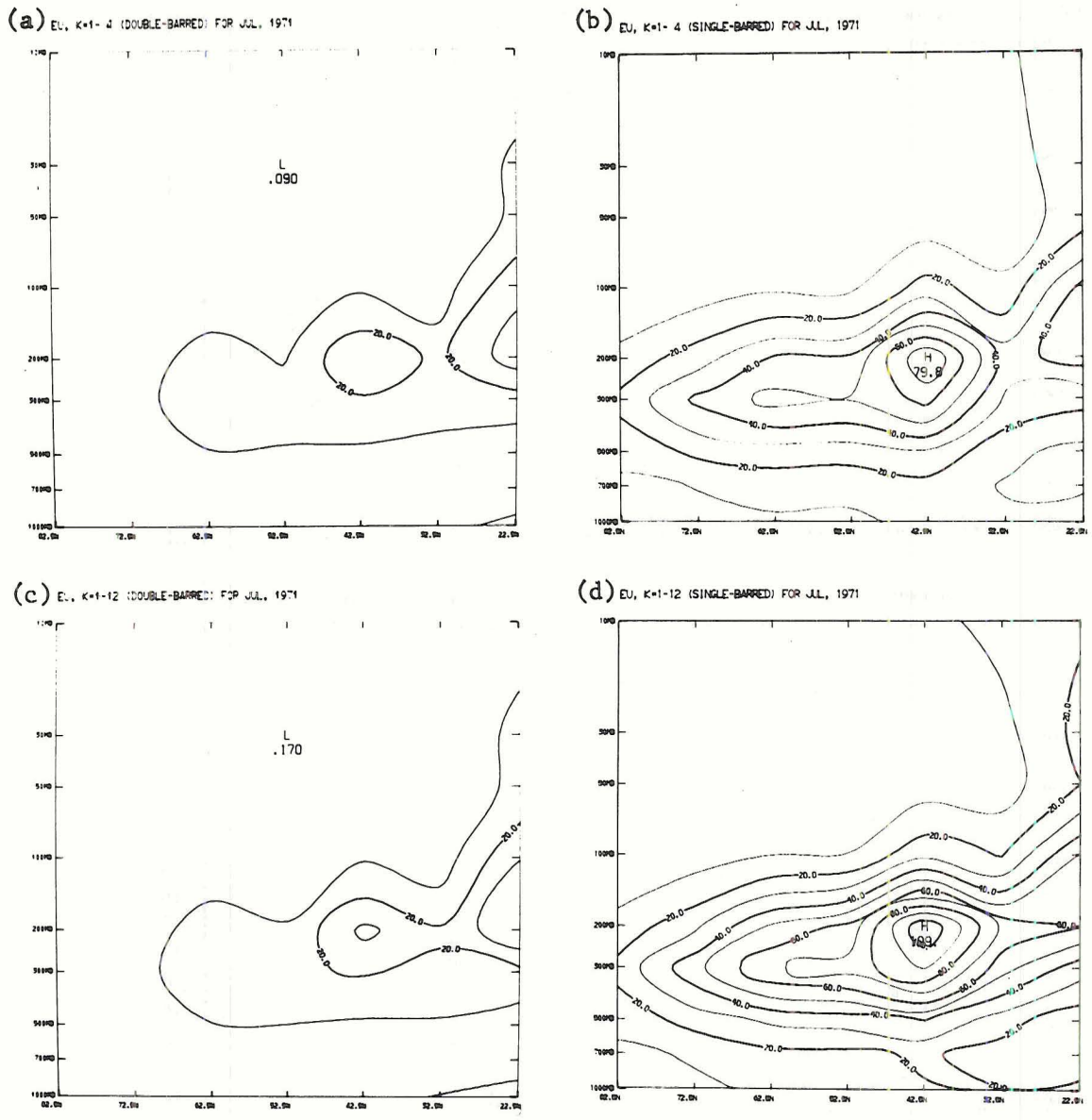

Figure 3.9 Same as Figure 3.7 except for July.

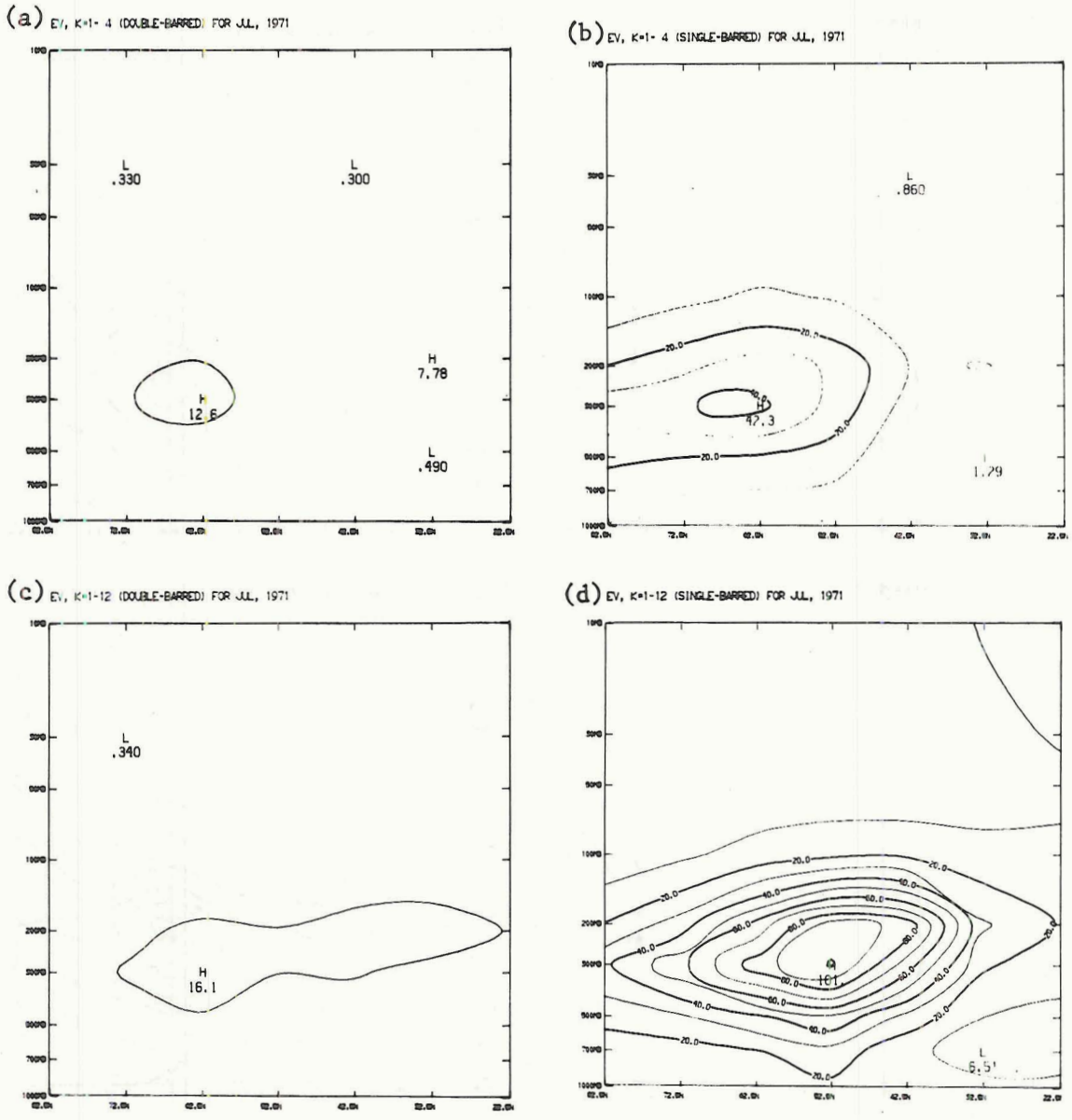

Figure 3.10 Same as Figure 3.7 except for the July meridional kinetic energy.

Van Mieghem, et al (1959, 1960) also computed zonal and meridional kinetic energy spectra from monthly normal geostrophic winds at the 500 mb level. They analyzed the first three waves for each of the twelve months and at each fifth degree of latitude from 20°N to 70°N. Their data is in the form of kinetic energy in a zonal ring of one centibar thickness and one meter of meridional width, so that the cosine of the latitude times the energies presented here are proportional to their values. Since cosϕ varies from .91 at 25°N to .42 at 65°N (the range of their diagrams) a comparison can be made allowing for the shrinking of the latitude circles. Their results show many similarities with the monthly mean spectral distributions for the year 1971 (not shown). For example, the maxima appear to be well defined, with the largest maxima occurring in mid-latitudes in the winter for all three waves. The minima are not very well defined, existing primarily in broad latitude bands throughout the warmer months. To a strong maximum of spectral zonal kinetic energy there oftentimes corresponds a strong maximum of spectral meridional kinetic energy generally from 10-15° of latitude further poleward.

Sato (1974) computed kinetic energy densities for an analysis of the vertical structure of planetary scale waves. This was also done here by multiplying the computed spectral energies by the standard air densities (from the U.S. Standard Atmosphere Supplements, 1966). This gives us a measure of energy per unit volume and compensates for the decrease of air density with height. Sato often observed a node-like structure or relative minimum of wave one kinetic energy density near 100 mb and 60°N during the winter months. He ascribes this phenomenon to interferences of vertically propagating waves and the existence of

a critical level through which the wave does not propagate (high velocity stratospheric zonal winds). As in his study maximum wave energies per unit volume in 1971 appear at the 300 mb level with generally decreasing values in the stratosphere. In January, at 72.5°N a node-like structure does appear near the 100 mb level for the wave one zonal plus meridional kinetic energy densities (not shown). However, it does not occur at any of the other latitudes or for any of the other waves analyzed in this study.

3.3 Transport of Relative Westerly Momentum.

Most of the theories of the maintenance of the general circulation of the atmosphere are founded on the principle of meridional and vertical exchange of absolute angular momentum. Most of the total meridional transport of this quantity is a transport of relative angular momentum, the rest is a transport of earth-angular momentum (Lorenz, 1967). The vertical transport of momentum seems to be dominated by the flux of earth angular momentum (Palmén and Newton, 1969), and while the vertical flux of relative westerly momentum is smaller than this, it has been found that in winter the mean meridional circulation produces a vertical flux of relative westerly momentum which is an order of magnitude larger than that by the monthly mean eddies (Oort and Rasmusson, 1971). Furthermore, Srivatsangam (1976) has developed a technique using harmonic analysis to compute vertical fluxes of relative westerly momentum by the individual waves. However, the vertical exchange by smaller scales of motion cannot be adequately studied through the use of zonal harmonic analysis.

In this section, the meridional flux of relative westerly momentum by horizontal atmospheric wave motions will be presented, keeping in

mind that the computational procedures used here automatically eliminate the momentum transport by the direct meridional cells since they are entirely non-geostrophic (Lorenz, 1967).

The meridional flux of relative westerly momentum can best be determined by computing the single-barred monthly means. With this approach the contributions to the momentum flux by transient and standing atmospheric disturbances are retained. The distribution of the spectral fluxes, then, can be easily separated into their transient and stationary components.

Following Oort and Rasmusson (1971), the total meridional flux (that is, the single-barred flux) can be divided into three parts:

i) The flux resulting from transient waves (single-barred flux minus double-barred flux);

ii) The flux resulting from standing waves (double-barred flux); and

iii) The flux resulting from the mean meridional circulation (which is zero here because of the geostrophic assumption).

The single- and double-barred relative westerly momentum fluxes have been computed for each month of 1971 and for wave numbers one through twelve using Equation 3.6 in Chapter 2. The fluxes presented here represent the zonally averaged flux across a parallel of latitude and should be multiplied by cos ϕ to be proportional to the total flux across any latitude.

To aid in the interpretation, the single- and double-barred momentum flux data for the individual waves one through three, and the sum of waves one through four and one through twelve are presented here using pressure-latitude diagrams similar to Figures 3.5 - 3.10.

Figure 3.11 depicts the January flux of relative westerly momentum by wave one (a and b), wave two (c and d), and wave three (e and f) due to the standing part of the waves (left) as well as the total flux (right) for each wave. The difference between the single- and double-barred fluxes for a given wave gives the magnitude and direction of the flux produced by the transient part of the wave (positive values indicate a northward flux while negative values indicate a southward flux). For this reason, when the single-barred flux has a lower value than the double-barred flux, it can de deduced that the transient wave is transporting westerly momentum southward. Furthermore, the direction of the standing and transient wave fluxes are often diametrically opposed.

It can be seen in Figure 3.11 that the total January wave one flux of momentum (b) is distributed very similarly to the standing wave contribution (a). The flux is small and primarily northward at lower latitudes in the troposphere, southward in polar regions, and rather strong northward in the vicinity of the polar-night jet. It is also apparent from these diagrams that the transient wave one flux (b minus a) is somewhat smaller than the standing wave one flux and opposite in direction. The wave two flux (d) is directed strongly to the south in the troposphere, with most of this flux by the standing wave component (c). The transient wave two (d minus c) produces a northward flux in the stratosphere of about equal magnitude to the standing part of wave one. The standing part of wave three (e) contributes very little to the total wave three flux of momentum (f), while the transient part (f minus e) produces a northward flux which is strong in the mid-stratosphere

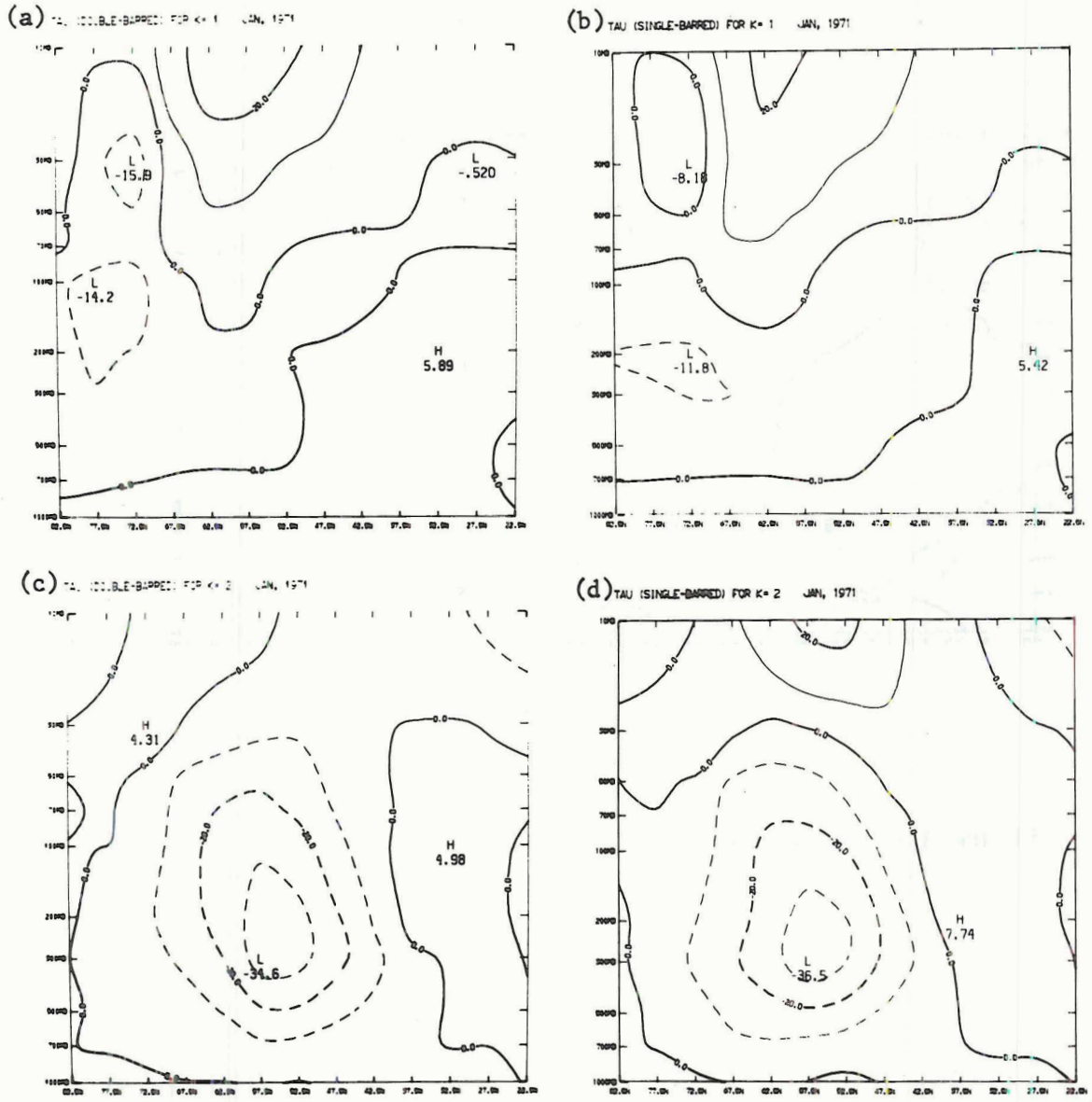

Figure 3.11 January meridional flux of relative westerly momentum by wave (a) one (double-barred), (b) one (single-barred), (c) two (double-barred), (d) two (single-barred), (e) three (double-barred), and (f) three (single-barred). Solid lines indicate northward (or zero) flux; dashed lines indicate southward flux. Isopleth interval is 10 m^2/s^2.

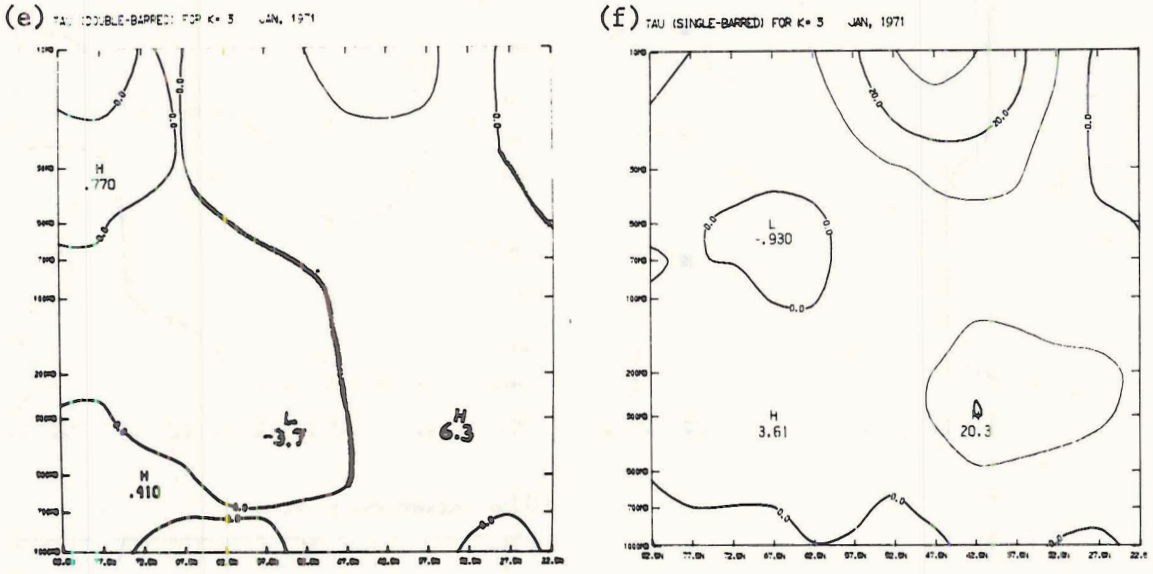

Figure 3.11 Continued.

near 50°N and in the troposphere near 40°N, but weak elsewhere. The wave four flux (not shown) is quite small everywhere.

The transient parts of waves three, five, and six together account for 57% of the total transient eddy flux (assumed to be the same as the transient flux by waves one through twelve) and 44% of the total flux (single-barred flux by waves one through twelve) at 200 mb and 37.5°N. Waves five and six at this latitude, with a wavelength of 6352 km and 5293 km, approximate the scale of mid-latitude synoptic disturbances.

In Figure 3.12 the sum of the momentum fluxes in January by waves one through four and one through twelve are presented. The total flux distribution by waves one through twelve (d) shows three very distinct regions: directed northward near the subtropical jet and in the stratosphere, and directed southward in the troposphere north of about 47.5°N. These regions happen to correspond with areas of strong westerly zonal flow in the Northern Hemisphere. The sharp dividing line between northward and southward transfer of relative westerly momentum near 47.5°N in the troposphere corresponds to the abrupt shift in the horizontal tilt of the ridge and trough lines north of the mean latitude of the polar front (from Equation 3.7, Chapter 2).

The magnitude, direction, and distribution of the total double-barred fluxes of relative westerly momentum (meaning the sum of the first twelve wave fluxes in Fig. 3.12c) agree well with the zonally averaged total stationary eddy transports in January computed by Oort and Rasmusson (1971) from observed winds. For example, in the troposphere they found a peak southerly flux at 300 mb and 65°N of 28 m^2/s^2, and a peak northerly flux at 200 mb and 30°N of 19 m^2/s^2. Furthermore,

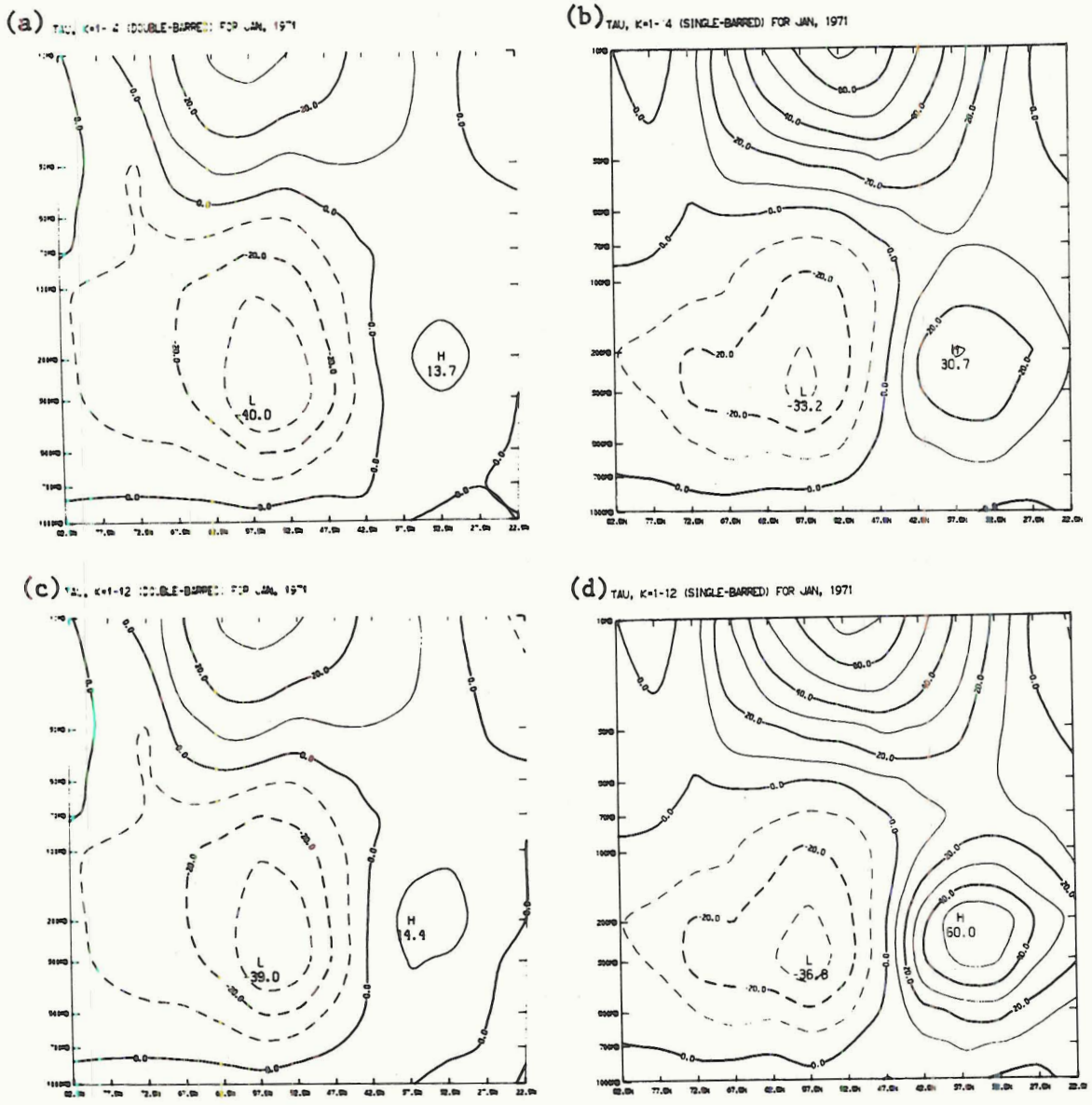

Figure 3.12 January meridional flux of relative westerly momentum by waves (a) one through four (double-barred), (b) one through four (single-barred), (c) one through twelve (double-barred), and (d) one through twelve (single-barred).

they found a peak northward flux by transient eddies at 300 mb and 30°N of 19 m^2/s^2 (comparable to d minus c in Fig. 3.12).

Quite a bit of additional information can be obtained from a perusal of the four diagrams in Figure 3.12. The long standing waves (k=1 through 4) account for nearly all of the standing wave flux of relative westerly momentum in January. The difference d minus b in Figure 3.12 gives the momentum flux by waves five through twelve and shows that these shorter waves are contributing significantly to the total flux just to the north of the mean subtropical jet stream (near 35°N). In fact, they account for roughly 50% of the total northward flux in this region. The computed mean transfers show waves five through seven to be primarily responsible for this flux, with the higher wave-numbers contributing negligible amounts. The importance of the transient waves can also be determined by looking at the differences between the diagrams for the single- and double-barred values of the flux. The most pronounced differences (for transient waves one through twelve: d minus c) appear near the subtropical jet where the transient waves of all sizes account for roughly 75% of the total flux of relative westerly momentum. Of this quantity, the short transient waves (with wave-numbers from five to twelve) are responsible for 60%. The contribution by the long transient waves (b minus a) accounts for roughly half of the flux in the vicinity of the polar night westerlies, with the peak values about five to ten degrees of latitude south of the main flux by the long stationary waves (which account for most of the other half). The long transient waves in the polar troposphere transport westerly momentum northward.

In April (not shown) several changes in the flux pattern appear. The stratospheric polar vortex has weakened to the extent that it is no longer an agent in the overall transport of relative westerly momentum. Throughout the mid-latitude troposphere, the short (k=5 through 12) transient waves transport a greater percentage of relative momentum in April than in January. The transient part of wave one produces a northward transport in polar latitudes of the upper troposphere. The region of southward flux noted in January comprises only a 15° latitude belt in April and is produced mainly by transient eddies (half by wave two; the rest by a combination of other waves).

In July (Fig. 3.13) the shorter waves (d minus b) contribute an even greater percentage than in April of the total flux of momentum which itself is quite negligible except in the upper troposphere south of about 50°N. Again, most of the northward flux is by transient eddies of various scales, but generally for wavenumbers greater than three (this doesn't show up in the figures but is quite clear in the computed data). Comparisons of the July standing and transient meridional fluxes of relative westerly momentum (c and d minus c, respectively) also agree quite well with Oort and Rasmusson's (1971) mean July calculations. For example, Oort and Rasmusson found a maximum northerly flux by stationary waves of 14.8 m^2/s^2 at 200 mb and 30°N, and a peak northerly flux by transient waves amounting to 20.7 m^2/s^2 at 200 mb and 40°N.

By October (not shown), a flux distribution very similar to that of January develops, although shifted slightly north. The stationary parts of waves one and three, and the transient parts of waves five through seven accomplish most of the large northward transport of relative westerly momentum in mid-latitudes of the troposphere. The

westerly winds of the stratospheric polar-night vortex have begun to develop with long wave perturbations transporting relative westerly momentum northward. A southerly flux in the polar troposphere can be attributed to the stationary part of wave one and the transient part of wave four.

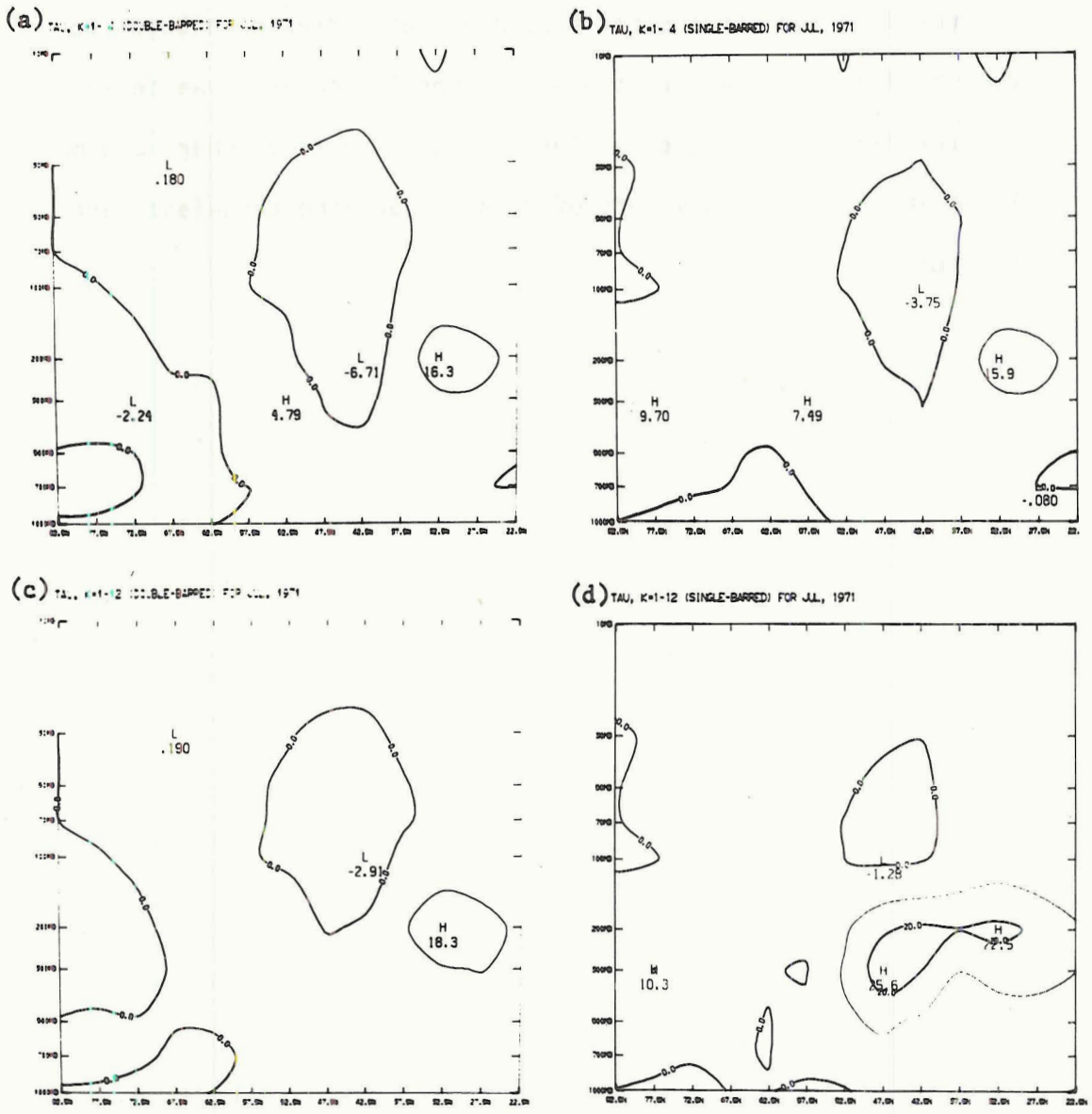

Figure 3.13 Same as Figure 3.12 except for July.

4. STRATOSPHERIC SUDDEN WARMING OF JANUARY, 1971

A phenomenon called a major stratospheric sudden warming occurs in midwinter when a poleward movement of planetary scale thermal systems (advecting warmer air into polar regions) results in a reversal of the polar circulation at 10 mb or below (Quiroz, et al., 1975). At times, "minor" warmings occur without producing a circulation reversal in the stratosphere below the 10 mb level (Quiroz, 1975).

The dynamics of these warmings haven't been completely explained, yet it seems plausible that the forcing is directed from the troposphere into the stratosphere, a point stressed by a number of authors (Julian and Labitzke, 1965; Murakami, 1965; Miller, 1970).

Matsuno (1970, 1971) developed a linear dynamic model of the stratospheric sudden warming which primarily consists of upward propagation of waves with zonal wave numbers one or two and their interactions with zonal winds. The stratospheric sudden warmings are complicated phenomena, but he suggests only three characteristic features during the course of the event:

i) the deformation and subsequent breakdown of the high velocity polar-night westerly vortex;

ii) a reversal of the normal winter meridional temperature gradient produced by excessive warming near the pole; and finally

iii) the onset of easterly winds at polar latitudes.

This sequence of events fairly well describes a warming event in general terms, yet with each stratospheric sudden warming event a unique although similar synoptic situation is revealed.

4.1 Synoptic Discussion.

The daily Northern Hemisphere maps of temperature and geopotential heights at the 50 mb level published in the Meteorologische Abhandlungen of the Free University of Berlin (1971) depict quite clearly the development of the sudden warming during January 1971. Figure 4.1 reveals the 50 mb contour heights and isotherms in the northern hemisphere for 1 January and 19 January 1971.

On 1 January a strong westerly vortex existed which was considerably asymmetric, or eccentric with respect to the pole (Fig. 4.1a). Coldest temperatures (below -80°C) were located at high latitudes (70° - 75°N) near the longitude sector of Scandinavia. A warm tongue (-40°C) existed at approximately 60°N near the Bering Sea, while the interpolated temperature at the pole was about -75°C. This basic flow pattern existed for several days, finally beginning to split on 8 January with a well developed two-wave circulation pattern being established by 10 January. In conjunction with this the cold and warm centers mentioned above each split and diverged along about the 70°N parallel with a tongue of warm air directed toward the north pole. The two main troughs at about 65°N over eastern Canada and central Siberia became cut off from the zonal flow, consequently producing easterly flow on their northern sides. At this time the zonally averaged flow at high latitudes was still westerly, but only slightly (i.e., the polar vortex had broken down). This can be seen at 10 mb and 72.5°N in Figure 4.2 as a sharp decrease of the zonally averaged geostrophic flow between 9 and 11 January. On 10 January the 50 mb temperature at the pole had warmed to about -67°C, and by 19 January a temperature of about -40°C existed at this level over the pole (Fig. 4.1b). This warming reversed

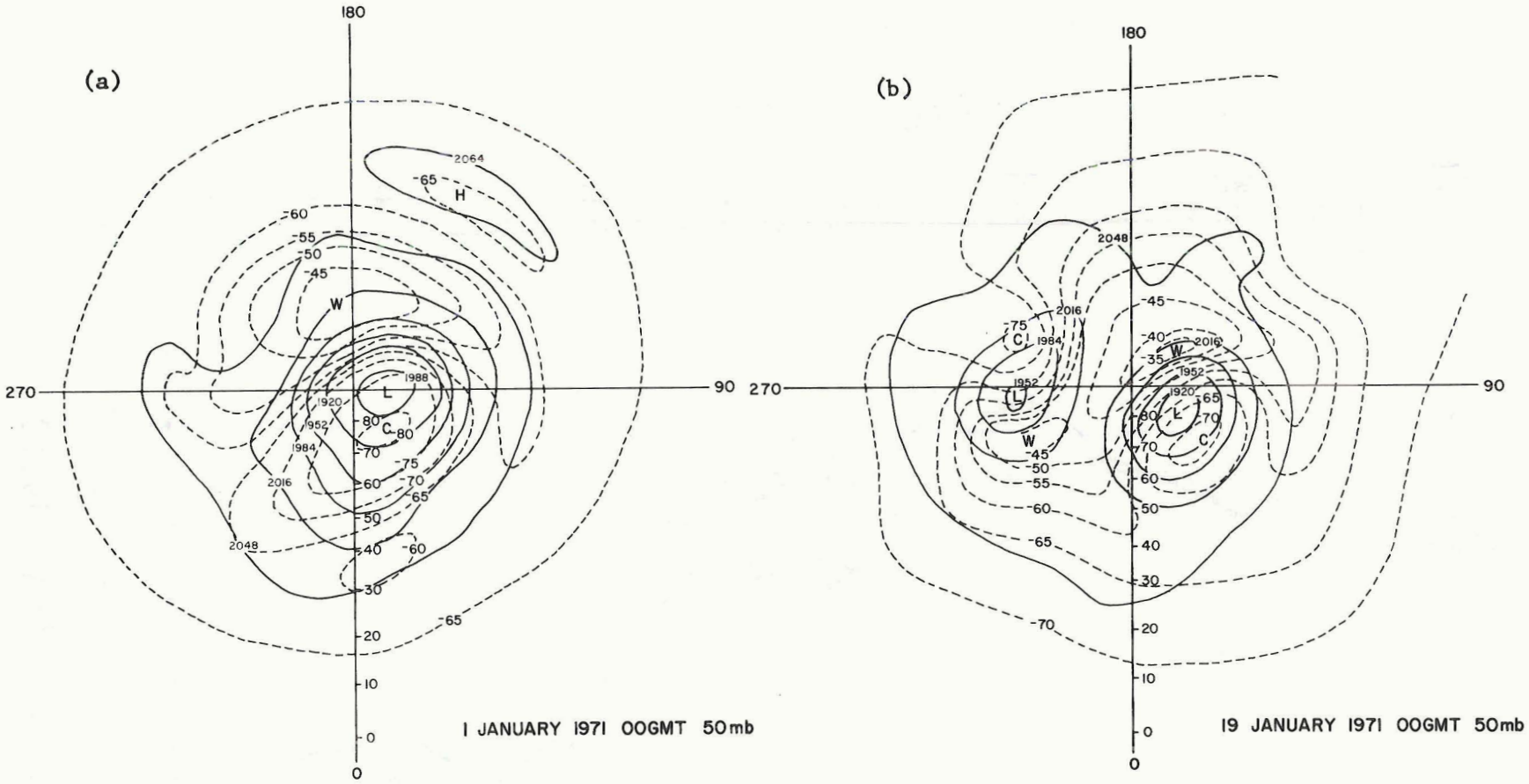

Figure 4.1 50 mb Northern Hemisphere synoptic charts for (a) 1 January 1971 and (b) 19 January 1971. Solid lines are contour heights (decameters) and dashed lines are isotherms (°C). After Free Univ. of Berlin, 1971.

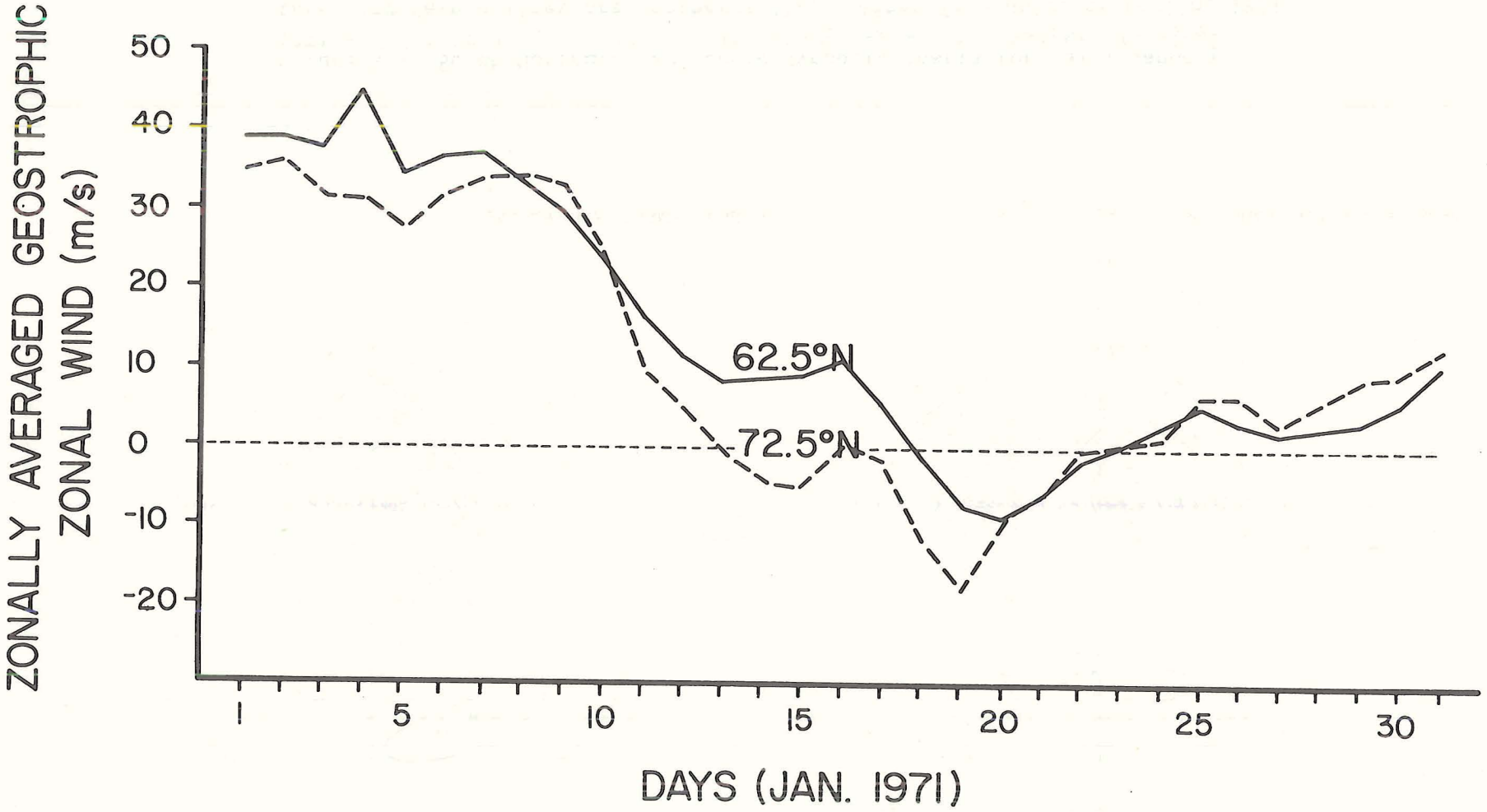

Figure 4.2 Day-to-day variation of the zonally averaged geostrophic zonal wind at 62.5°N (solid line) and 72.5°N (dashed line) at the 10 mb level. Units are m/s.

the normal zonally averaged temperature gradient sufficiently to allow easterly winds to predominate at high latitudes (see also Barnett, 1974). This can also be seen in Figure 4.2 as a reversal of the zonal flow with maximum easterly winds occurring on 19 January at 72.5°N and 20 January at 62.5°N. The cut off vortex over Siberia then began to move northwestward while the vortex over Canada filled. By early February, a strong circumpolar westerly flow was again established.

4.2 Amplitudes and Phases of the Long Waves.

As in the case of the January monthly means, the daily geopotential height fields for January, 1971 can be represented to a good approximation by the amplitudes and phases of the first two zonal harmonic waves in the stratosphere. The day-to-day variations of the amplitudes and phases for waves one and two at three stratospheric levels (10 mb, 70 mb, and 200 mb) and at one mid-tropospheric level (500 mb) at 70°N are plotted in Figures 4.3 and 4.4.

In early January the amplitude of wave one (Fig. 4.3a) is quite high at all levels, as is apparent on the synoptic maps. On 5 January the amplitude of wave one begins to decrease, except at 10 mb where this doesn't occur until 8 January (the minor flucutation on 10 January being disregarded). Throughout early January the amplitude of wave one shows a strong increase with height. Its fluctuations at upper levels appear to lag behind the lower levels with relative minimums at 500 mb, 200 mb, 70 mb, and 10 mb occurring on the 10th, 10th, 11th, and 19th of January, respectively. Relative maximums at these same levels reach their peak on the 16th, 16th, 19th, and 22nd, respectively. These dates should not be construed as absolute since some of the minor fluctuations are probably due to observational and analysis errors.

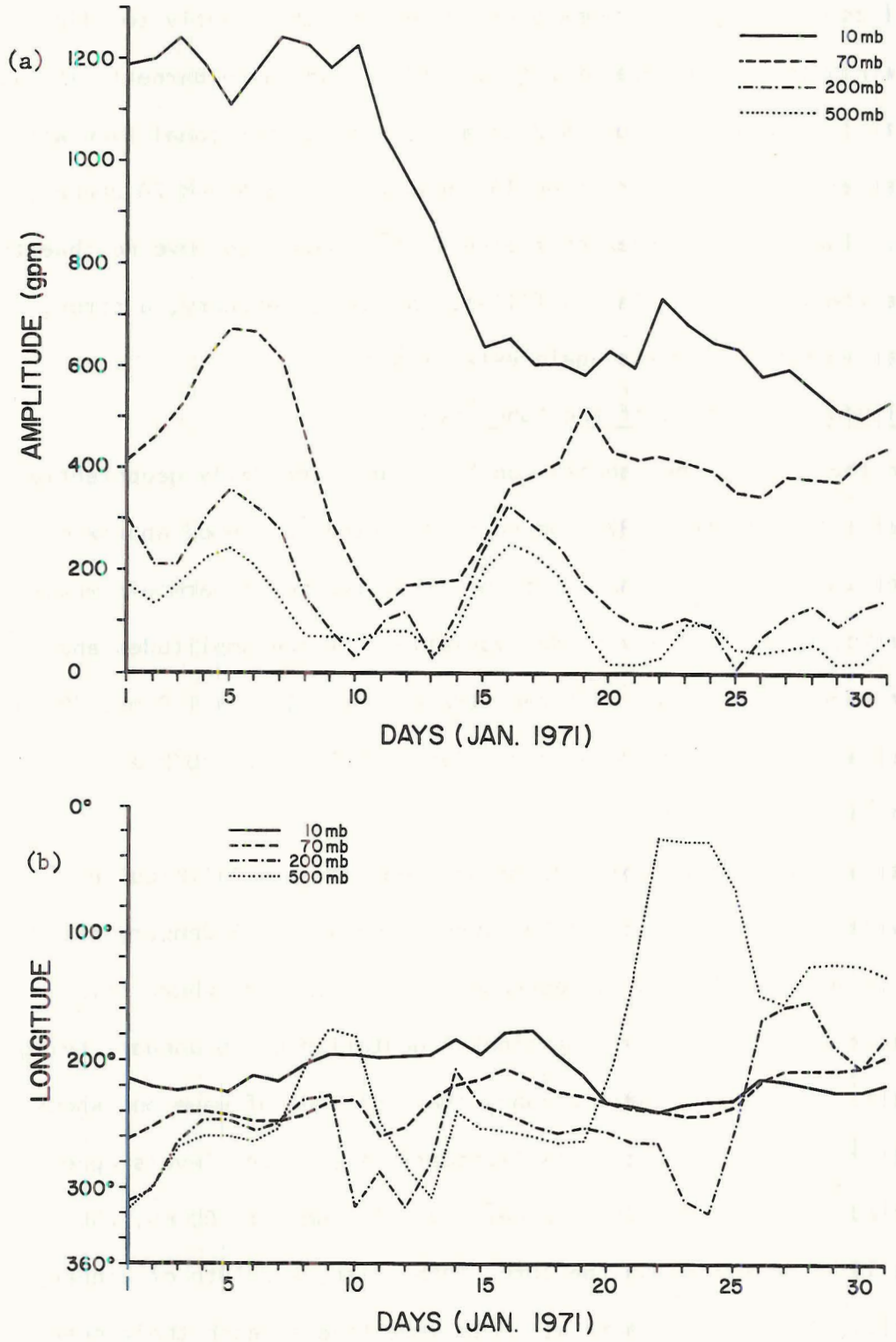

Figure 4.3 January day-to-day variation of the wave one (a) amplitude and (b) longitude of the first ridge line east of Greenwich at 10 mb (solid line), 70 mb (dashed line), 200 mb (dashed-dotted line), and 500 mb (dotted line) at 70°N.

This same behavior is exhibited by wave two (Fig. 4.4a) with relative maxima occurring on the 13th at 500 mb, the 14th at 200 mb, the 14th at 70 mb, and the 15th and 17th at 10 mb. The wave two minima also lag behind at upper levels. This same phenomenon isn't apparent for wave three but it is interesting to note that the amplitudes of waves two and three increase as the amplitude of wave one decreases. This apparent negative correlation has also been observed during other stratospheric sudden warmings (see, for instance Hirota and Sato, 1969). The amplification of wave two commencing on 6 January parallels the synoptic development of a two wave pattern becoming established by 10 January. It remains a question whether or not this represents nonlinear barotropic interactions of the long waves, since Matsuno's (1971) model simulates a warming event fairly well using linearized equations for waves one and also for wave two.

During the early part of the 1971 stratospheric warming (through 7 January) the phase angle of wave one indicates a westward tilt with height (Fig. 4.3b). At 70°N on 1 January the ridge at 500 mb is centered over northeastern Canada, while at 10 mb the ridge is located some 100° of longitude further west or over the Alaska-Canada border. Wave one is stationary at all levels between 3-7 January, as the amplitude reaches its peak values. However as the amplitude increases again later in the month (15-20 January), the ridge returns to its original position. In the meantime (9-14 January) the ridge had moved first eastward and then westward with this movement being most pronounced at the lower levels where the amplitude was small.

Wave two in January (Fig. 4.4b) exhibits an absence of tilt in the vertical when the amplitude is high (10-17 January), and the wave moves

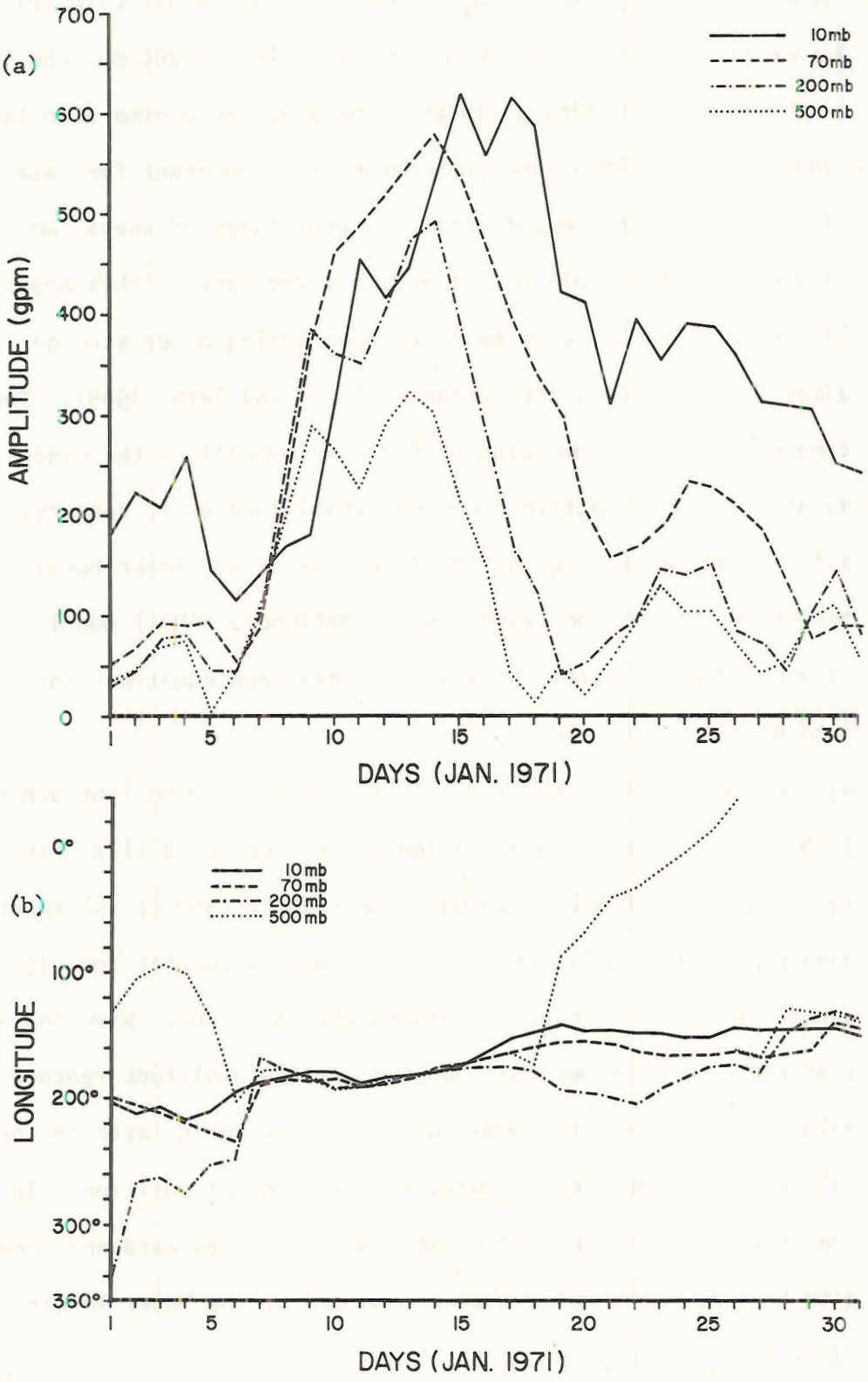

Figure 4.4 Same as Figure 4.3 except for wave two.

slowly towards the west during this period. The increase with height of the wave two amplitude is not quite as pronounced as that of wave one.

During the period 8-17 January, the zonally averaged westerly flow in the stratosphere is decreasing and at some point producing favorable conditions for vertical wave propagation (Charney and Drazin, 1961). However at the same time and at some other height a critical level can exist upon which the vertically propagating wave is absorbed and hence reducing the normal increase of wave amplitude with height (Matsuno, 1971).

The vertical structure of these long waves is shown on pressure-latitude diagrams similar to those presented in the previous chapter. In these figures the contour interval is 20 meters for amplitudes less than 300 meters, but changes to 50 meters at amplitudes above 300 meters for clarity. Figure 4.5 shows the amplitude distribution for wave one on selected days during the month of January. In the troposphere, this wave loses intensity through the early part of the month with a peak amplitude of only 107 meters at 45°N and 300 mb on 13 January. By this date, wave one appears intense only in the stratosphere with peak amplitudes consistently observed between 65°N and 70°N at the 10 mb level through 17 January. At this time the wave intensifies at lower levels of the stratosphere with the maximum amplitude at the 30 mb level. This may be the response to an easterly wind regime (which had developed at polar latitudes by this time) or to a critical level which prohibits any upward propagation of the wave.

Wave two (Fig. 4.6) has a rather small amplitude in early January, but it begins to intensify initially in the mid-latitude troposphere on 6 January and then explosively between 7-12 January through the

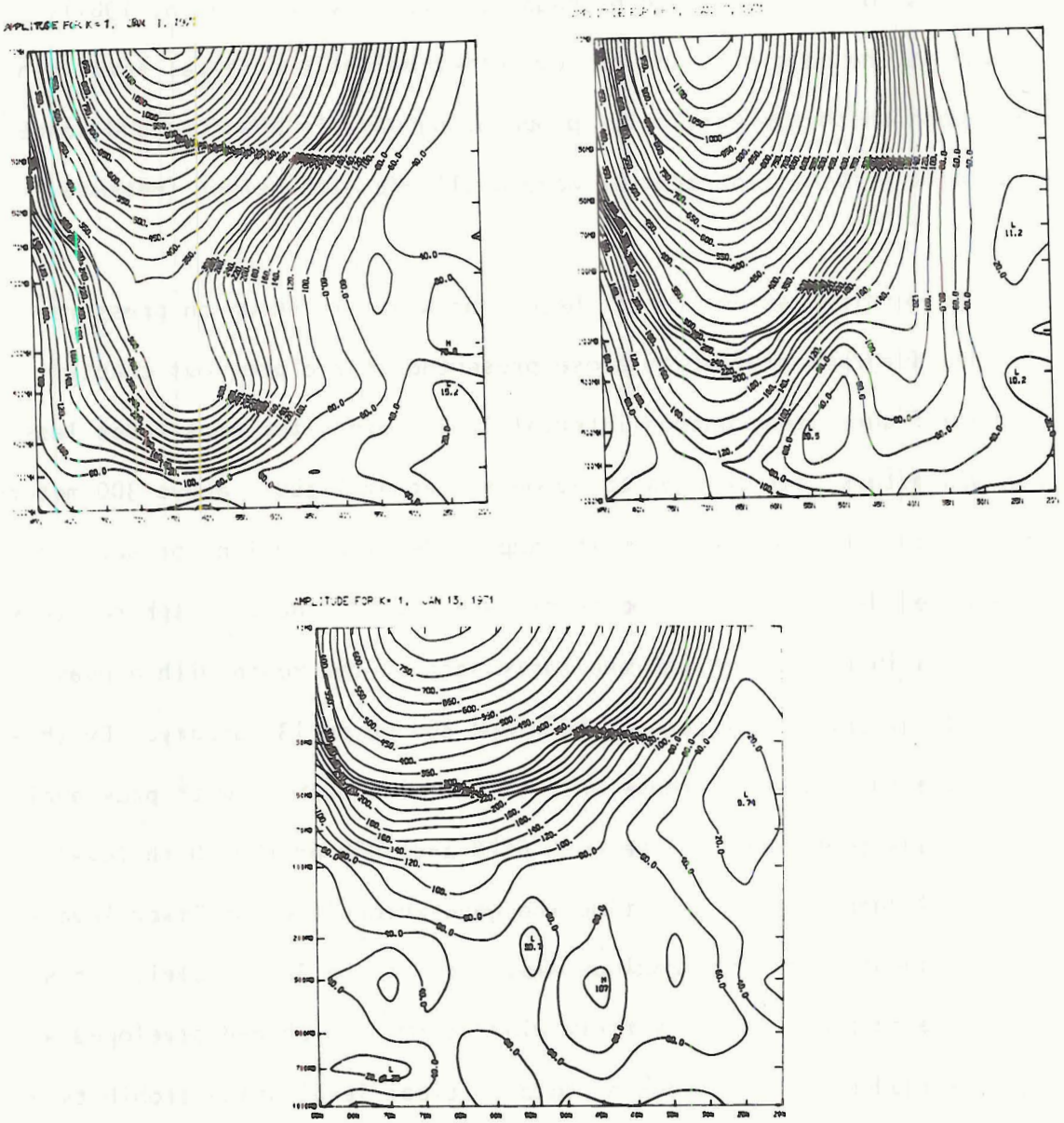

Figure 4.5 Wave one amplitude distribution for every 6th day of January. Contour interval of 20 m except 50 m at amplitudes above 300 m.

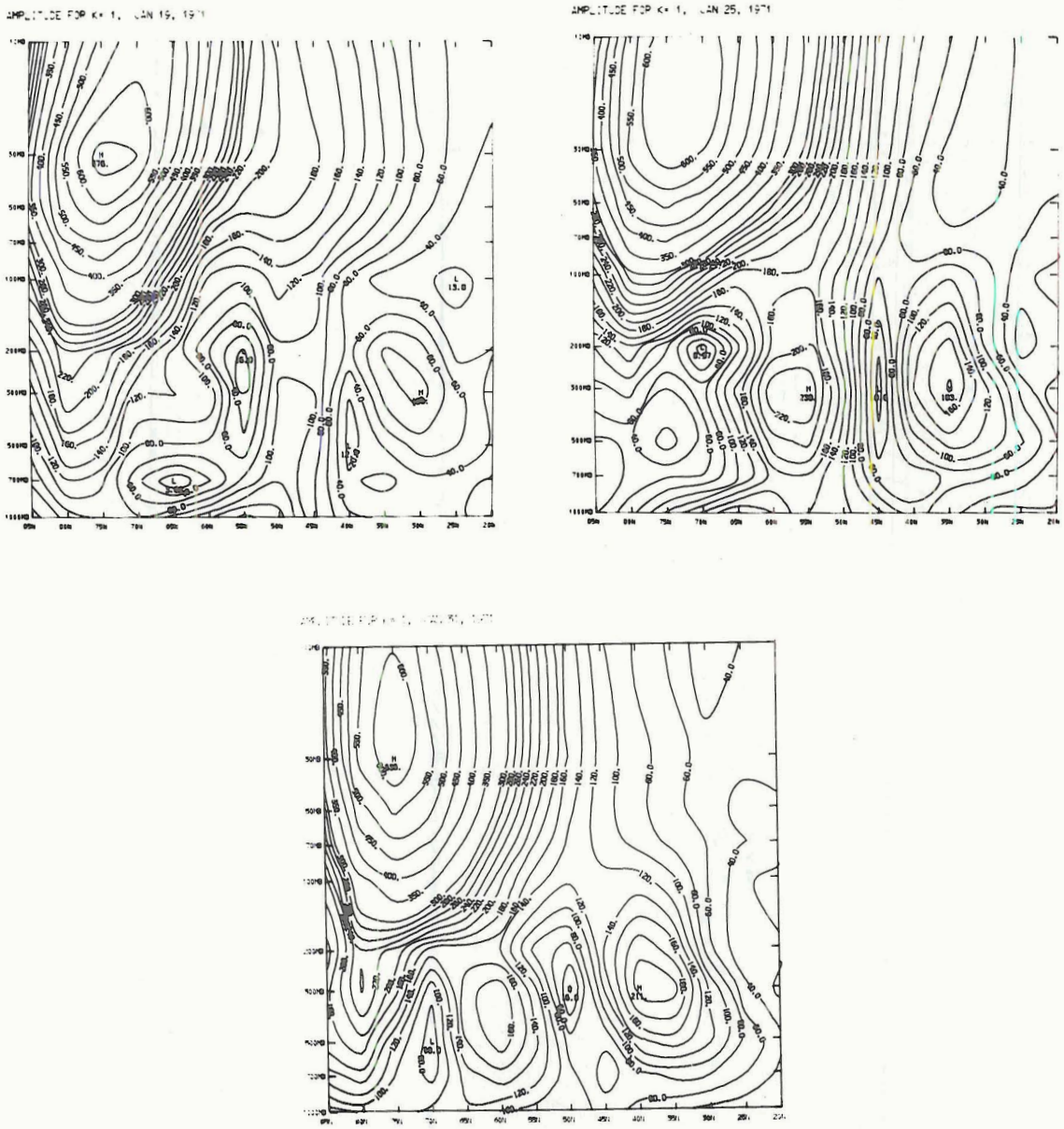

Figure 4.5 Continued.

stratosphere and at higher latitudes in the troposphere. The diagram for 13 January (Fig. 4.6) exemplifies the distribution of wave two at its most intense stage. The highest amplitude in the stratosphere during the period 9-17 January appears first at 50 mb, then at 30 mb, and finally at 10 mb where the peak amplitude exists for the remainder of the month. Wave two has a similar development to wave one in that after the period of highest amplitudes at all levels the wave becomes quite weak in the troposphere, but with a relative maximum near 45°N and 300 mb (i.e., wave one, 13 January; and wave two, 19 January) which subsequently amplifies. Following this amplification both waves one and two have more than one peak at various latitudes in the troposphere.

The amplitude of wave three (Fig. 4.7) shows considerably more variability during the month of January than either wave one or two. As with wave two, the peak amplitude of wave three in the stratosphere decreases drastically between 6-7 January. The wave then begins to amplify on 9 January, reaching a peak of over 300 meters at 65°N and 10 mb by 15 January (the sequences of these events can be seen in Fig. 4.7 but not for the specific days mentioned here). During most of the month two peaks exist, one in the troposphere and one in the stratosphere. The former appears near 300 mb between 35-65°N (often with two peaks: one each at higher and lower mid-latitudes).

The shorter waves (with wavenumbers greater than or equal to four) damp out quite rapidly in the stratosphere while occasionally reaching amplitudes of greater than 200 meters in the troposphere for waves 4-6.

4.3 Kinetic Energy and Relative Momentum Flux.

This section is concerned with the distribution and variations in time of the kinetic energy of the first three harmonic waves as well as

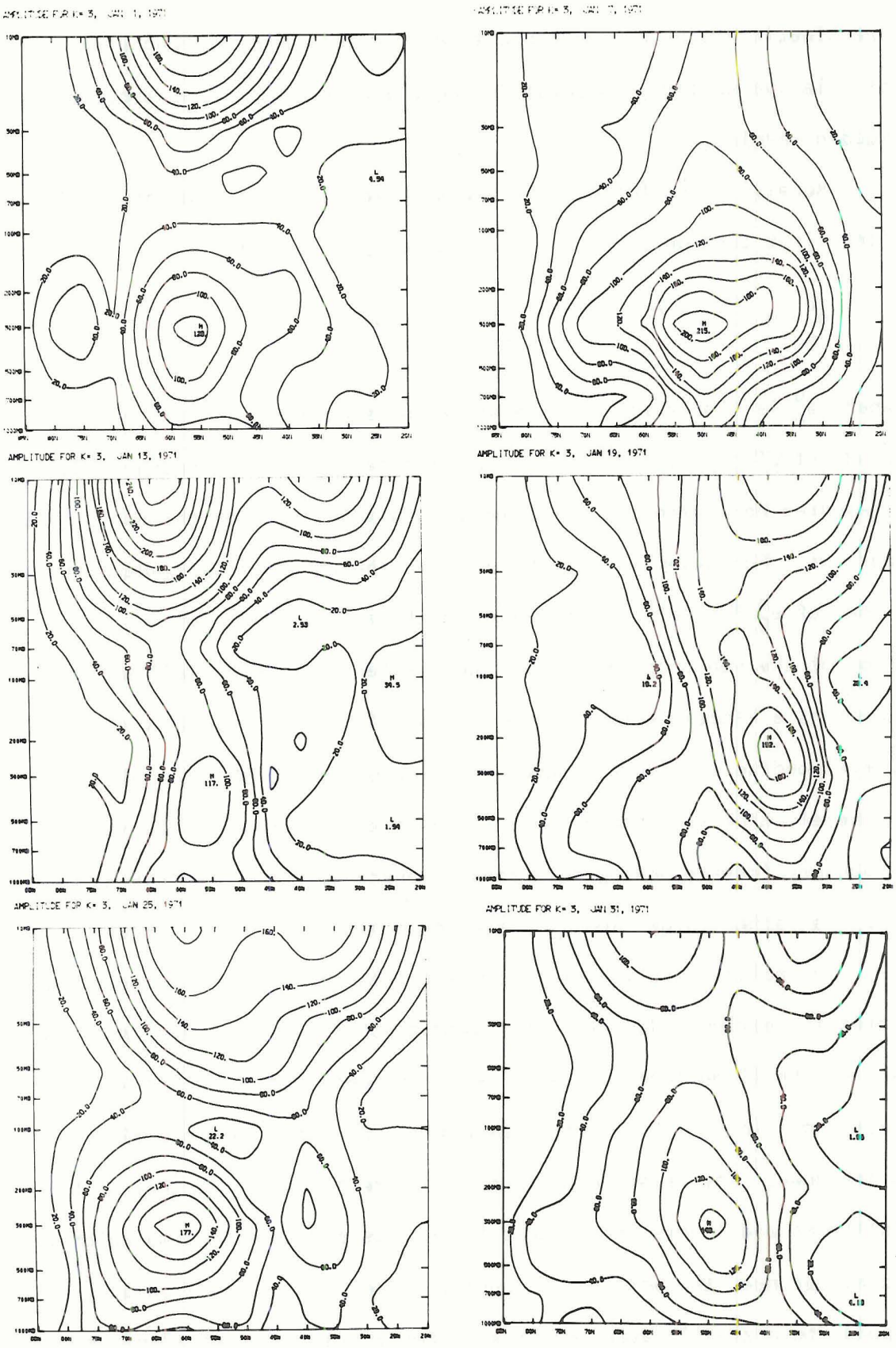

Figure 4.7 Same as Figure 4.5 except for wave three.

the kinetic energy of the basic zonal current, and the long wave fluxes of relative westerly momentum during the course of the stratospheric sudden warming.

Recalling the formula for the kinetic energy of the zonal current (the first term on the r.h.s of Equation 3.2, Chapter 2),

$$e_0^u = \frac{1}{2}(a_0^u)^2,$$

where a_0^u is simply the geostrophic wind associated with the meridional gradient of contour heights, we can relate the kinetic energy diagrams presented here with the geostrophic wind velocities of the basic zonal current. For example, Figure 4.8 shows the pressure-latitude distributions of e_0^u for selected days during the month. On 1 January the zonal flow of the sub-tropical jet stream, centered at about 32°N and 200 mb, contains a kinetic energy per unit mass of greater than 1200 m^2/s^2, corresponding to a zonally averaged wind of nearly 50 m/s. This extremely high wind speed and its subsequent decrease to the values of 7 January (corresponding to a zonally averaged wind of nearly 35 m/s) imply a rather large flow of energy or conversion to a different form.

The polar-night vortex in the stratosphere reaches its greatest intensity early in January with maximum zonal kinetic energy near 60°N and at the 10 mb level. The values here reach 1000 m^2/s^2 on 4 January (not shown in Fig. 4.8) after which time the polar vortex begins to break down. The relative maximum in Figure 4.8 on 19 January at high latitudes and levels is produced by the easterly wind regime which began to appear near the pole on 13 January. The maximum on 19 January corresponds to a zonally averaged peak easterly wind of about 18 m/s at the 10 mb level.

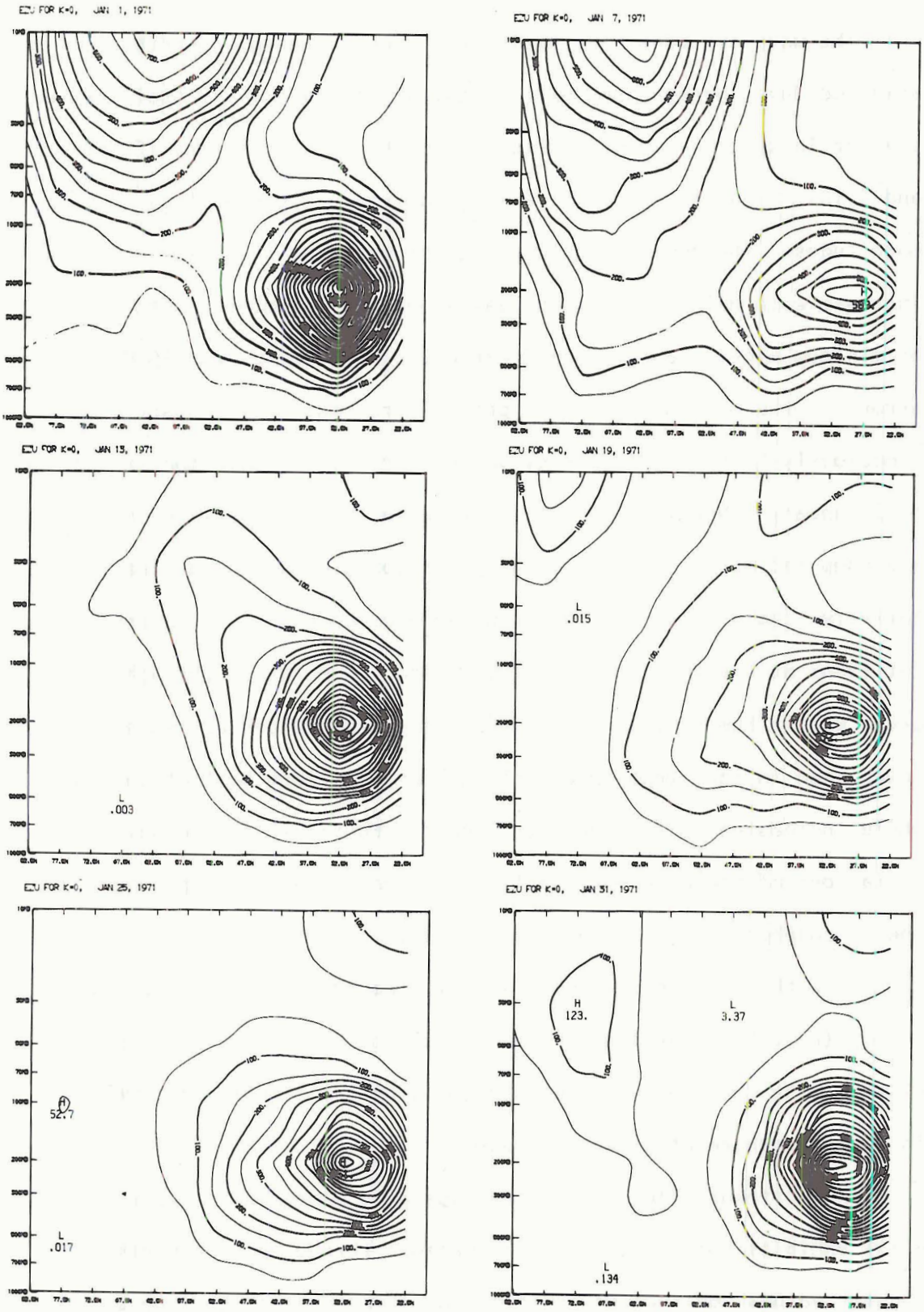

Figure 4.8 Kinetic energy of the zonal current (k=0) for every 6th day of January. Contour interval of 50 m^2/s^2.

The wave one zonal and meridional kinetic energy distribution for selected days through the month (Figs. 4.9 and 4.10) are qualitatively similar in spatial appearance to the monthly mean diagrams (Figs. 3.9 and 3.10). However, there is a large day-to-day variability of the magnitudes. The zonal kinetic energy of wave one (Fig. 4.9) shows an increase with height during the early part of the month, with a tongue of minimum kinetic energy again extending vertically near 65°N. Small errors in the original data are probably responsible for part of the anomalously high kinetic energy values north of 70°N in the stratosphere on 7 January. However, it must be remembered that the kinetic energies are computed as the square of the geostrophic winds so, at least qualitatively, the highest wave one zonal energy occurs on 7 January in high latitudes at the 10 mb level, after which it decreases through 19 January. Within the troposphere, the zonal energy values are substantially lower than in the stratosphere throughout the first half of the month, while increasing during the latter half. Furthermore, the day-to-day variations of the wave one zonal kinetic energy are more pronounced in the troposphere than in the stratosphere.

As with the wave one zonal kinetic energy, the meridional kinetic energy (Fig. 4.10) attains highest values on 7 January at 10 mb. The distribution does not vary as much throughout the month, however, except in the troposhere at high latitudes.

The northward flux of relative westerly momentum for wave one (Fig. 4.11) exhibits some irregular fluctuations throughout the month. The highest values again occur in the polar stratosphere, but the direction of the flux alternates several times during the month as the meridional tilt of the trough and ridge lines of wave one vary. The peak flux at

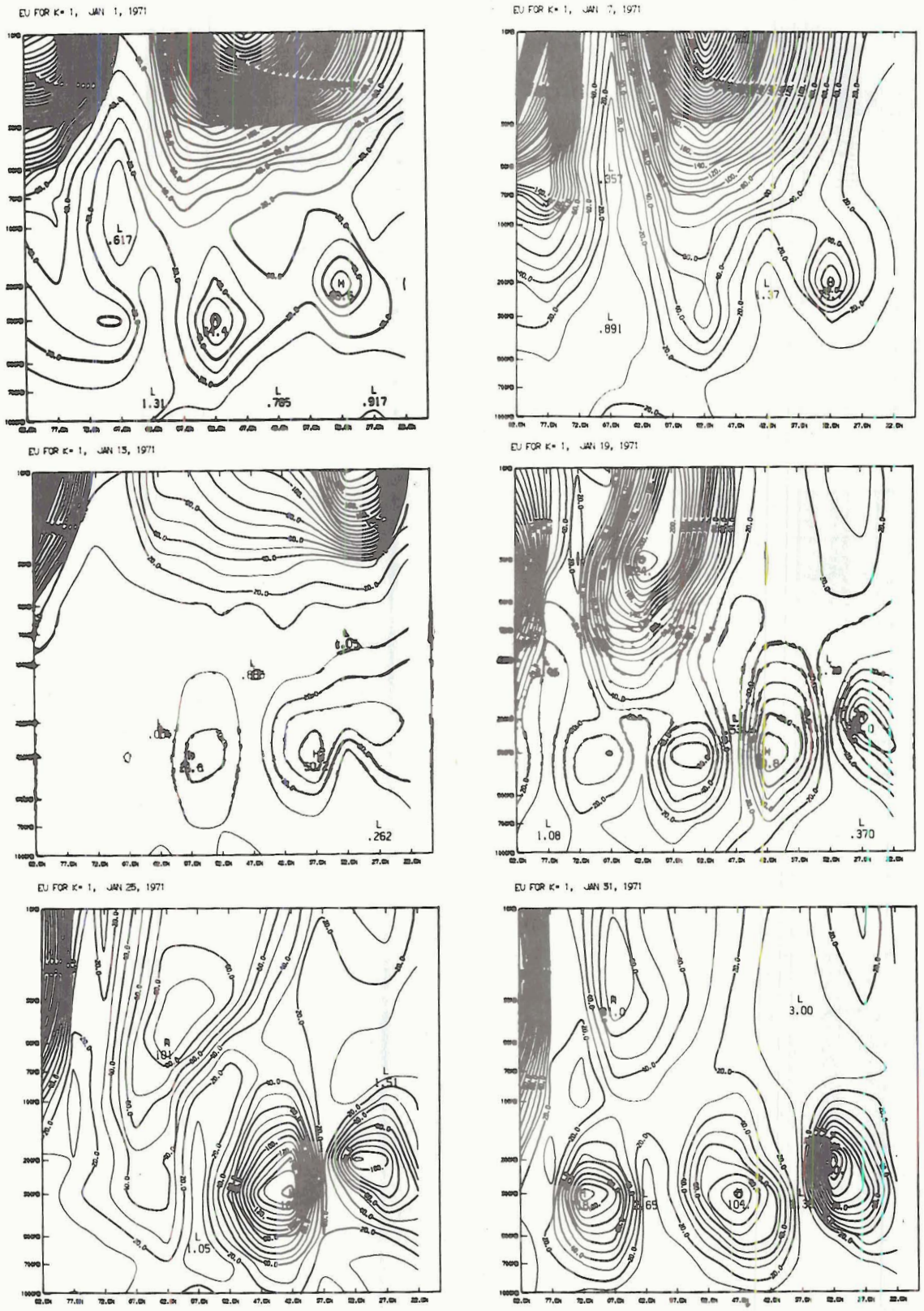

Figure 4.9 Kinetic energy of the zonal flow by wave one for every 6th day of January. Contour interval of 10 m^2/s^2.

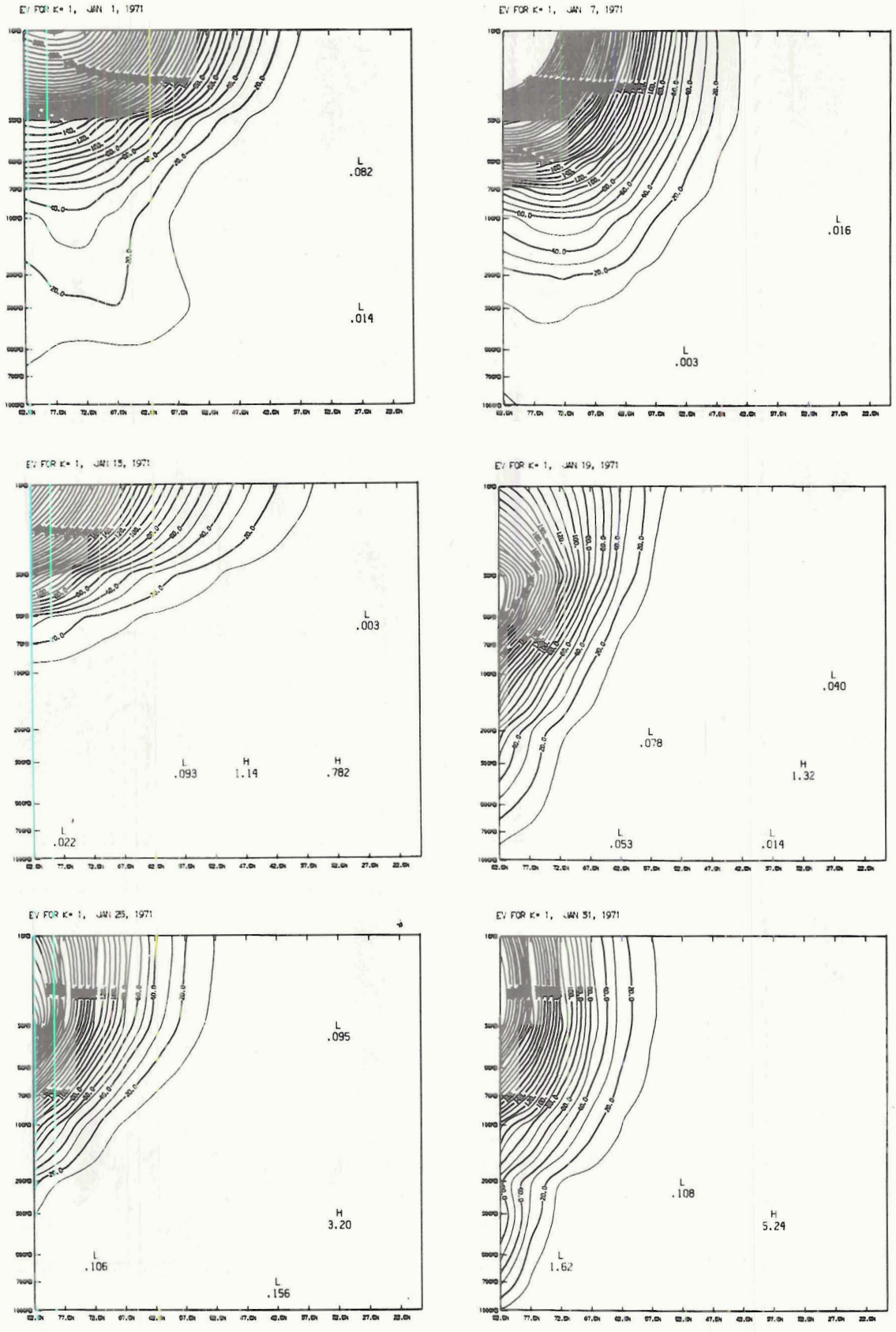

Figure 4.10 Same as Figure 4.9 except for the meridional flow.

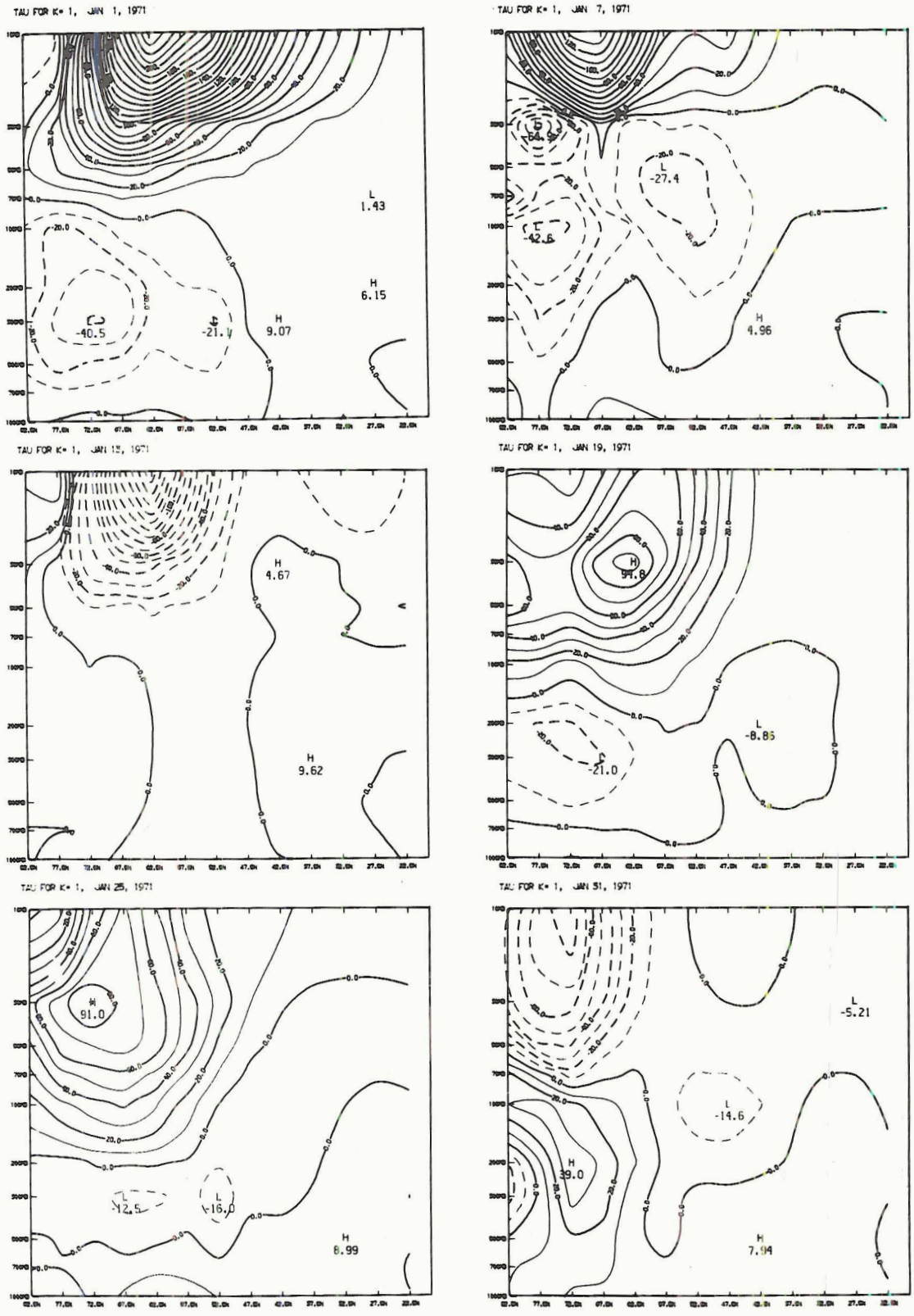

Figure 4.11 Meridional flux of relative westerly momentum by wave one for every 6th day of January. Solid lines indicate northward (or zero) flux; dashed lines indicate southward flux. Contour interval of $10 m^2/s^2$.

10 mb is northward through the first eight days of the month, southward from 9-14 January, then northward again through 27 January, and finally southward for the last few days of the month. The first change of sign appears at nearly the same time as the vortex splitting as well as when the wave one amplitude (Fig. 4.3a) decreases rapidly.

Figures 4.12 - 4.14 depict daily distributions of the wave two zonal kinetic energy, meridional kinetic energy, and northward flux of relative westerly momentum, respectively. The wave two zonal kinetic energy (Fig. 4.12) increases rapidly in the troposphere between 4 January and 7 January, at the same time that the kinetic energy of the mean zonal flow decreases rapidly (Fig. 4.8), and then in the stratosphere by 13 January, again a consequence of the vortex splitting and amplification of wave two. Also on this day localized high zonal kinetic energy values occur simultaneously near 10 mb and 30°N for wave one, wave two, and the basic zonal current. Through the remainder of the month the wave two zonal kinetic energy generally decreases in the stratosphere and fluctuates in the troposphere. The wave two meridional kinetic energy (Fig. 4.13) amplifies explosively between 7-13 January throughout the atmosphere at high latitudes and then decreases rapidly in the troposphere and more gradually in the stratosphere during the remainder of the month. In the troposphere, however, the wave two meridional kinetic energy reappears with some magnitude towards the end of January. The wave two flux of relative westerly momentum (Fig. 4.14) becomes very high in magnitude around 13 January and transports westerly momentum southward through most of the troposphere and northward through most of the mid-stratosphere during this period. By 19 January, when the zonal flow is reversed, this wave transports relative westerly momentum

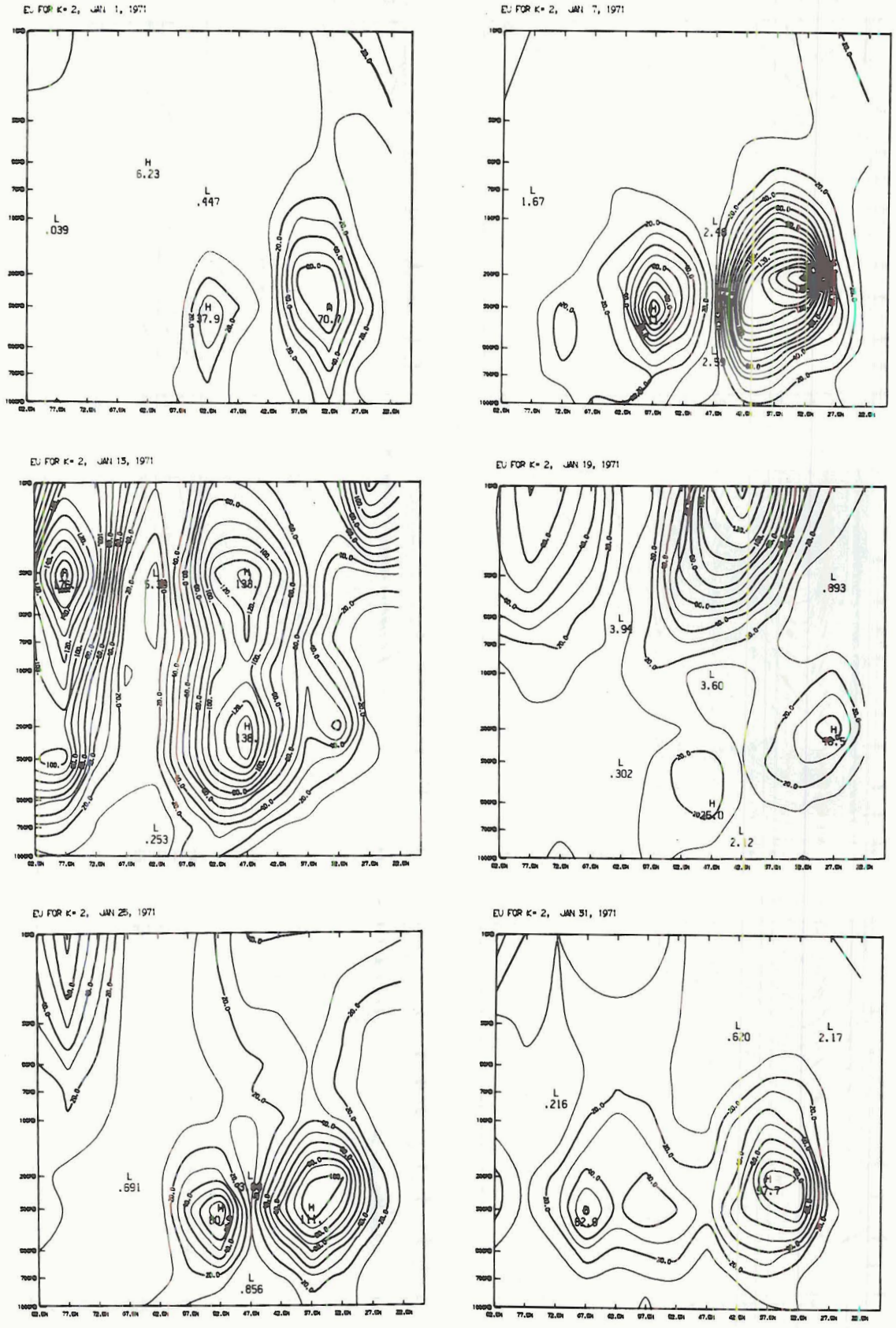

Figure 4.12 Same as Figure 4.9 except by wave two.

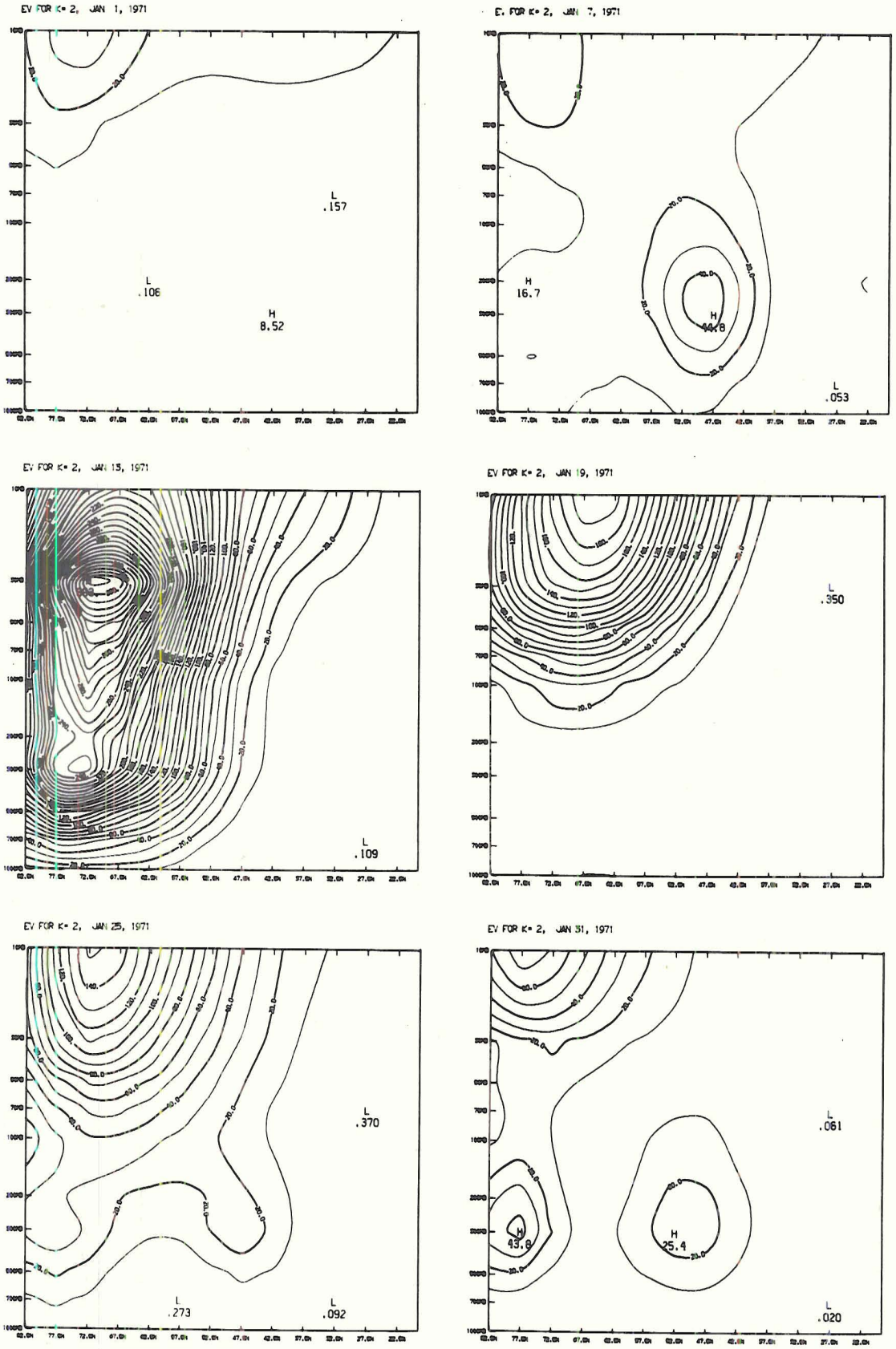

Figure 4.13 Same as Figure 4.9 except by wave two meridional flow.

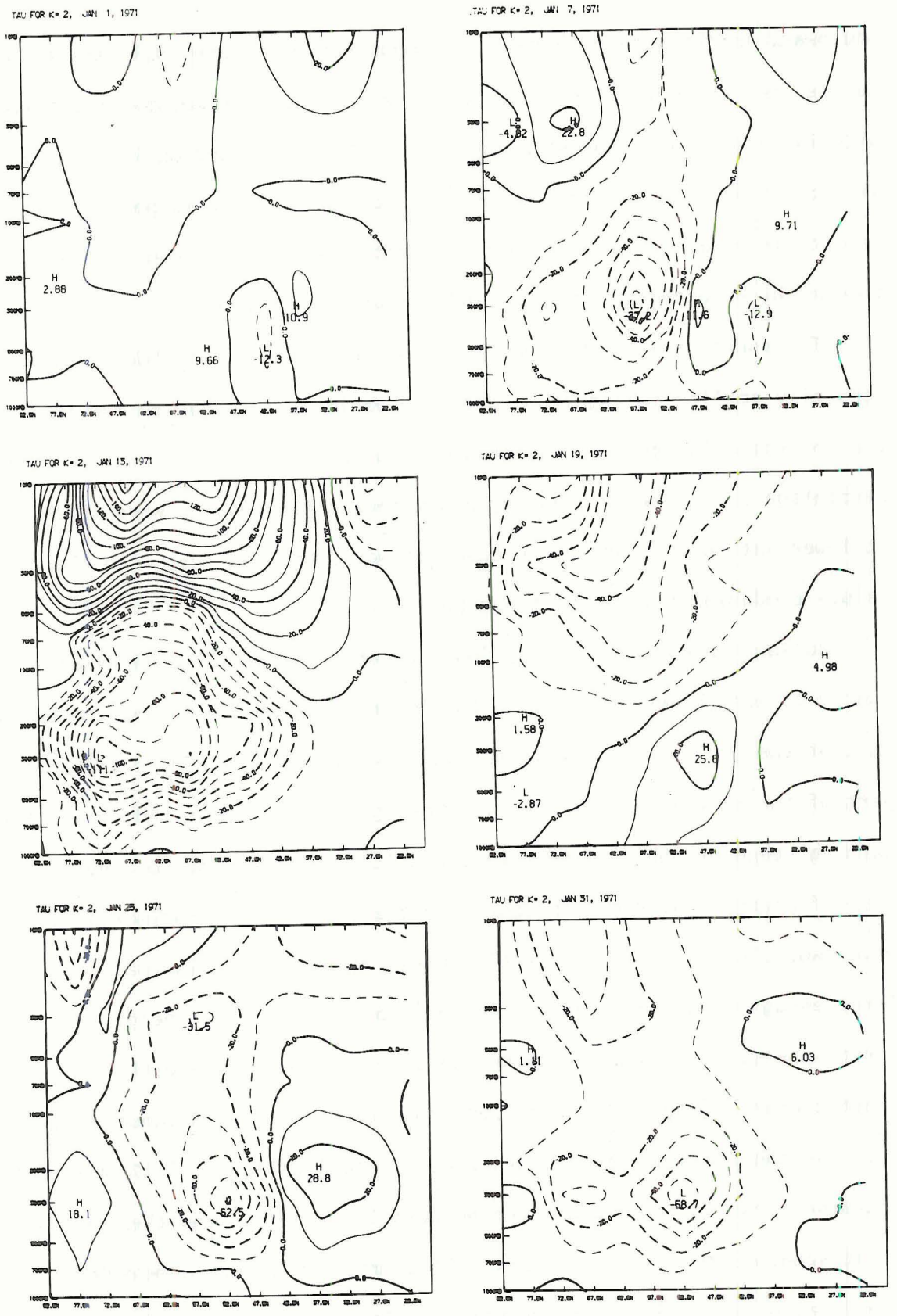

Figure 4.14 Same as Figure 4.11 except by wave two.

southward in the stratosphere. By comparison of Figures 4.11 and 4.14 we see that the directions of fluxes due to waves one and two are opposite in direction in the stratosphere on 13 January and on 19 January with the flux by each wave changing direction during this period. This results in a smaller zonally averaged net transport for the two waves than might be expected from the individual wave fluxes.

The energies and momentum fluxes of wave three (not shown) are generally smaller in magnitude and more variable from day to day than the corresponding quantities for waves one and two. In general a greater percentage of the kinetic energy and momentum flux due to wave three is at lower latitudes than in the cases of waves one and two, with the peak values predominantly in the troposphere.

Julian and Labitzke (1965) found a net transfer of zonal kinetic energy to eddy kinetic energy in the lower stratosphere during the early part of the 1963 stratospheric warming, and Iwashima (1974) attributed part of the increase of eddy kinetic energy which he measured during the warming stage of the 1967-68 stratospheric sudden warming to a vertical flux of energy from the troposphere to the stratosphere (primarily by wave two) since the dip in kinetic energy of the zonal flow was not large enough to account for the increase of eddy kinetic energy in the stratosphere. This appears to be the case here also, since the zonal kinetic energy (Fig. 4.8) decreases drastically from 7-13 January while the wave two zonal and meridional kinetic energies (Figs. 4.12 and 4.13) increase first in the troposphere between 1-7 January, and then in the stratosphere between 7-13 January. Of course, this development by wave two is also revealed on the synoptic charts as a splitting of the

stratospheric circumpolar vortex and establishment of a strong two wave pattern.

5. SUMMARY AND CONCLUSIONS

From the monthly mean data for 1971 several distinct spatial and temporal variations of hemispheric scale atmospheric parameters in the wavenumber domain were determined. The basic data of the investigation consisted of the first thirteen harmonic coefficients of geopotential heights computed by daily Fourier analyses of geopotential heights at 36 grid points around 14 latitude circles from 20°N to 85°N and at 10 pressure levels from 1000 mb to 10 mb. The parameters computed from these coefficients are the amplitudes, phase angles of the harmonic waves, kinetic energies per unit mass of the zonal and meridional geostrophic wind components, and meridional fluxes of relative westerly momentum.

Two types of calculations were used to compute monthly means of the nonlinear (kinetic energy and momentum flux) parameters (Chapter 2.4). First, the parameters were computed directly from the monthly mean harmonic coefficients, and then the same parameters were computed daily from the daily harmonic coefficients and averaged for the month. It was then possible to analyze the intensity of the day-to-day variations of the different scales of motion by looking at the differences between the two types of means.

The importance of the long waves ($k \leq 4$) in the monthly mean general circulation during the winter season was verified by inspection of the amplitude and variance distributions during the month of January which showed an increasing predominance of the longest waves at higher latitudes and levels (Chapter 3.1). It was also found that the ratio of the

amplitudes of the short waves to the long waves increased from winter to spring and remained fairly high in the summer.

The dominant feature of the seasonal amplitude distributions was the disappearance of the strong waves 1 and 2 in the stratosphere in conjunction with the final breakdown of the polar night vortex (Chapter 3.1). There appeared to be only small amplitude wave activity in the stratosphere in July, while in the troposphere waves 1-6 appear fairly active. Wave one in July was found in many cases to be 180 degrees out of phase with the January wave suggesting thermal forcing (Chapter 3.1).

The spectra of zonal and meridional geostrophic kinetic energy were analyzed for January and July revealing the zonal kinetic energy spectrum to be dominated by waves one through three in both months (Chapter 3.2). An appreciable part of the meridional kinetic energy spectrum is contained in the wavenumber band from five through twelve at lower and mid-latitudes of the troposphere in January and July. But at high latitudes and levels waves one through three dominated the meridional kinetic energy spectrum (Chapter 3.2).

In January roughly two thirds of the contribution of wave one to the zonal kinetic energy is produced by the standing part of the wave except in the vicinity just north of the subtropical jet where the transient component is nearly equal in magnitude (Chapter 3.2). The wave one meridional kinetic energy increases with latitude and height, and is produced mainly by the standing wave component. Also during January, the wave two zonal kinetic energy is produced mainly by the transient component. In general, the transient waves appear responsible for the major part of the tropospheric meridional kinetic energy with the long transient waves (one through four) predominating in polar

latitudes and the shorter transient waves (five through twelve) dominating elsewhere. On the other hand, most of the zonal kinetic energy (other than that of the mean zonal current) can be accounted for by the long standing wave elements in both the troposphere and the stratosphere (Chapter 3.2).

In July, the transient eddies are responsible for most of the tropospheric zonal and meridional kinetic energies, with the long transient waves accounting for roughly half of the total zonal wave kinetic energy. The meridional kinetic energy in July is produced mainly by shorter transient waves at lower latitudes and by long transient waves at polar latitudes. The stratosphere contains very little eddy kinetic energy in July; however, a fairly strong easterly mean zonal flow exists (Chapter 3.2).

The long standing waves account for nearly all the standing wave transport of relative westerly momentum in January and July, with wave two in January primarily responsible for the strong southerly flux in the troposphere north of the polar front jet. The transient parts of waves five through seven account for a large part of the northward flux of relative westerly momentum near the subtropical jet while the standing part of wave one and the transient part of wave two together account for most of the northerly flux in the stratosphere (Chapter 3.3).

The flux of relative westerly momentum in July is much smaller than in January and is produced primarily by transient waves with wavenumbers greater than three.

The stratospheric sudden warming of January 1971 was preceded by a very strong zonal current which became asymmetric with respect to the pole, followed in time by a strong two wave pattern (actually two

cut-off lows, or vortices) producing warming near the pole and easterly winds at high latitudes (Chapter 4.1) Both waves one and two exhibited westerly vertical tilts of the troughs and ridges when the amplitudes were high (Chapter 4.2). Waves two and three appear to gain energy at the expense of the zonal current and possibly other waves (Chapter 4.3). The amplitude of wave three shows considerably more variability than either waves one or two. The shorter waves are insignificant in the stratosphere, and of significantly smaller magnitude than waves one and two in the troposphere.

During the course of the stratospheric sudden warming relative westerly momentum is transported southward by wave one and northward by wave two just prior to the onset of easterly winds while reversed roles appear after this (Chapter 4.3).

It appears from this study that harmonic analysis is a useful tool in the understanding of various scales of atmospheric wave motions, particularly in the upper troposphere and stratosphere.

REFERENCES

Adams, J.C., A.K. Cline, M.A. Drake and R.A. Sweet, 1975: NCAR Support Library, Vol. III, NCAR Tech. Note NCAR-TN/IA-105. Atmospheric Technology Division, NCAR, Boulder, Colorado.

Barnett, J.J., 1974: The mean meridional temperature behaviour of the stratosphere from November, 1970 to November, 1971 derived from measurements by the Selective Chopper Radiometer on Nimbus IV. Quart. J. R. Met. Soc., 100, 505-530.

_____, R.S. Harwood, J.T. Houghton, C.G. Morgan, C.D. Rodgers, and E.J. Williamson, 1971: Stratospheric Warming Observed by Nimbus 4. Nature, 230, 47-48.

Charney, J. and P.G. Drazin, 1961: Propagation of planetary-scale disturbances from the lower into the upper atmosphere. J. Geophys. Res., 66, 83-110.

Craig, R.A., 1965: The Upper Atmosphere: Meteorology and Physics, Academic Press, 509 pp.

Cressman, G.P., 1959: An operational objective analysis system. Mon. Wea. Rev., 87, 367-374.

Deland, R.J., 1973: Spectral analysis of traveling planetary scale waves: vertical structure in middle latitudes of northern hemisphere. Tellus, XXV, 355-374.

Eliasen, E., 1958: A study of the long atmospheric waves on the basis of zonal harmonic analysis. Tellus, X, 206-215.

Free University of Berlin, 1971: Meteorologische Abhandlungen, Band 120/ Heft 1.

Haney, R.L., 1961: Behavior of the principal harmonics of selected 5-day mean 500 mb charts. Mon. Wea. Rev., 89, 391-396.

Hildebrand, F.B., 1956: Introduction to Numerical Analysis, McGraw-Hill, 511 pp.

Hirota, I., and Y. Sato, 1969: Periodic variation of the winter stratospheric circulation and intermittent vertical propagation of planetary waves. J. Met. Soc. Jap., 47, 390-402.

Iwashima, T., 1973: Observational studies of the ultra-long waves in the atmosphere (I). J. Met. Soc. Jap., 51, 209-229.

_____, 1974: Observational studies of the ultra-long waves in the atmosphere (II). J. Met. Soc. Jap., 52, 120-142.

Jenne, R.L., 1975: Data sets for meteorological research. NCAR Tech. Note, NCAR-TN/IA-111, National Center for Atmospheric Research, 168 pp.

Julian, P.R. and K.B. Labitzke, 1965: A study of atmospheric energetics during the January-February 1963 stratospheric warming. J. Atmos. Sci., 22, 597-610.

Kertz, Walter, 1956: Die thermische Erregungsquelle der atmosphärschen Gezeiten. Nachr. Ak. Wiss. Göttingen, Mathem.-Phys. Kl. Nr. 6/1956, 145-166.

LaSeur, N.E., 1954: On the Asymmetry of the middle-latitude circumpolar current. J. of Met., 11, 43-57.

Lorenz, E.N., 1967: The Nature and Theory of the General Circulation of the Atmosphere. World Meteorological Organization Publication No. 218, 161 pp.

Matsuno, T., 1970: Vertical propagation of stationary planetary waves in the winter northern hemisphere. J. Atmos. Sci., 27, 871-883.

_____, 1971: A dynamical model of the stratospheric sudden warming. J. Atmos. Sci., 28, 1479-1494.

Miller, A.J., 1970: The transfer of kinetic energy from the troposphere to the stratosphere. J. Atmos. Sci., 27, 388-393.

Murakami, T., 1965: Energy cycle of the stratospheric warming in early 1958. J. Met. Soc. Jap., 43, 262-283.

Murgatroyd, R.J., 1969: The structure and dynamics of the stratosphere. The Global Circulation of the Atmosphere. Roy. Met. Soc., 159-195.

Oort, A.H. and Rasmusson, 1971: Atmospheric Circulation Statistics. NOAA Professional Paper 5, U.S. Dept. of Commerce, 323 pp.

Palmén, E. and C.W. Newton, 1969: Atmospheric Circulation Systems, Their Structure and Physical Interpretation. International Geophysics Series No. 13, Academic Press, 603 pp.

Panofsky, H.A. and G.W. Brier, 1958: Some Applications of Statistics to Meteorology. The Pennsylvania State University, 224 pp.

Quiroz, R.S., 1975: The stratospheric evolution of sudden warmings in 1969-74 determined from measured infrared radiation fields. J. Atmos. Sci., 32, 211-224.

_____, A.J. Miller and R.M. Naganti, 1975: A comparison of observed and simulated properties of sudden stratospheric warmings. J. Atmos. Sci., 32, 1723-1736.

Sato, Y., 1974: Vertical structure of quasi-stationary planetary waves in several winters. J. Met. Soc. Jap., 42, 272-281.

Srivatsangam, S., 1976: Atmospheric eddy transports and their efficiencies. Environmental Research Paper 3, Atmospheric Science Department, Colorado State University, Fort Collins, Co., 26 pp.

U.S. Committee on Extension to the Standard Atmosphere, 1966: U. S. Standard Atmosphere Supplements, 1966. U. S. Government Printing Office, 289 pp.

van Loon, H. R., R. L. Jenne, and K. Labitzke, 1973: Zonal harmonic standing waves. J. Geophys. Res., 78, 4463-4471.

Van Mieghem, J., 1961: Zonal harmonic analysis of the northern hemisphere geostrophic wind field. (I.A.M.A.P. Presidential address, Helsinki) I.U.G.G. Monog., No. 8, Paris, 57 pp.

_____, 1973: Atmospheric energetics. Oxford Univ. Press, 206 pp.

_____, P. Defrise and J. Van Isacker, 1959: On the selective role of the motion systems in the atmospheric general circulation. Rossby Memorial Volume, 230-239.

_____, P. Defrise and J. Van Isacker, 1960: Harmonic analysis of the normal monthly northern hemisphere geostrophic flow at 500 mb. Med. Kon. VL. Acad. van België, Kl., der Wet., Jg. XXII-4, 1-38.

BIBLIOGRAPHIC DATA SHEET	1. Report No. CSU - ATSP-245	2.	3. Recipient's Accession No.

4. Title and Subtitle

THE STRUCTURE OF ATMOSPHERIC PARAMETERS IN WAVENUMBER-SPACE

5. Report Date: March, 1976

6.

7. Author(s): David Wackter

8. Performing Organization Rept. No. CSU - ATSP-245

9. Performing Organization Name and Address

Atmospheric Science Department
Colorado State University
Fort Collins, Colorado 80523

10. Project/Task/Work Unit No.

11. Contract/Grant No.

GA-4152 and
DES 74-001917 A01

12. Sponsoring Organization Name and Address

National Science Foundation
Washington, D.C. 20550

13. Type of Report & Period Covered

14.

15. Supplementary Notes

16. Abstracts

Zonal harmonic analysis of geopotential heights was performed at each fifth degree of latitude from 20°N to 85°N and at fourteen standard pressure levels from 1000 mb to 10 mb for each day of 1971. Computed parameters include the first twelve harmonic amplitudes, phase angles of contour heights, geostrophic wind components, kinetic energies of the zonal and meridional geostrophic flow, and the meridional fluxes of relative westerly momentum. Two types of calculations were used to compute monthly means, thereby allowing the introduction of "standing" and "transient" wave contributions.

The most dominant feature of the seasonal amplitude distributions was the disappearance of the strong wavenumbers one and two in the stratosphere following the spring breakdown of the polar night vortex.

(Continued on other side)

17. Key Words and Document Analysis. 17a. Descriptors

Mean Meridional Profiles
Stratospheric Sudden Warming
Vertical Structure
Zonal Harmonic Analysis

17b. Identifiers/Open-Ended Terms

17c. COSATI Field/Group

18. Availability Statement	19. Security Class (This Report) UNCLASSIFIED	21. No. of Pages 94
	20. Security Class (This Page UNCLASSIFIED	22. Price

Wavenumbers one through three dominated the zonal kinetic energy spectrum in January and July, and also the meridional kinetic energy spectrum at high latitudes and levels. An appreciable part of the meridional kinetic energy was contained in the wavenumber band from five through twelve at lower and mid-latitudes of the troposphere.

The standing and transient components of the wave energy showed preferred modes with, in general, the transient waves predominantly responsible for the meridional kinetic energy and the standing waves responsible for a major part of the zonal kinetic energy.

The development of a stratospheric sudden warming was analyzed in the same manner, but on a daily basis. When amplitudes of wavenumbers one and two were high there occurred a noticeable westerly tilt with height. Waves two and three appear to gain energy at the expense of wave one and the mean zonal current as the polar night vortex begins to break down.